Maraa eastern transect: Sites M0015–M0018[1]

Expedition 310 Scientists[2]

Chapter contents

Operations

Hole M0015A

After completing Hole M0007C, ~300 m to the northwest, the *DP Hunter* moved to Site M0015 in 72.15 m of water. After a short bathymetry traverse to locate a site for Hole M0015A, drilling operations began at 0030 h on 27 October 2005 and continued until 0325 h on 28 October. Total depth (TD) was 42.28 meters below seafloor (mbsf). There was generally good core recovery, usually with <1 m core runs between bit blocking, and 72.71% average recovery for the hole.

Prior to logging, Hole M0015A was reamed and flushed for 1 h, after which the core barrel was removed and the drill string rerun with a casing shoe. Logging commenced at 0630 h on 28 October. Initially, the casing depth was set at 7 mbsf, but the logging tools would not pass downhole beyond 20 mbsf, so they were removed. The casing was run to the base of the hole and then pulled back to 20 mbsf. Logging was then possible in the bottom part of the borehole, but one tool was stuck for a while and had to be eased free with the downhole hammer. Thereafter, logging continued successfully; the casing was pulled back to 7 mbsf, and the remainder of the hole was logged, with overlap. Logging operations in Hole M0015A were completed by 1930 h on 28 October. The string was then tripped to deck, and Seacore's drilling and reentry template (DART) was lifted off the seabed.

Hole M0016A

After moving to new Site M0016, a tautwire bathymetry traverse was conducted to locate a site for Hole M0016A. By 2400 h on 28 October 2005, the *DP Hunter* was positioned above Hole M0016A in 80 m water depth. Shortly after midnight on 29 October, coring operations began. Throughout the day, coring continued with fairly poor recovery, and drilling indicated that the formation had many cavities. Coring in Hole M0016A was terminated at 0620 h on 30 October at a TD of 38.31 mbsf. This was because of difficulty in overcoming bit blocking, and, after a string trip to clean the whole core barrel system, the HQ inner barrel could not reenter the outer pipe because of the string bending. It is most likely that the DART had moved on the seabed, possibly through subsidence.

[1] Expedition 310 Scientists, 2007. Maraa eastern transect: Sites M0015–M0018. *In* Camoin, G.F., Iryu, Y., McInroy, D.B., and the Expedition 310 Scientists. *Proc. IODP,* 310: Washington, DC (Integrated Ocean Drilling Program Management International, Inc.). doi:10.2204/iodp.proc.310.106.2007
[2] Expedition 310 Scientists' addresses.

doi:10.2204/iodp.proc.310.106.2007

Hole M0016B

Hole M0016B was located 5 m east of Hole M0016A. Initially, the noncoring insert bit was used to drill down to 17 mbsf, and then coring continued with variable but generally good core recovery. Coring operations ended at 0230 h on 31 October 2005 at a TD of 44.62 mbsf.

Site M0006

After moving to previous Site M0006, a tautwire site survey was conducted along a short transect. This survey was abandoned after the DART touched down on the seabed unexpectedly, indicating that the bathymetry for this area was not accurate. After running the downpipe camera to check for stinger damage and lifting the DART higher from the seabed, a new tautwire survey was conducted 10 m east of the previous transect. A suitable site was found, but when the DART was lowered it touched the seabed 2 m deeper than indicated by the tautwire. The topography of the seafloor was suspected to be very uneven at this survey location, so a new survey transect was initiated 10 m to the east. During this survey, the DART unexpectedly touched seabed again. The seabed depth at Site M0006 appeared to change rapidly, and the changes were not evident on the bathymetry data. Therefore, the search for a new site was abandoned, the DART was lifted into the moonpool, and the *DP Hunter* returned to previous Site M0015.

Hole M0015B

The *DP Hunter* moved back to previous Site M0015 to start new Hole M0015B in 71.53 m water depth. Coring operations began at 1330 h on 31 October 2005 and were completed by 1730 h on 1 November at a TD of 40.12 mbsf. Because very short core runs were being achieved in the lower part of the hole and most liners were being crushed, the last four or five runs were made using the split chromed steel liners commonly used elsewhere in this type of coring. The immediate result was longer core runs before jamming, better core recovery, and improved preservation of delicate structures. Some horizons that would previously have been crushed were kept intact or in their correct cored position.

Hole M0017A

Hole M0017A was located ~60 m north of Hole M0015B in 56.5 m water depth. Before touching down with the DART, a seabed camera survey was run to check for living corals. None were observed, and coring operations began at 2300 h on 1 November 2005. A faster penetration rate was achieved because of the use of steel split liners, which gave the drillers a much more sensitive indicator of bit blocking. As a consequence, they were able to detect bit blocking much more quickly and were sometimes able to avoid it. This meant that core runs were longer and the number of wireline trips was reduced. Core recovery also improved. No problems were encountered with the subsequent curation or science through the use of steel split liners. Coring was completed by 1600 h on 2 November at a TD of 40.56 mbsf.

Prior to logging Hole M0017A, the hole was flushed. There was some difficulty with a stuck HQ pipe while trying to trip the drill string, which could be rotated but not lifted. The string eventually came free. A casing shoe was fitted for the logging operation. Logging commenced in Hole M0017A at 2130 h on 2 November and was completed by 0350 h on 3 November. Resistivity, acoustic imaging, optical imaging, hydrochemical, caliper, and sonic tools were run. Starting depth of the tools varied because of tools catching in cavities (between 31.55 and 23.23 mbsf), and the depth of the casing pipe was 13.35 mbsf. The core barrel fishing cable was used on one occasion to pull the sonic tool, which was stuck just below the casing, up to the surface. This process damaged a portion of the logging winch cable, which was cut at ~85 m. Reheading of the winch cable was completed well before the next logging operation.

Hole M0018A

A short echo sounder survey (30 m × 20 m grid) was conducted ~120 m south-southeast of proposed Site TAH-03A 1 to locate a suitable site for Hole M0018A. At 0915 h on 3 November 2005, the DART was lowered at the chosen site and touched the seabed 14 m deeper than suggested by the echo sounder survey. The specific site was resurveyed using the lead-line, and a new site was chosen nearby. The DART was unable to be drilled in at this site at first (a solid carbonate crust was evident on the camera survey) but was successfully drilled in on the second attempt (after the crust was broken by the stinger?). At 1640 h on 3 November, coring operations began in Hole M0018A, and they continued until 1200 h on 4 November. TD of the hole was 40.05 mbsf, with a total recovery of 61.50%. The nature and quality of the material collected indicated that most of the coreable material was being collected. A camera survey was conducted after withdrawing the drilling equipment from the hole. No undue disturbance was observed, although there was a significant mound where the DART was situated with a slight "tail" of what appeared to be cuttings coming from it and going down the presumed slope.

Prior to departing the Maraa area, the tautwire was respooled and the DART was lifted onto the deck of the *DP Hunter* and secured. Once on deck, the stinger below the DART was found to be missing, and a new stinger was fitted. The vessel departed the Maraa area at 1750 h on 4 November and arrived at the Faaa area at 2030 h.

Sedimentology and biological assemblages

The eastern transect drilled in the region of Maraa (southwest Tahiti) includes, with increasing distance from the island, Sites M0017, M0015, M0018, and M0016, ranging in depth from 56.45 to 81.8 meters below sea level (mbsl).

Last deglacial sequence (Unit I)

Packstone-grainstone intervals: Cores 310-M0017A-1R and 3R

Coral/algal rubble intervals: Section 310-M0015A-8R-1, Cores 310-M0016A-13R, 14R, and 16R, Section 310-M0016B-21R-2, and Cores 310-M0017A-4R, 10R, 12R, and 14R and 310-M0018A-9R, 10R, 13R, 17R, 19R, 21R, and 22R

Skeletal sand intervals: Sections 310-M0015A-15R-1 and 16R-1

The thickness of the last deglacial sequence (lithologic Unit I) ranges from 30 m in Hole M0015A at 72.15 mbsl to 40 m in Hole M0018A at 81.8 mbsl. The base of the unit has been recovered from 96 mbsl at the inner sites to 121 mbsl at the outer sites.

In Hole M0017A, the top of the last deglacial sequence comprises a well-consolidated packstone-grainstone composed mainly of *Halimeda* segments associated with foraminifers (benthic and encrusting foraminifers), bryozoans, echinoids, and mollusks. Rhodoliths are observed in Core 310-M0017A-1R.

In Hole M0016A, the top of the last deglacial sequence consists of rubble of coral fragments (encrusting agariciids, *Porites,* and *Montipora*) and rhodoliths. The surfaces of the skeletal fragments are usually stained and bored.

This sequence is primarily composed of coralgal-microbialite frameworks commonly interlayered with loose skeletal sediments, including coral and algal rubble.

Coral and algal rubbles are mostly composed of accumulations of fragments of corals (mostly composed of encrusting *Acropora* and *Montipora* and branching *Pocillopora* and *Porites*), microbialite crusts and mollusks, *Halimeda* segments, and rounded lithoclasts (e.g., skeletal sandstone rich in volcanic grains) (Figs. F1, F2) (e.g., intervals 310-M0017A-12R-1, 138–146 cm, and 310-M0018A-21R-1, 18–32 cm); benthic foraminifers are usually scarce. Coral fragments are commonly coated with thin crusts of nongeniculate coralline algae. The surface of the coral fragments usually displays evidence of extensive bioerosion and, locally, reddish staining. Pebbles of basalt and sand-sized volcanic grains occur locally.

Skeletal sand corresponds to *Halimeda* sand and is rich in fragments of corals (e.g., branching *Porites*), echinoids, and mollusks.

The frameworks that form the bulk of the last deglacial sequence include three subunits, each displaying distinctive coral assemblages and internal structure.

Subunit IA

Intervals: Cores 310-M0015A-1R through 7R, 310-M0015B-1R through 7R-1, 310-M0016A-2R through 11R, 310-M0017A-3R-1 through 8R, and 310-M0018A-1R through 9R

Subunit IA primarily comprises locally well lithified coralgal bindstone that forms the upper part of the last deglacial sequence in all holes: from 56.45 to 68.1 and 80 mbsl in the inner holes (Holes M0017A and M0015B, respectively) and from 81 to 97 mbsl in the outer holes (Holes M0016 and M0018, respectively).

In Holes M0015B and M0018A, the top of the subunit is characterized by the occurrence of a hardground and yellowish-reddish staining of the rock surface; bioerosion is extensive (Figs. F3, F4) (e.g., intervals 310-M0015B-1R-1, 0–10 cm, and 310-M0018A-1R-1, 0–6 cm).

Coral assemblages are dominated by encrusting colonies of *Montipora,* agariciids represented by *Pavona, Porites, Leptoseris,* and *Leptastrea,* and foliaceous colonies of *Pachyseris* (Figs. F5, F6, F7, F8, F9, F10, F11, F12) (e.g., intervals 310-M0015B-1R-1, 20–40 cm, and 2R-1, 35–50 cm, 310-M0016A-7R-1, 40–50 cm, 310-M0017A-3R-CC, 1–10 cm, and 4R-1, 7–17 cm, and 310-M0018A-1R-1, 16–29 cm, 1R-1, 79–90 cm, and 3R-1, 60–80 cm). Associated corals include massive colonies of *Porites,* branching colonies of *Porites, Pavona,* and *Pocillopora* (including robust branching colonies), and tabular colonies of *Acropora* in the lower part of this subunit (Fig. F13) (e.g., interval 310-M0018A-7R-1, 70–80 cm).

Corals are usually thinly encrusted with nongeniculate coralline algae, except in the lower part of the subunit where the crusts are significantly thicker (up to 2 cm thick) and include vermetid gastropods and serpulids. The last stage of encrustation over coral

colonies corresponds to thick microbialite crusts dominated by massive laminated fabrics.

Some primary cavities are partly filled with well- and moderately consolidated skeletal sands or are veneered with microbialites; locally the walls of the cavities exhibit brownish staining.

Subunit IB

Intervals: Cores 310-M0015A-7R through 12R, Sections 310-M0015B-7R-2 through 21R-2, and Cores 310-M0017A-9R through 17R.

Subunit IB is mostly composed of coralgal-microbialite frameworks in which coral assemblages are dominated by tabular colonies of *Acropora* (Figs. **F14, F15, F16, F17**) (e.g., intervals 310-M0015A-7R-1, 20–35 cm, and 10R-1, 70–80 cm, 310-M0015B-19R-1, 53–69 cm, and 310-M0017A-12R-1, 57–65 cm). This distinctive subunit occurs only at the inner sites of the transect (i.e., in Holes M0017A [68–85 mbsl], M0015A [79.4–85.7 mbsl], and M0015B [80–86.44 mbsl]).

Associated corals include encrusting colonies of *Montipora* (locally dominant [e.g., Cores 310-M0015B-14R through 16R]), *Porites, Leptastrea, Montastrea,* and agariciids, massive colonies of *Porites* (e.g., Sections 310-M0015B-9R-2 and 10R-1 and Core 11R) and *Montastrea,* and branching colonies of *Porites, Pocillopora,* and *Acropora* (Figs. **F18, F19, F20, F21**) (e.g., intervals 310-M0015A-9R-1, 28–40 cm, 310-M0015B-9R-1, 0–12 cm, and 310-M0017A-9R-1, 10–17 cm, and 14R-1, 87–103 cm). Robust branching colonies of *Acropora* and *Pocillopora* occur in the lower part of this subunit where they are locally dominant (Figs. **F22, F23**) (e.g., intervals 310-M0015B-21R-1, 85–105 cm, and 310-M0017A-13R-1, 21–36 cm, and Cores 310-M0017A-15R through 17R).

Corals are generally coated with thick crusts of nongeniculate coralline algae, up to a few centimeters, in which vermetid gastropods and serpulids occur. Very thick microbialite crusts form the last stage of encrustation and are mostly composed of massive laminated fabrics locally overlain by dendritic accretions (Figs. **F24, F25, F26**) (e.g., intervals 310-M0017A-13R-1, 3–12 cm, 310-M0017B-16R-1, 87–98 cm, and 310-M0015B-21R-1, 84–92 cm).

Coral colonies usually exhibit traces of bioerosion; brownish-yellowish staining is conspicuous on some surfaces.

Large primary cavities are partly filled with coarse skeletal sand rich in *Halimeda* segments and fragments of mollusks and echinoids.

Subunit IC

Intervals: Cores 310-M0015A-12R through 36R, Sections 310-M0015B-22R-1 through 38R-2, and Cores 310-M0016A-12R through 36R, 310-M0016B-1R through 23R-1, 310-M0017A-17R through 21R, and 310-M0018A-9R through 22R-1

Subunit IC comprises coralgal-microbialite frameworks dominated by branching colonies of *Porites* (Figs. **F27, F28, F29, F30**) (e.g., intervals 310-M0015A-20R-1, 55–68 cm, and 30R-1, 74–84 cm, and 310-M0015B-33R-1, 112–139 cm, and 34R-1, 13–34 cm). The top of this subunit occurs at 85 mbsl in the inner holes (Holes M0017A, M0015A, and M0015B) and deeper than 90 mbsl in the outer holes (Holes M0016A, M0016B, and M0018A). The base of Unit I was recovered from 94 mbsl at the inner sites to 121 mbsl at the outer sites.

A well-diversified coral assemblage is associated with branching colonies of *Porites* (Figs. **F31, F32**) (e.g., intervals 310-M0016B-11R-1, 20–34 cm, and 310-M0017A-18R-1, 77–91 cm) and includes branching and robust branching colonies of *Pocillopora* and *Acropora* (e.g., Cores 310-M0015A-14R, 16R, 17R, 27R, and 34R, 310-M0015B-26R and 31R, and 310-M0016A-26R and 27R), massive colonies of *Montastrea,* encrusting colonies of *Porites, Montipora, Leptastrea, Millepora,* agariciids (*Pavona* and *Leptoseris*), and *Psammocora,* and tabular colonies of *Acropora* (Figs. **F33, F34, F35, F36, F37, F38, F39, F40, F41**) (e.g., intervals 310-M0015A-23R-1, 18–42 cm, and 26R-1, 8–31 cm, 310-M0015B-21R-1, 85–90 cm, and 25R-1, 40–65 cm, 310-M0016A-22R-1, 13–20 cm, 23R-1, 0–16 cm, 29R-1, 38–60 cm, 30R-1, 14–24 cm, and 21R-1, 52–66 cm, and 310-M0018A-13R-1, 25–35 cm). Massive colonies of *Porites* dominate in Cores 310-M0016A-33R through 36R (e.g., interval 310-M0016A-3R-1, 23–33 cm).

Coral colonies are generally coated with thick crusts of nongeniculate coralline algae locally associated with vermetid gastropods and serpulids. In those frameworks, microbialites (laminated and thrombolitic microbial fabrics) form massive crusts (up to 20 cm thick) over corals and coralline algae and usually represent the major volumetric and structural component of the frameworks (Fig. **F42**) (e.g., interval 310-M0015A-14R-1, 23–49 cm). They usually correspond to a two-stage encrustation composed of very thick laminated fabrics overlain by thrombolitic accretions that usually represent the last stage of encrustation. Large primary cavities are partly filled with micritic sediments, including *Halimeda* segments and fragments of mollusks and echinoids (Figs. **F43, F44, F45**) (e.g., intervals 310-M0015A-14R-1, 48–60 cm, and 21R-1, 19–31 cm, and 310-

M0015B-26R-1, 50–75); brown crusts occur in some cavities. Some surfaces of the reef rocks display yellowish to reddish staining.

Corals exhibit alteration in Cores 310-M0018A-12R and 14R; yellowish, brownish to reddish staining is conspicuous on some surfaces in Cores 18R through 20R.

In Hole M0015B, the base of the last deglacial sequence comprises an algal bindstone composed of crusts and branches of nongeniculate coralline algae.

Volcanic silt and sand and occasional granules and pebbles appear only as minor components in some of the carbonate units at the base of Holes M0015A and M0015B. In Hole M0015A, volcanic sediments first appear in Section 310-M0015A-35R-1; in Hole M0015B, they only appear in Section 310-M0015B-38R-2.

Older Pleistocene sequence (Unit II)

Intervals: Cores 310-M0015A-37R through 41R, Sections 310-M0015B-38R-2 and 38R-3, 310-M0016B-23R-CC through 24R, and 310-M0017A-21R-1 through 21R-3, and Core 310-M0018A-22R

The older Pleistocene sequence (lithologic Unit II) is primarily composed of irregular alternations of yellow, gray to beige poorly sorted skeletal limestone (grainstone to rudstone-floatstone) and coralgal frameworks with local intercalations of coral and algal rubble that display a conspicuous alteration.

Postdepositional diagenetic processes of the older Pleistocene sequence is indicated by the diagenetic alteration of coral skeletons and the occurrence of large solution cavities that display yellow, brown to red-brown staining and cement lining (Figs. **F46, F47, F48, F49**) (e.g., intervals 310-M0015A-40R-1, 10–24 cm, and 41R-1, 105–118 cm, 310-M0015B-38R-3, 92–102 cm, and 310-M0015A-40R-1, 30–38 cm). Some solution cavities are partly filled with internal sediments.

Grainstone, rudstone, and floatstone are rich in fragments of corals (e.g., robust branching *Pocillopora,* branching and massive *Porites,* branching *Acropora,* and encrusting *Montipora*), coralline algae, echinoids and mollusks, and *Halimeda* segments (Figs. **F50, F51, F52, F53, F54, F55, F56, F57, F58**) (e.g., intervals 310-M0015A-37R-1, 40–55 cm, 39R-1, 63–80 cm, 39R-1, 115–129 cm, 40R-1, 29–32 cm, and 41R-1, 25–35 cm, 310-M0015B-38R-3, 40–55 cm, 310-M0016B-22R-CC, 10–24 cm, 24R-1, 57–70 cm, and 24R-1, 79–94 cm, and 310-M0017A-21R-3, 92–119 cm). Skeletal elements are usually extensively bioeroded. Sand-sized volcanic grains are commonly associated with the skeletal grains. Intraclasts are common.

Coralgal frameworks are composed of encrusting and branching colonies of *Porites,* tabular colonies of *Acropora,* encrusting and massive colonies of *Montipora,* and encrusting colonies of agariciids (Figs. **F59, F60, F61**) (e.g., intervals 310-M0015A-38R-1, 63–75 cm, and 310-M0017A-21R-1, 98–118 cm, and 22R-2, 32–64 cm); massive colonies of *Porites* occur locally. These corals are thickly encrusted with nongeniculate coralline algae associated with vermetid gastropods and serpulids.

Petrophysics

Recovery at Maraa eastern transect sites, on the southwestern side of the island of Tahiti, was partial (Hole M0016A = 56%, Fig. **F62;** Hole M0016B = 51%, Fig. **F63;** Hole M0017A = 56%, Fig. **F64;** Hole M0018A = 61%, Fig. **F65**) and good (Hole M0015A = 72%, Fig. **F66;** Hole M00015B = 71%, Fig. **F67**). Cores 310-M0015A-12R, 14R, 15R, 16R, and 38R, 310-M0015B-28R, 310-M0016A-02R, 310-M0017A-04R, and 310-M0018A-19R were left unsaturated and therefore have different data coverage and quality (see the **"Methods"** chapter for more details). Water depths are as follows: Hole M0015A = 72.15 mbsl, Hole M0015B = 72.30 mbsl, Hole M0016A = 80.85 mbsl, Hole M0016B = 80.35 mbsl, Hole M0017A = 56.34 mbsl, and Hole M0018A = 81.80 mbsl.

Density and porosity

Two methods were used to evaluate bulk density at Maraa eastern transect sites. Gamma ray attenuation (GRA) on the MSCL provided an estimate of bulk density from whole cores. Discrete moisture and density (MAD) samples facilitated a second, independent measure of bulk density and provided grain density and porosity data.

From 0 to 37 mbsf (e.g., Cores 310-M0015A-1R through 37R and 310-M0015B-1R through 37R; last deglacial sequence [lithologic Unit I]), density ranges between 1.9 and 2.4 g/cm^3. The downhole profile shows small-scale density variations, which are directly reflected in porosity. Porosity ranges between 20% and 50%. In some cases, MAD values deviate as much as 0.5 g/cm^3 from GRA bulk density (Fig. **F67**). This deviation is most likely due to the presence of large pores in the core area over which the density is calculated. Below 37 mbsf (Cores 310-M0015A-37R through 41R and 310-M0015B-38R; older Pleistocene sequence [lithologic Unit II]), MAD bulk density correlates with maximum GRA values. The high GRA bulk densities are always >2.1 g/cm^3 with a maximum of 2.45 g/cm^3, corresponding to the diageneti-

cally altered older Pleistocene sequence (see **"Older Pleistocene sequence [Unit II]"**). As a result of diagenesis, porosities are toward lower values in the range of 10%–25% with few outliers to 35%, corresponding to local intercalations of gravel and sand layers. None of the older Pleistocene sequence was recovered in Hole M0016A (Fig. **F62**).

Grain density has an average value of 2.73 g/cm³ and considerable scatter from 2.67 to 2.80 g/cm³. Values <2.67 g/cm³ are rare and may be the result of grain volume measurement error.

Porosity, calculated from MAD data (see **"Moisture and density"** in the "Methods" chapter), ranges from 47% at, for example, 8 mbsf (Fig. **F62**) to <9% at, for example, 37 mbsf (Fig. **F66**). The lowest porosity (6%–8%) occurs in the hardground between at the last deglacial–older Pleistocene sequence transition (Holes M0015A and M0015B, 37 mbsf; Figs. **F66, F67**).

P-wave velocity

P-wave velocities were provided through multisensor track (MST) *P*-wave logger (PWL) on whole cores and discrete measurements on core plugs. In Unit I, the velocity profile is highly scattered, reflecting small-scale variability in velocity as a result of porosity changes. Values range from 1800 to 4900 m/s and show no clear downhole trends. Discrete measurements confirm excursions in velocities toward the higher velocity spectrum. The older Pleistocene sequence shows distinct higher velocities with values mostly >4000 m/s. In Hole M00015A (Fig. **F66**), at 36–37 mbsf, this hardground shows constant velocities >4500 m/s, indicating tight and dense matrix properties. Discrete measurements reveal velocities as high as 5212 m/s (Hole M0015B, 38 mbsf; Fig. **F67**). A cross plot of velocity versus porosity for the Maraa western transect sites shows a general inverse relationship (Fig. **F68**). For the time-average empirical equation of Wyllie et al. (1956) and Raymer et al. (1980), the traveltime of an acoustic signal through rock is a specific sum of the traveltime through the solid matrix and the fluid phase. The general trend appears to be approximately linear, with the largest deviations between porosities of 0% and 15% and scattered observations in the high-porosity domain. Downhole sonic logging data for Hole M0017A (Fig. **F64**) are available for the interval 15–27 mbsf and display a highly variable velocity profile in correlation with scattered V_P MST observations. This profile correlates with the high abundance of macro pores that makes the interval difficult to core intact; the interval velocities tend to be lower because of the presence of seawater (~1535 m/s) making up to 50% of the medium through which the acoustic wave propagates, which results in a decrease in overall "averaged" velocity values (Fig. **F69**).

Magnetic susceptibility

Magnetic susceptibility values in the last deglacial sequence are generally low but are still higher than expected for clean carbonates. Values rarely exceed 100 × 10^{-5} SI units. The largest excursions can be found in the uppermost 10 mbsf (e.g., Holes M0015A, M0015B, and M0016A; Figs. **F62, F66, F67**). The zone above the transition to the older Pleistocene sequence appears to contain very few magnetizable minerals with a magnetic susceptibility maximum of ~30 × 10^{-5} SI units (e.g., Hole M0018A, 30–33 mbsf; Fig. **F65**). This same zone can be observed in Hole M0017A at 31–35 mbsf (Fig. **F64**). The older Pleistocene sequence shows an increase in magnetic susceptibility but only in individual excursions as high as 220 × 10^{-5} SI units. Average response is ~50 × 10^{-5} SI units.

Resistivity

See **"Resistivity"** in the "Maraa western transect" chapter.

Diffuse color reflectance spectrophotometry

The downhole trend in Holes M0015A and M0015B (Figs. **F66, F67**) is a slight increase in L* values from 55 L* units (average = shallower than 10 mbsf) to 62 L* units (average = deeper than 32 mbsf). This trend reflects lithological changes from gray microbialite-dominated lithofacies in the last deglacial sequence to light yellowish/brown rudstone lithofacies in the older Pleistocene sequence. Many peaks of high L* values (up to 80 L* units) in the interval 9.1–11.8 mbsf originate from an above average abundance of corals, such as massive *Porites* (Fig. **F70**).

No clear downhole trends are observed in the last deglacial sequences of Holes M0016A and M0017A (Figs. **F62, F64**). On the other hand, in Hole M0016B (Fig. **F63**), L* values (up to 80 L* units) decrease from the lower part to the middle part of the last deglacial sequence. This trend corresponds to lithological changes from coralgal framework–dominated lithofacies (including some massive *Porites*) to microbialite-dominated lithofacies. The decrease of L* values observed at 49.2 mbsf in Hole M0016B (Fig. **F63**) corresponds to the unconformity between coralgal bindstone in the last deglacial sequence and rudstone in the older Pleistocene sequence.

Downhole variations in L* values are observed in the last deglacial sequence of Hole M0018A (Fig. **F65**). Three "cycles" are observed that correlate with litho-

logical changes from coralgal framework–dominated (including *Porites* and *Acropora*) to microbialite-dominated lithofacies.

Hole-to-hole correlation

Borehole correlation patterns at Maraa eastern transect sites do not have obvious magnetic susceptibility responses. Density, porosity, and velocity profiles are scattered in the last deglacial sequence and do not permit direct correlation. One clear marker is the generally low response in the 4–5 m directly overlying the older Pleistocene sequence. The main correlation surface is the last deglacial–older Pleistocene sequence transition, which centers around 39 mbsf in most boreholes except for Hole M0015A, where the transition can be found at 36 mbsf.

Site-to-site correlation

The last deglacial–older Pleistocene sequence transition, a sharp and abrupt unconformity, is the key correlation surface through all boreholes. Above this transition, the last deglacial sequence comprises an open coralgal-microbialite framework with highly variable density, porosity, and velocity values. Correlation of these properties has proven to be difficult. Magnetic susceptibility correlates well within sites, but over long distances it does not permit site-to-site correlation. The transition is characterized by a sharp and abrupt increase in density and velocity and a decrease in porosity. Subaerial exposures have altered the upper few meters of this sequence, implied by the occurrence of cement crusts, infillings of karst features with younger sediments, and other diagenetic features (see **"Sedimentology and biological assemblages"**). The depth of this transition is not constant. At Maraa eastern transect ridge sites, this level is present at ~120 mbsl for most sites except for the shallower Hole M0017A (Fig. **F64**), where the unconformity occurs at 93 mbsl. At Maraa western transect sites, this transition occurs at ~87 mbsl for all boreholes. This would indicate that the last deglacial sequence was deposited on an irregular topography with the underlying older Pleistocene sequence shallowing landward.

Downhole logging

Hole M0015A

Open borehole logging was carried out in two stages in Hole M0015A (72.15 mbsl) because of borehole instability. By positioning an open shoe casing at 20.0 mbsf, the bottom part of Hole M0015A could be logged. Borehole conditions were hostile, indicated by the caliper and image logs (Fig. **F71**); primary cavities up to 90 cm can be observed in the lower part of the section (below 22.5 mbsf). The optical imaging tool got stuck in the cavity at ~27.5 mbsf while logging up. Tool recovery resulted in cable head damage, and a complete changeover of the entire logging setup was necessary to continue downhole logging. It was therefore decided to stay above this interval in the second logging attempt; the basal part of the last deglacial sequence (lithologic Unit I) was imaged only with the acoustic borehole televiewer (ABI40). Its top part was logged by placing the open shoe casing at 7.5 mbsf.

The lowermost interval of the last deglacial sequence (Unit I) (base to 29.03 mbsf; Cores 310-M0015A-31R through 41R; Fig. **F72**) is characterized by an extremely large borehole diameter, isolated high-reflectivity fragments (coral fragments), and overall low reflectivity values, which can be classified as a rubbly lithofacies. Lithologies (~25.13–29.03 mbsf) consist of very open frameworks with branching coral colonies. Intervals displaying extensive development of microbialites are characterized by a more intense response in acoustic reflectivity. In Hole M0015A, the uppermost lithologies (23.0–25.13 mbsf; Cores 310-M0015A-23R through 26R) consist of coralgal-microbialite frameworks dominated by tabular and branching coral colonies. Striking images show cavities up to 90 cm in size and less intense (compared to Tiarei) microbialite encrusting (Fig. **F72**). Within these primary cavities, thrombolitic fabrics can often be observed "hanging" down from cavity ceilings. Formation electrical resistivity values gradually decrease from 2.6 to 0.9 m, where the lowest values can easily be correlated with cavities and the highest values can be correlated with intense microbialite encrustation. Sonic velocities (V_P) were very difficult to obtain; however, a range in V_P from ~1550 m/s (seawater in cavities) to 3531 m/s was recorded.

In the upper part of the last deglacial sequence (15.50-22.60 mbsf; Cores 310-M0015A-13R through 22R), formation resistivity slightly increases toward the top. V_P ranges from 1805 to 3718 m/s, and sonic Stoneley wave velocities are, on average, 1197 m/s. An optical image of a medium-sized cavity shows that this unit consists of thick branching coral assemblages (22.60–19.50 mbsf). The top 4 m shows an increase in thickness of the branches along with increasing intensity of microbialite encrusting.

From 15.50 mbsf upsection, a change in coral morphology can be observed. Large-sized cavities are absent, and microbialite lining of mostly tabular and locally encrusting corals can clearly be distinguished in the optical and acoustic images (e.g., 9.75–10.50 mbsf; Core 310-M0015A-9R). Formation resistivity values slightly decrease toward the top, where the

lowest values can be correlated with medium- to small-sized primary cavities.

Hole M0017A

Borehole conditions in Hole M0017A (56.45 mbsl) were extremely harsh, and it was difficult to deploy logging probes because the borehole was highly unstable and the relatively soft lithologies penetrated (overall low acoustic amplitude values in the ABI40 image log) resulted in very murky borehole fluids. Calipers show a large increase in borehole diameter at various intervals. Optical images are seriously affected by murky borehole waters; only at the top, just below the casing, is the quality reasonable. Acoustic images are not affected by this, and they are a high-quality visual representation (millimeter scale) of the lithologies cored (Fig. **F73**).

In Hole M0017A (Fig. **F74**), the last deglacial sequence can be divided into three intervals based on the downhole logging data:

- Interval 1 (31.55–29.75 mbsf; Cores 310-M0017A-18R through 19R) comprises assemblages of branching coral colonies with large-sized cavities. Formation electrical resistivity is low in this interval.
- Interval 2 (25.34–29.75 mbsf; Cores 310-M0017A-16R through 17R) has formation electrical resistivity values that gradually decrease from 3.0 (~29.45 mbsf) to 1.63 Ωm, where lowest values can easily be correlated with the cavities. Sonic velocities were very difficult to obtain; however, a clear decrease in V_P from 3603 to ~2173 m/s shows that analogs to the formation resistivity trend can be observed in this interval. Stoneley wave velocities could not be measured because at the end of the V_P run the sonic tool got stuck below the casing. During tool recovery, the wireline cable was badly damaged. At the time of logging operations, the temperature of the borehole fluid was ~27.3°C, pH values were ~7.82, and electrical conductivity was ~56.65 mS/cm (0.177 m). Comparing the acoustic reflectivity response in this interval with an ABI40 image of the same interval in Hole M0015A shows that this interval consists of a branching coral interval as well. Resistivity values increased from ~1.63 to 3.46 Ωm in the interval from 24.72 to 23.40 mbsf, marking the transition from the middle to the upper part of the interval.
- Interval 3 (13.50–23.40 mbsf; Cores 310-M0017A-10R through 15R) shows a gradual decrease in resistivity values from 3.46 to 1.92 Ωm. The temperature of the borehole fluid decreased from ~27.13°C, pH values were ~7.82, and electrical conductivity was ~56.65 mS/cm (0.177 m). V_P decreased at first from 3521 to 2032 m/s (24.03–21.64 mbsf). From 21.20 mbsf uphole, V_P ranged from 2024 to 3000 m/s over relatively short intervals. The upper part of Hole M0017B shows a more homogeneous acoustic reflectivity response, indicating that pronounced differences in lithologic components in the last deglacial sequence and large-scale cavities are absent.

Synthesis of geophysical downhole logging at Maraa

Wireline logging operations at Maraa sites produced nearly complete downhole coverage of the last deglacial sequence from 41.65 to 102 mbsl. Tools have different data coverage in various holes (see the "Downhole logging" sections in the individual site chapters). In Figure **F75,** borehole televiewer images, natural radioactivity logs (total counts), and electrical resistivity logs are plotted in meters below sea level. In each of the logged boreholes, the boundary between the last deglacial sequence and the older Pleistocene sequence is indicated. The depth below present-day sea level of the top of the older Pleistocene sequence is highly variable and therefore indicates a rugged morphology prior to the development of the last deglacial sequence. Resistivity does not show any direct signal, but spectral gamma ray logs indicate a significant increase of counts in the older Pleistocene sequence (Holes M0005D and M0007A). Caliper, borehole fluid characterization, and acoustic tools all contain particular information on parameters for specific intervals and lithologies.

References

Raymer, L.L., Hunt, E.R., and Gardner, J.S., 1980. An improved sonic transit time-to-porosity transform. *Trans. SPWLA 21st Annu. Log. Symp.,* Pap. P.

Wyllie, M.R.J., Gregory, A.R., and Gardner, L.W., 1956. Elastic wave velocities in heterogeneous and porous media. *Geophysics,* 21(1):41–70. **doi:10.1190/1.1438217**

Publication: 4 March 2007
MS 310-106

Figure F1. Rudstone with *Halimeda* segments and coral fragments encrusted with coralline algal crusts (Unit I; interval 310-M0017A-12R-1, 138–146 cm).

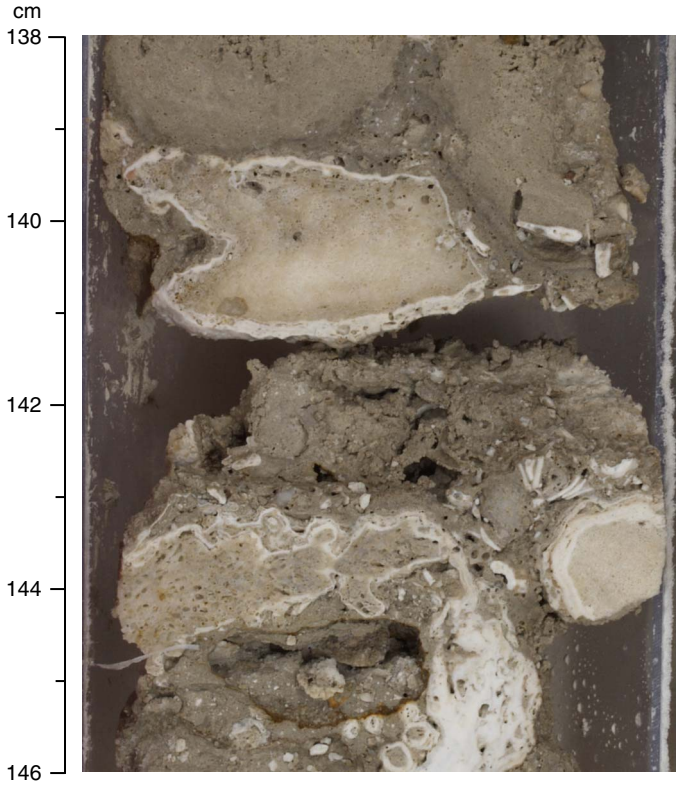

Figure F2. Rubble of encrusting *Leptastrea* and robust branching *Pocillopora* (Unit I; interval 310-M0018A-21R-1, 18–32 cm). Some fragments are fresh and others exhibit bioeroded surfaces.

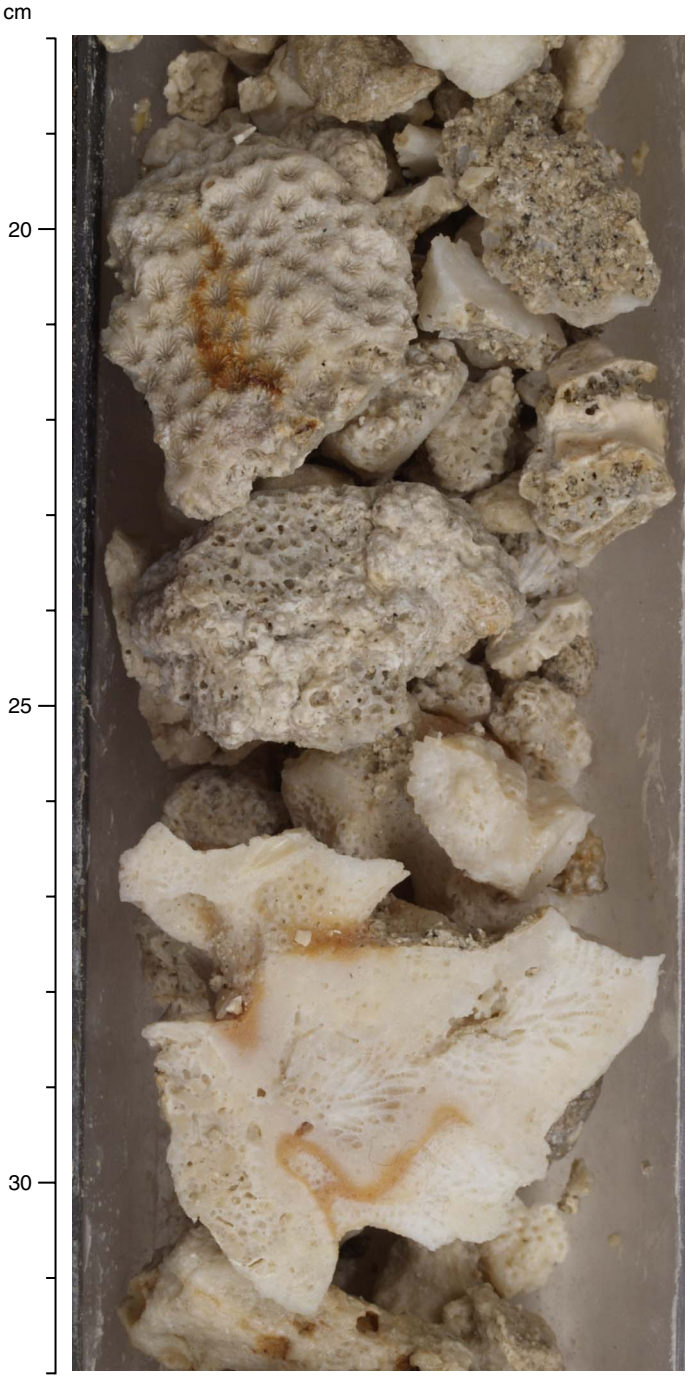

Figure F3. Top of Subunit IA (Subunit IA; interval 310-M0015B-1R-1, 0–10 cm). Note extensive bioerosion of sediment.

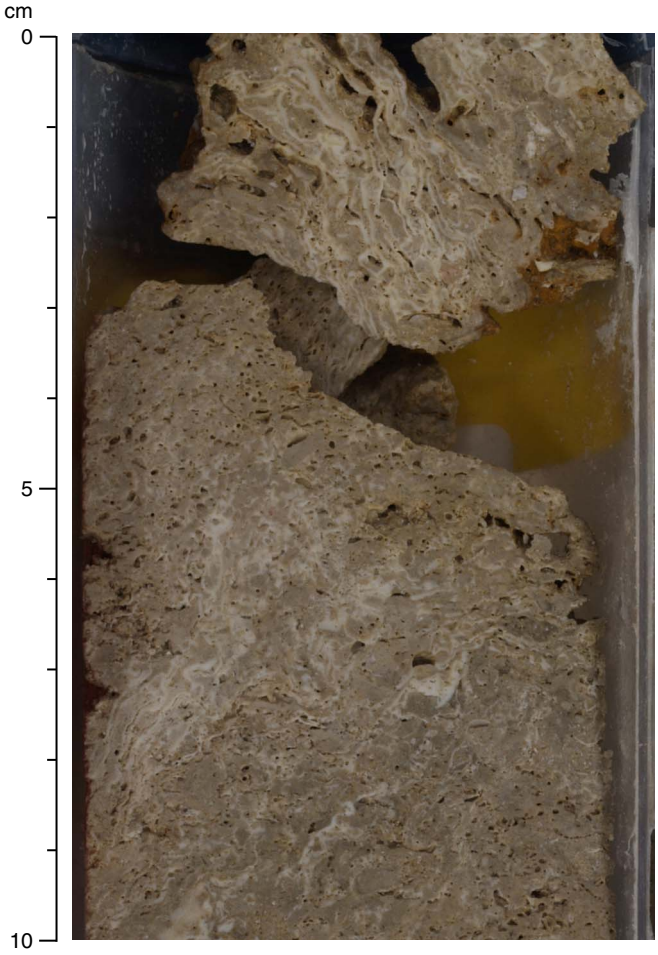

Figure F4. Abundant thin coralline algal crusts at the top of the subunit are extensively bioeroded (Subunit IA; interval 310-M0018A-1R-1, 0–6 cm). Note shells of boring bivalves.

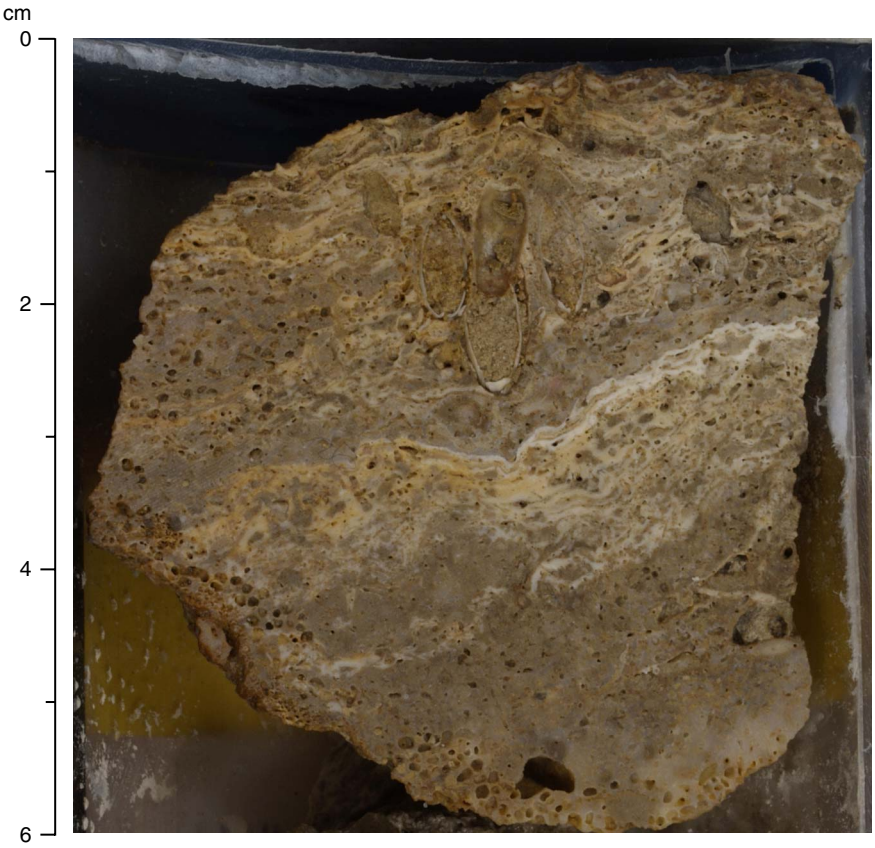

Figure F5. Coralgal bindstone with interlayered coralline algae and encrusting colonies of *Porites* and agaricids (Subunit IA; interval 310-M0015B-1R-1, 20–40 cm).

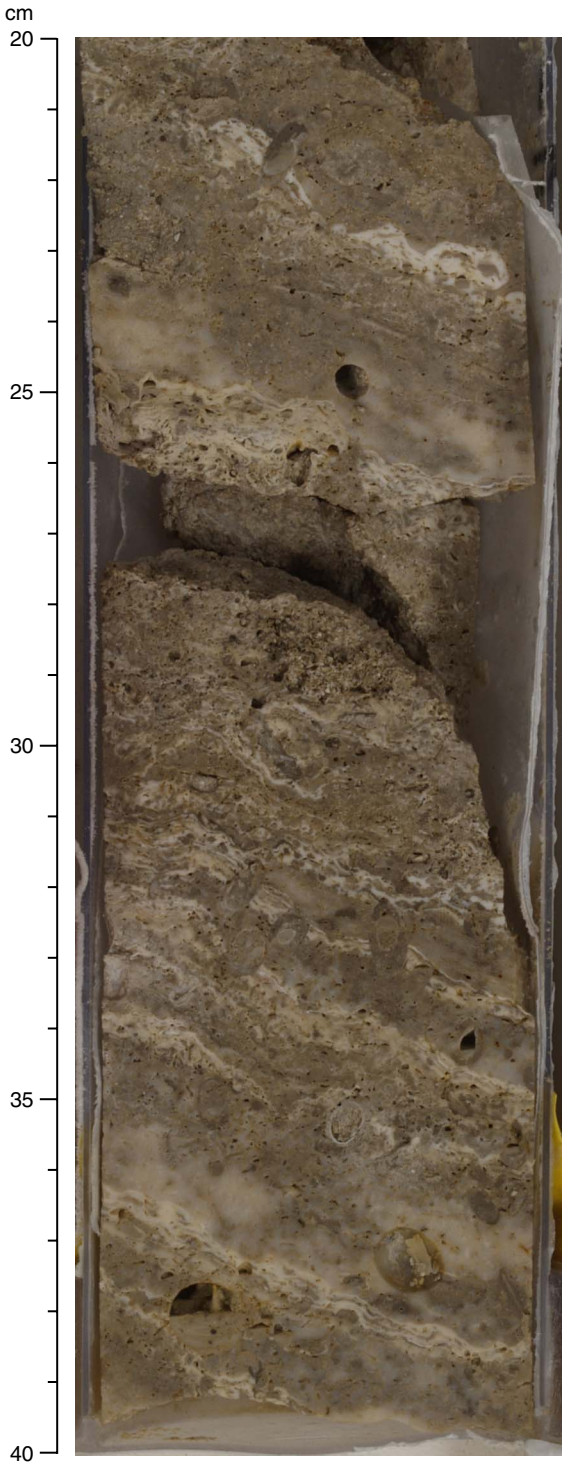

Figure F6. Interlayered encrusting coralline algae (Subunit IA; interval 310-M0015B-2R-1, 35–50 cm). Note intense bioerosion of coral colonies.

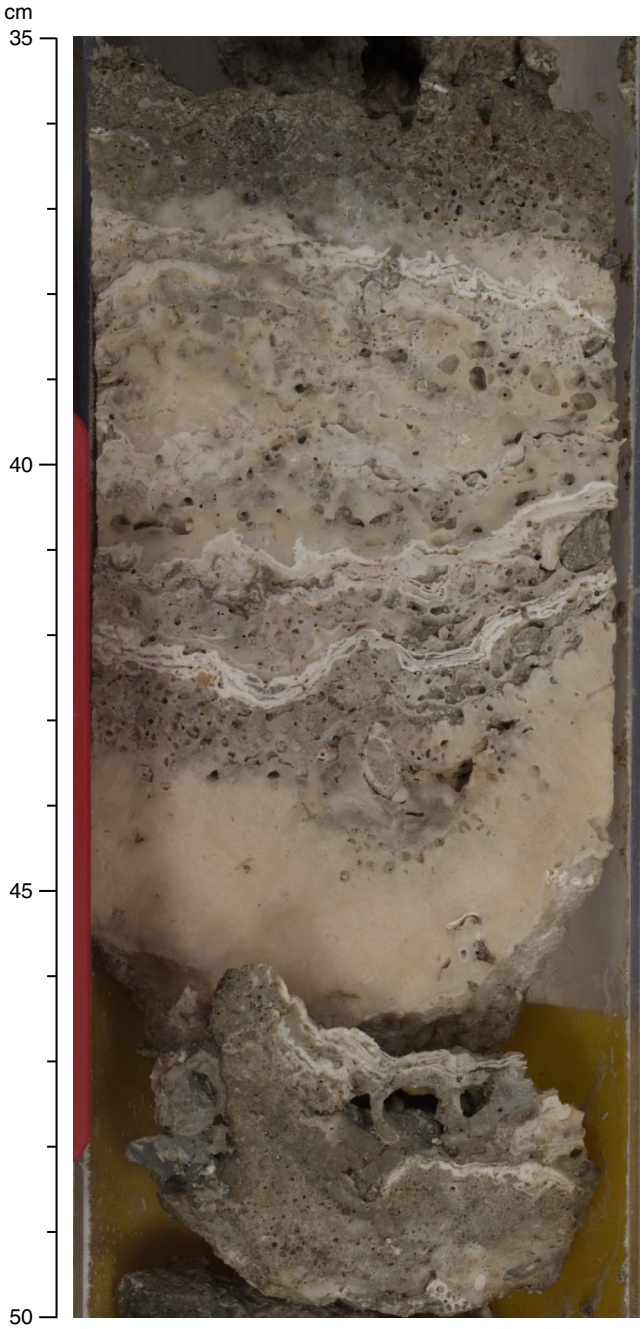

Figure F7. Encrusting colonies of *Montipora* covered with coralline algal crusts (Subunit IC; interval 310-M0016A-7R-1, 40–50 cm).

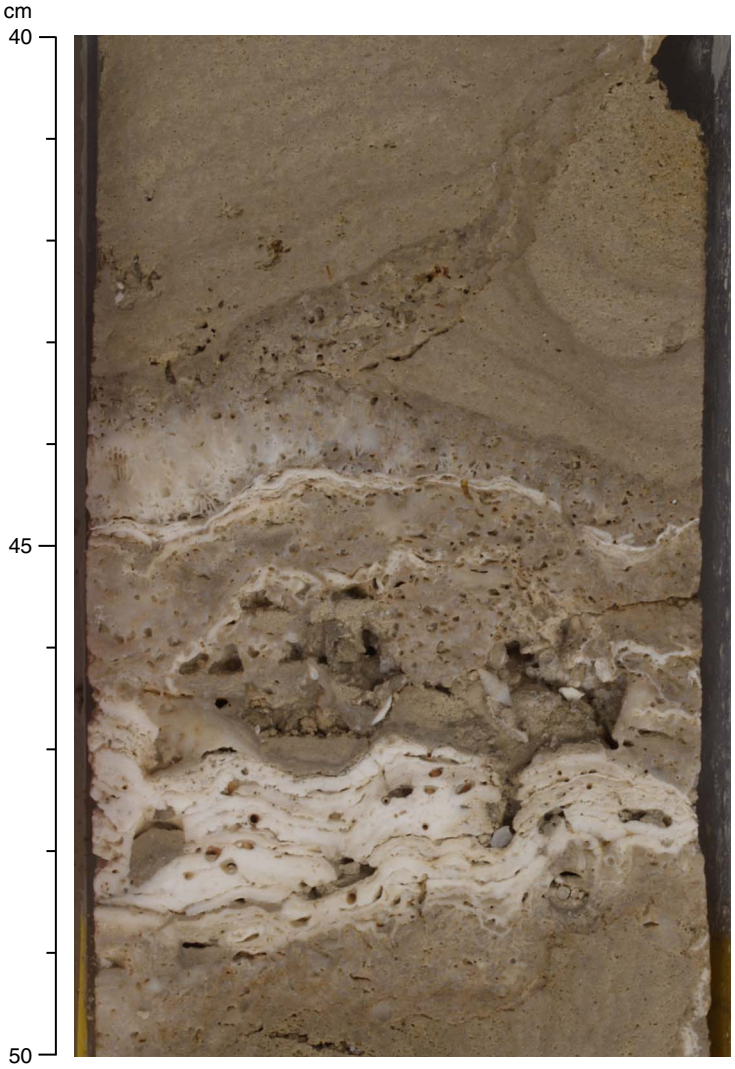

Figure F8. Encrusting colonies of *Montipora* and *Porites* encrusted with multiple thin crusts of coralline algae (Subunit IA; interval 310-M0017A-3R-CC, 1–10 cm).

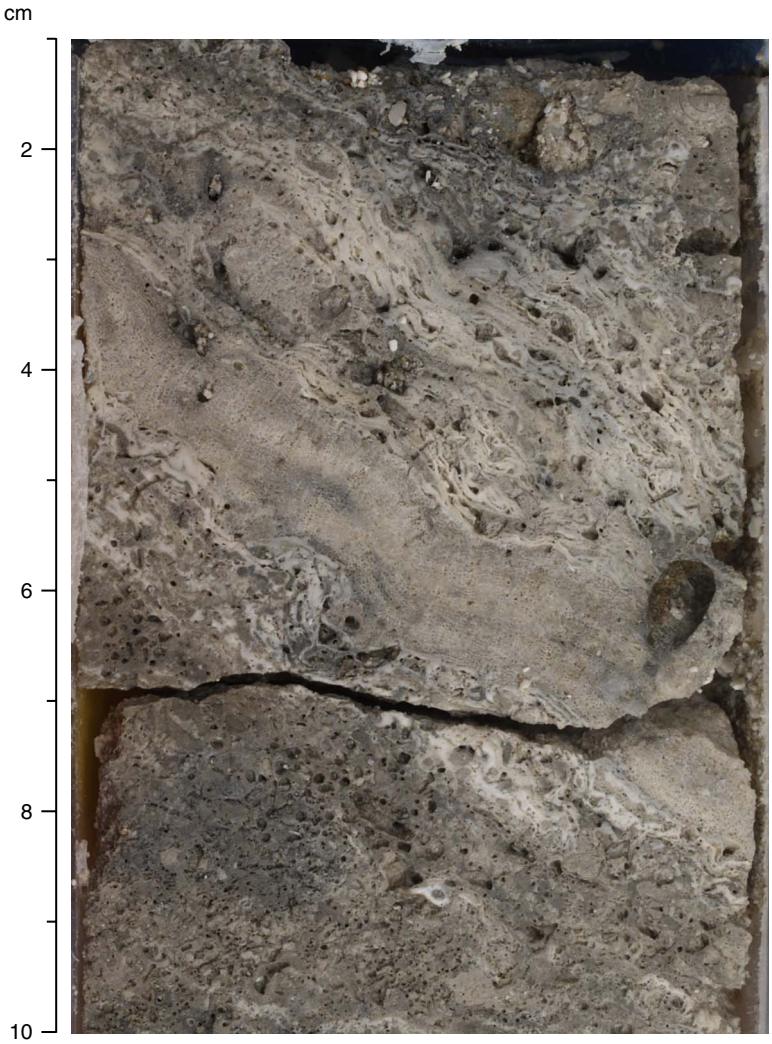

Figure F9. Multiple layers of encrusting agariciids (*Pavona*?) interlayered with coralline algal crusts (Subunit 1A; interval 310-M0017A-4R-1, 7–17 cm). Note strong bioerosion in corals.

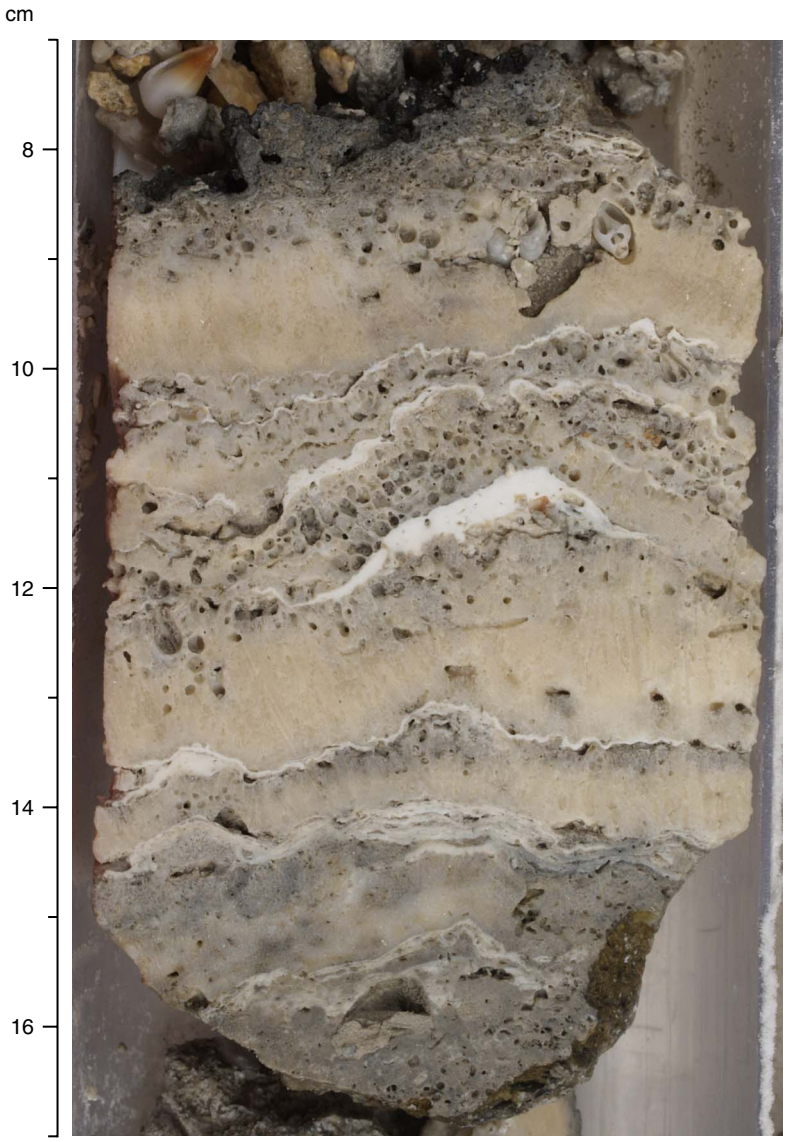

Figure F10. Interlayered encrusting agariciids (*Pavona*?) and coralline algae (Subunit IA; interval 310-M0018A-1R-1, 16–29 cm).

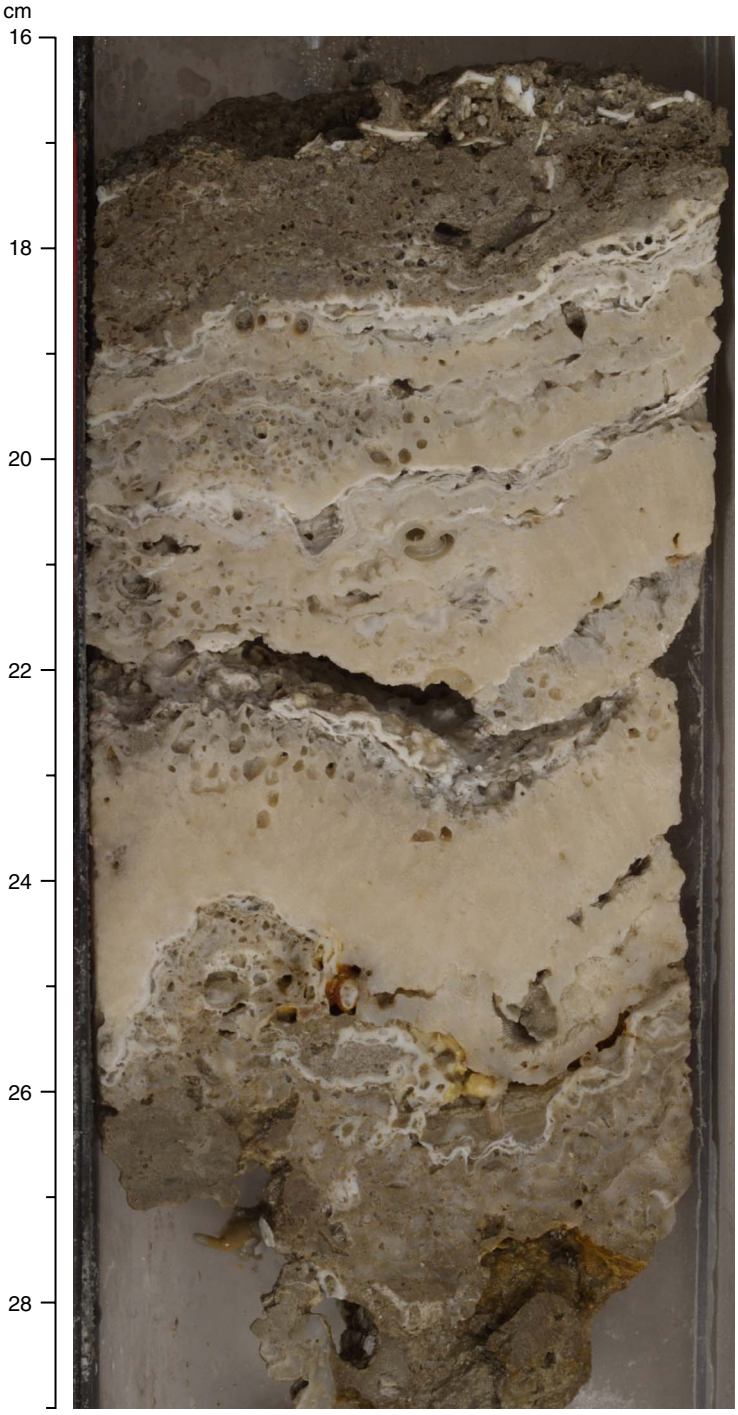

Figure F11. Interlayered encrusting coralline algae and encrusting corals (agariciids, *Montastrea,* and *Porites*) (Subunit IA; interval 310-M0018A-1R-1, 79–90 cm).

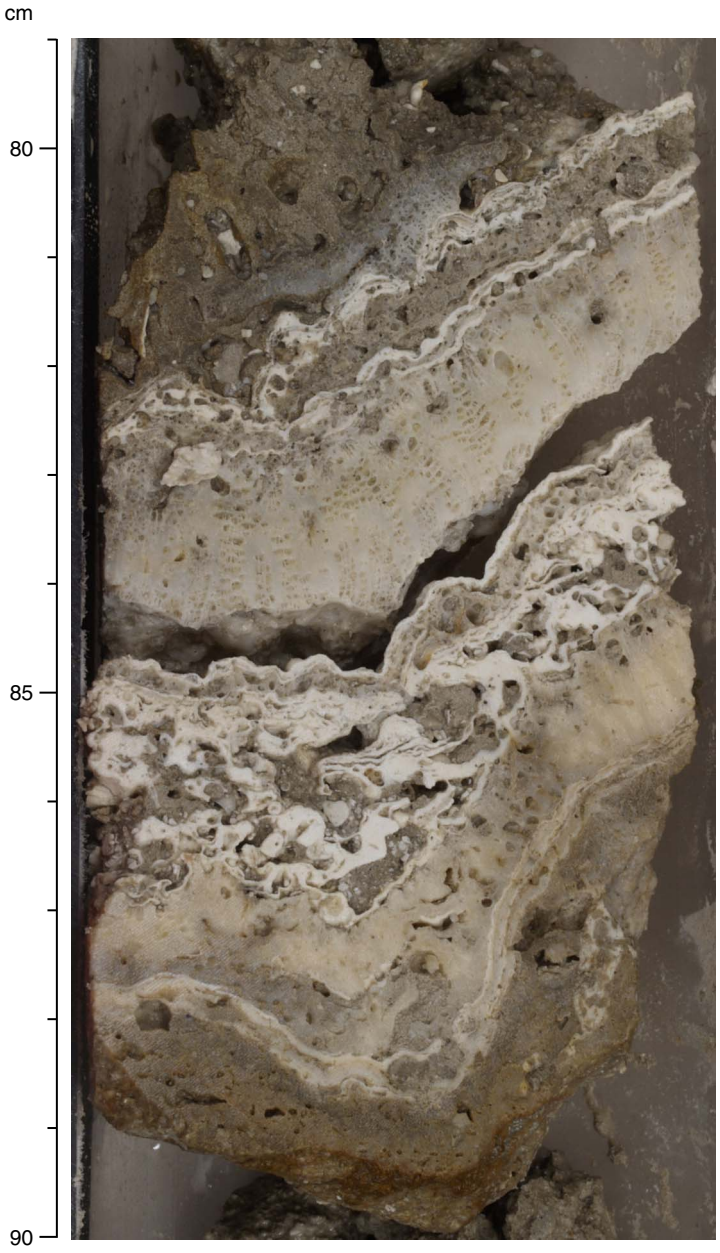

Figure F12. Framework of encrusting *Porites* and agariciids, thick multiple layers of encrusting coralline algae, and microbialites (Subunit IA; interval 310-M0018A-3R-1, 60–80 cm).

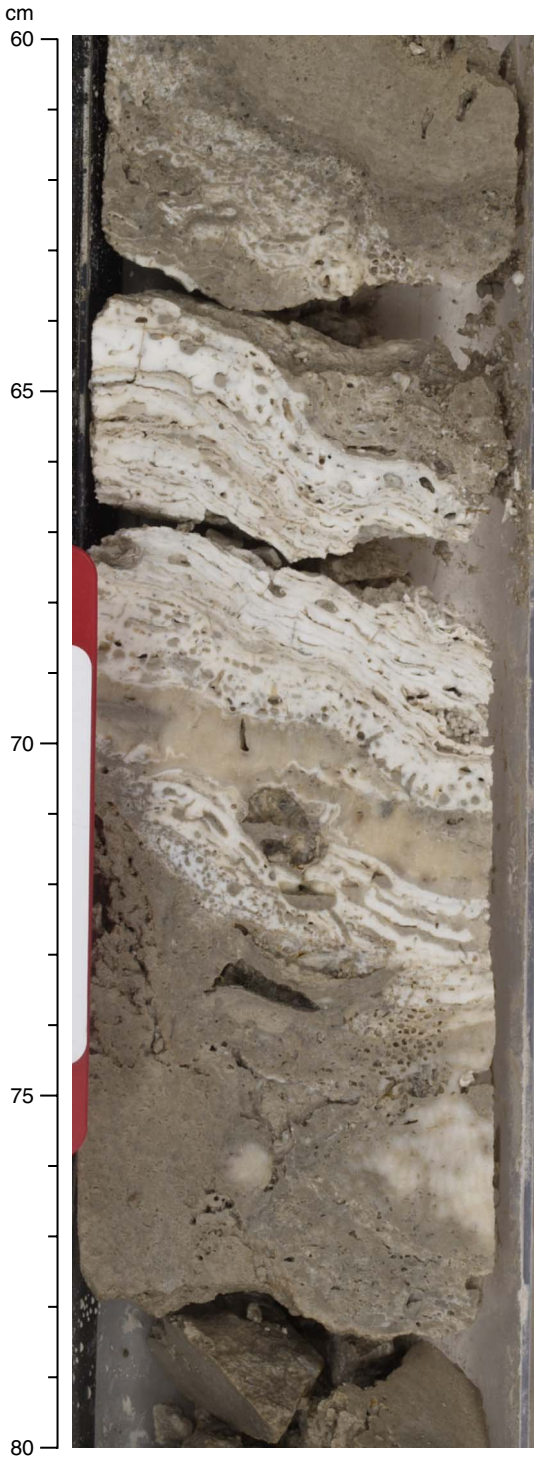

Figure F13. Encrusting *Montipora* and tabular *Acropora* colonies (Subunit IA; interval 310-M0018A-7R-1, 70–80 cm).

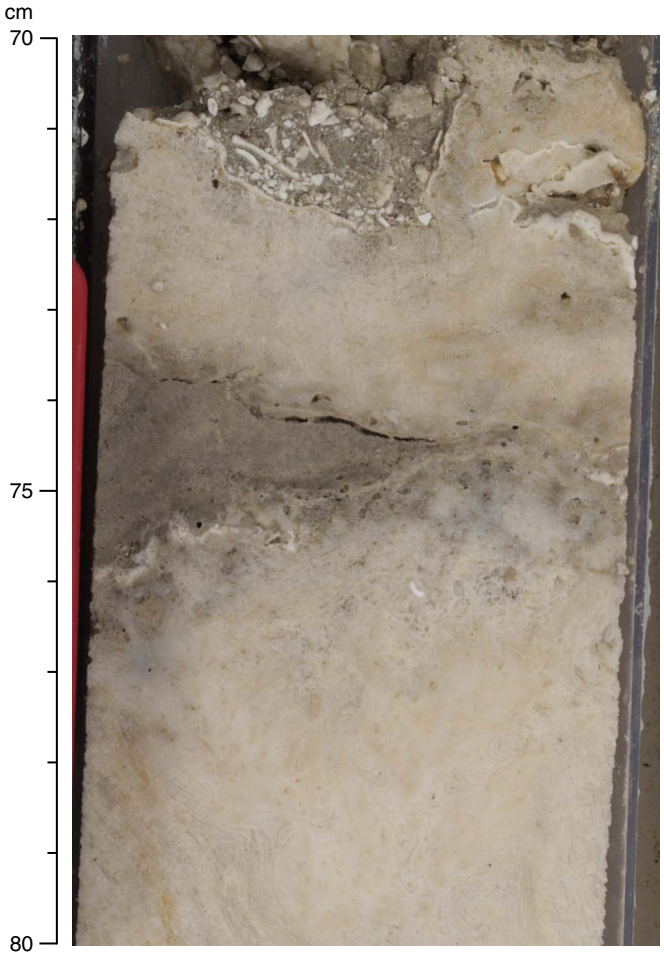

Figure F14. Coralgal-microbialite framework with thrombolitic microbialite crusts (Subunit IB; interval 310-M0015A-7R-1, 20–35 cm).

Figure F15. Tabular colonies of *Acropora* encrusted with coralline algae (Subunit IB; interval 310-M0015A-10R-1, 70–80 cm).

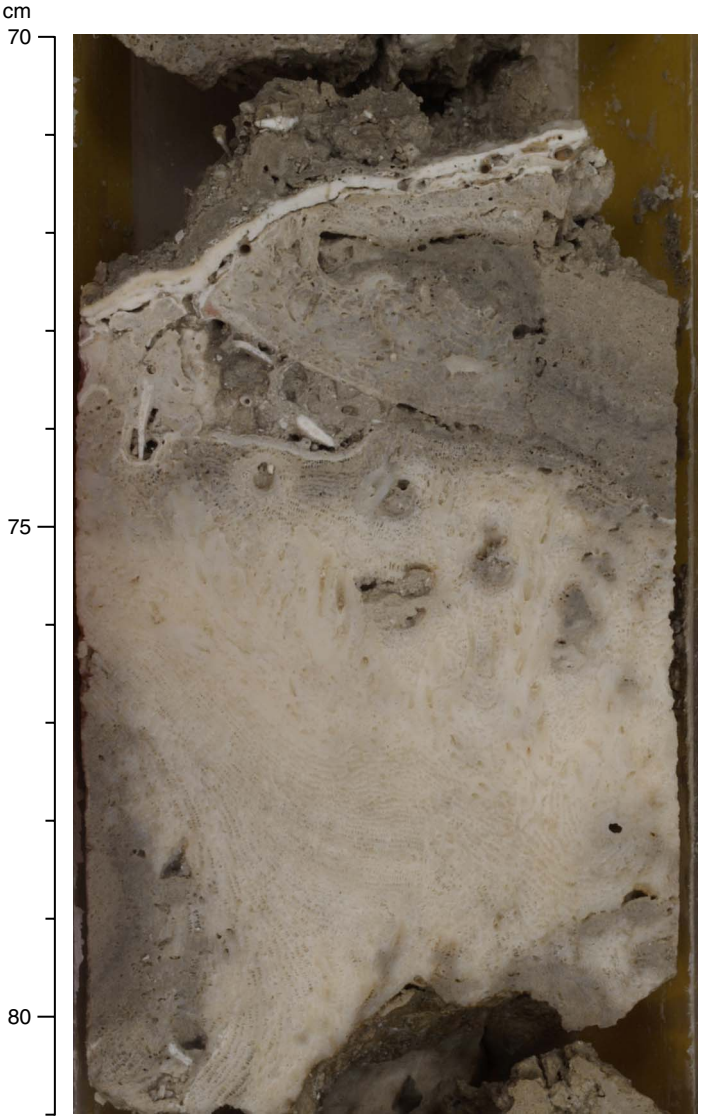

Figure F16. Coral framework composed of tabular *Acropora* encrusted with thick coralline algal crusts followed by laminated and dendritic microbialites (Subunit IB; interval 310-M0015B-19R-1, 53–69 cm).

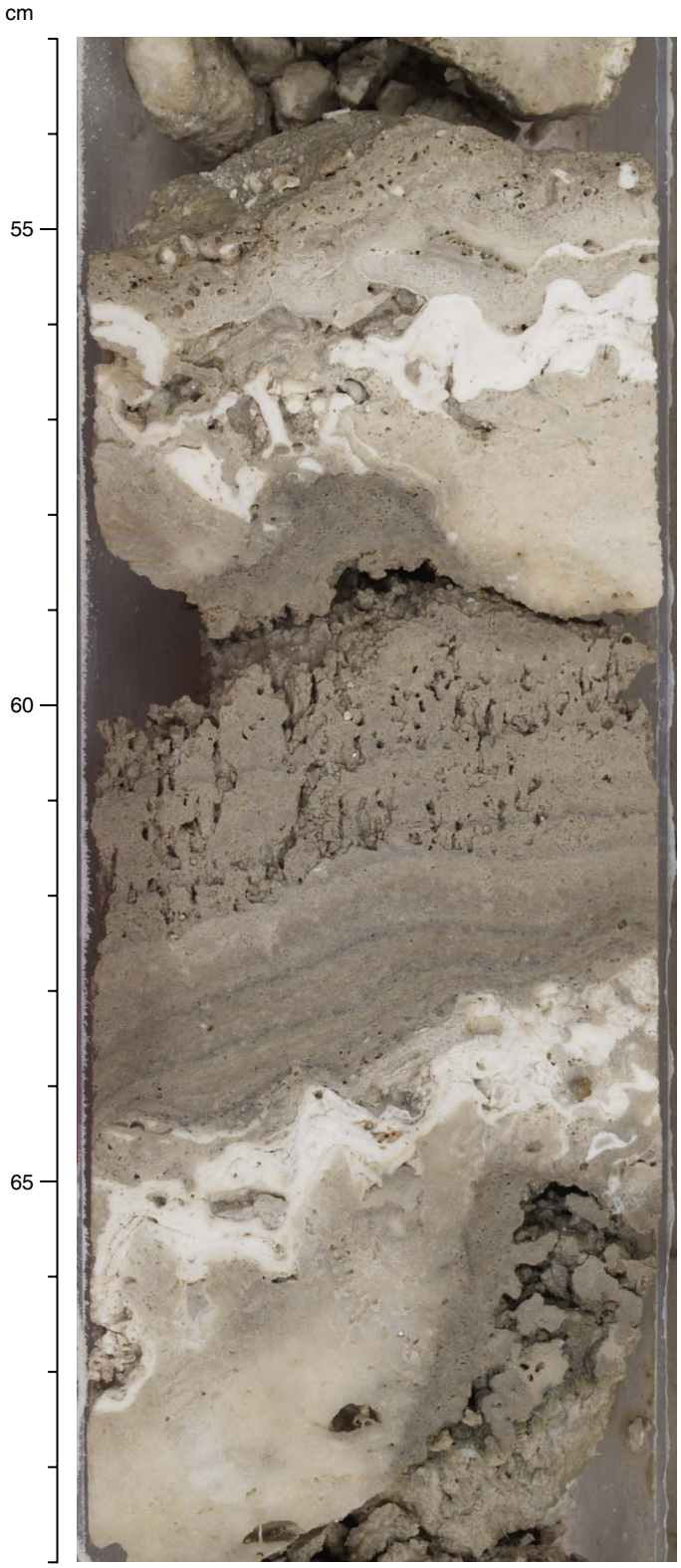

Figure F17. Interlayered encrusting *Montipora,* tabular *Acropora,* and coralline algae (Subunit 1B; interval 310-M0017A-12R-1, 57–65 cm).

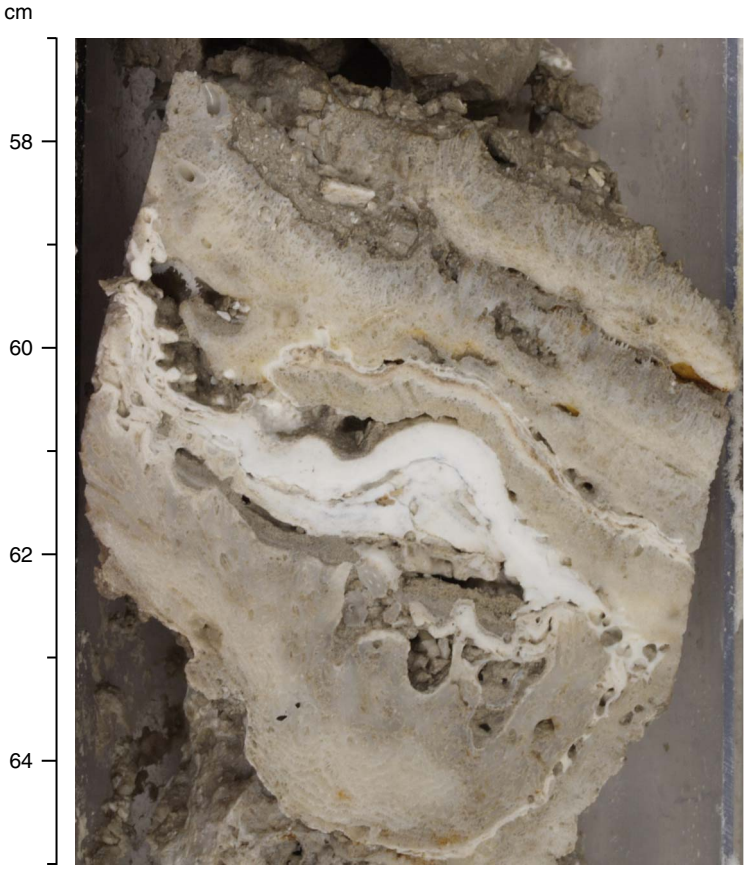

Figure F18. Encrusting colonies of *Porites* in microbialite-dominated interval (Subunit IB; interval 310-M0015A-9R-1, 28–40 cm).

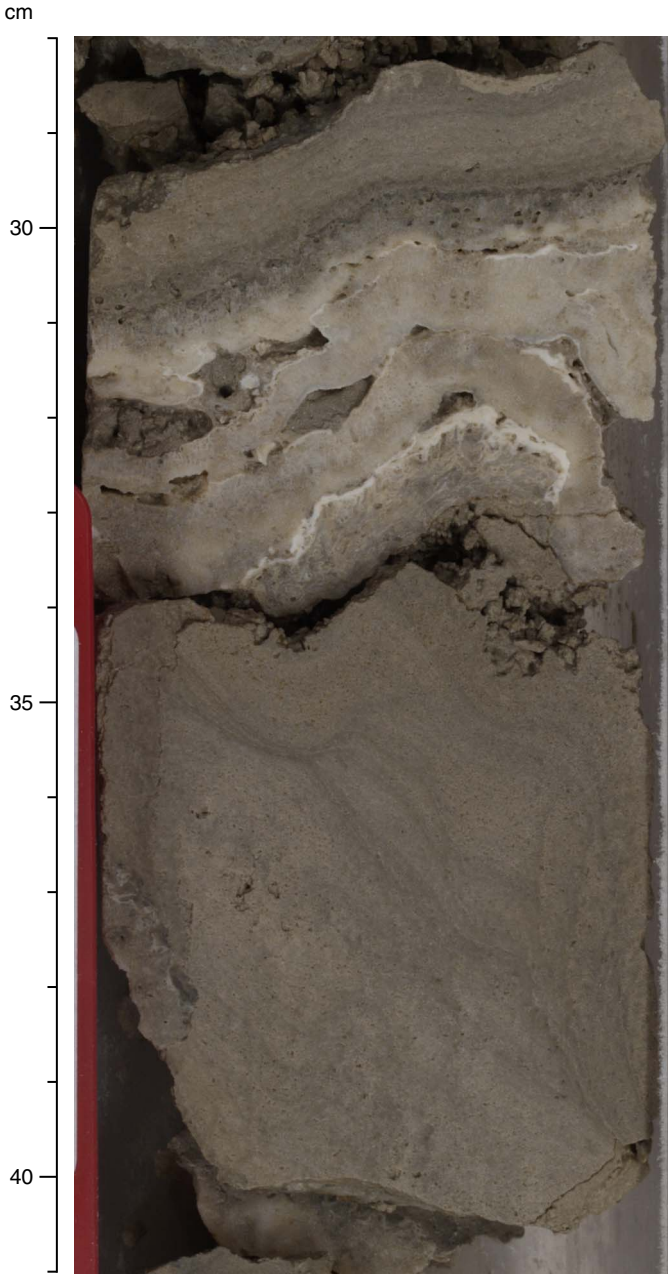

Figure F19. Coralgal framework dominated by branching *Porites* encrusted with multiple thin coralline algal crusts (Subunit IB; interval 310-M0015B-9R-1, 0–12 cm).

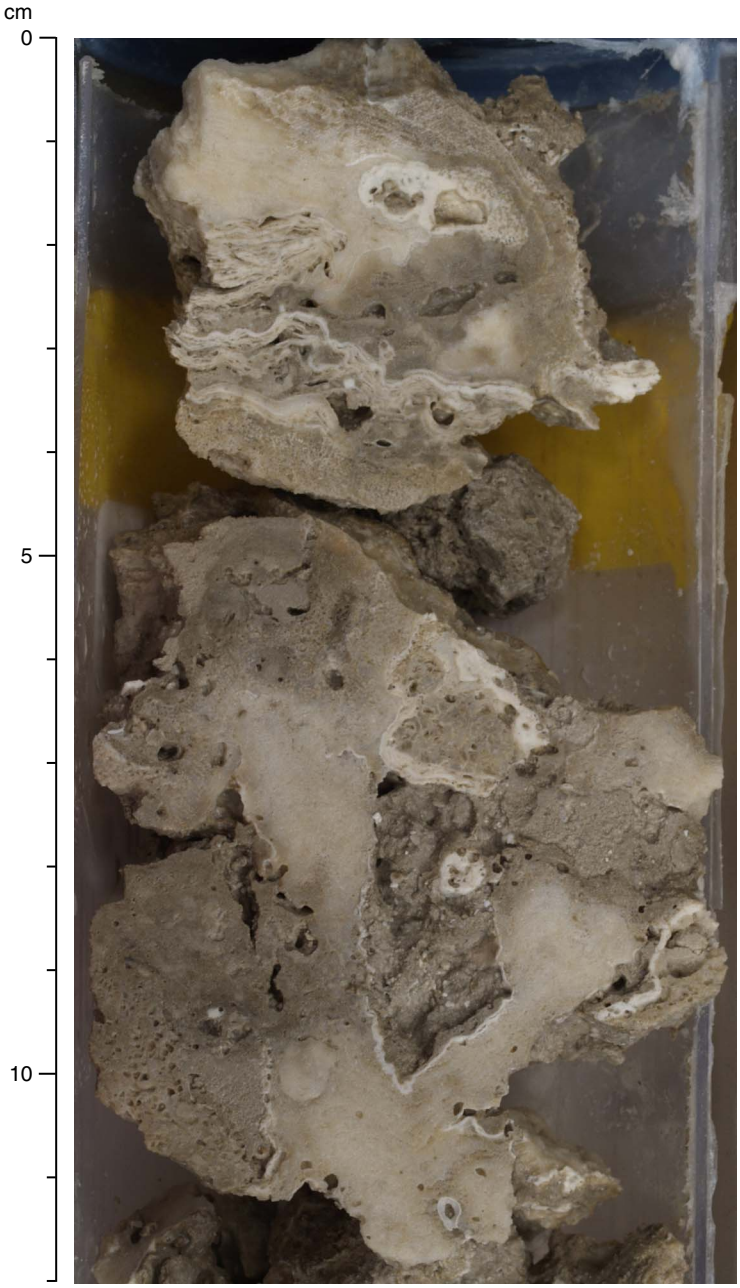

Figure F20. Massive colony of *Porites* (Subunit 1B; interval 310-M0017A-9R-1, 10–17 cm).

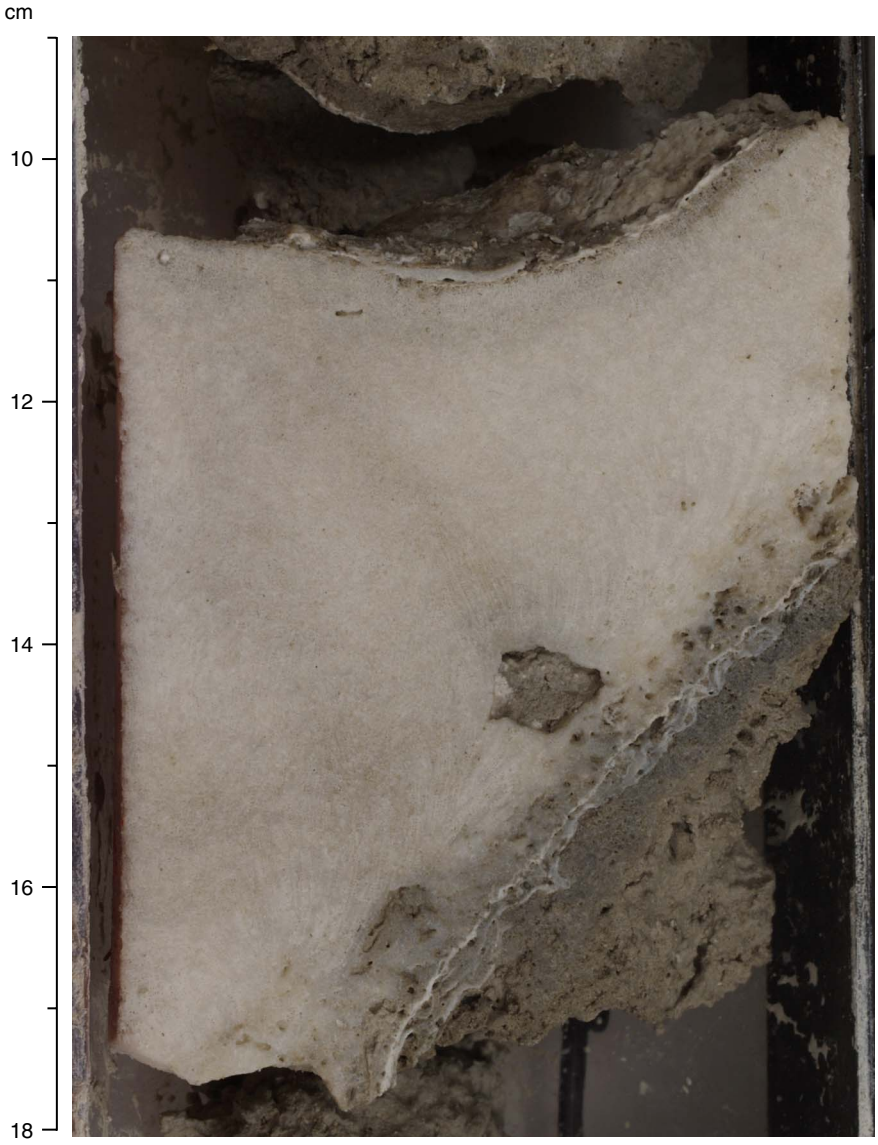

Figure F21. Interlayered encrusting corals (*Lepastrea,* agariciids, *Porites,* and *Montipora*) (Subunit 1B; interval 310-M0017A-14R-1, 87–103 cm).

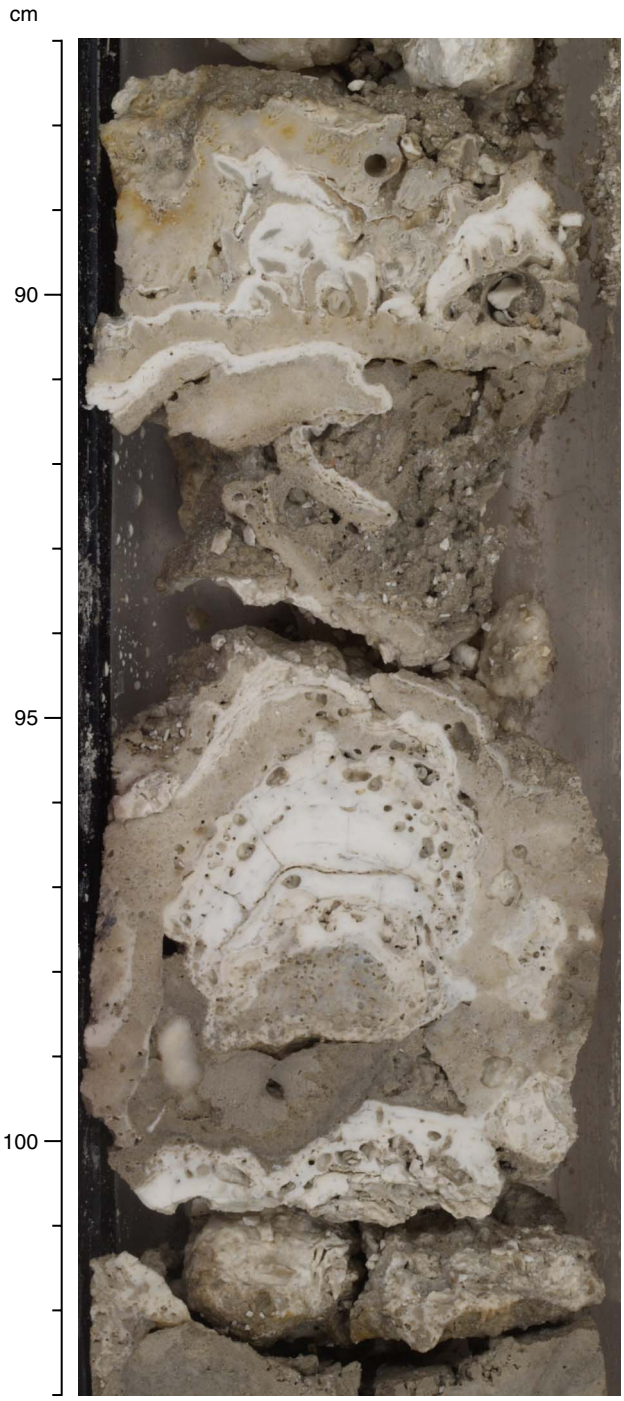

Figure F22. Robust branching colonies of *Pocillopora* (Subunit IB; interval 310-M0015B-21R-1, 85–105 cm).

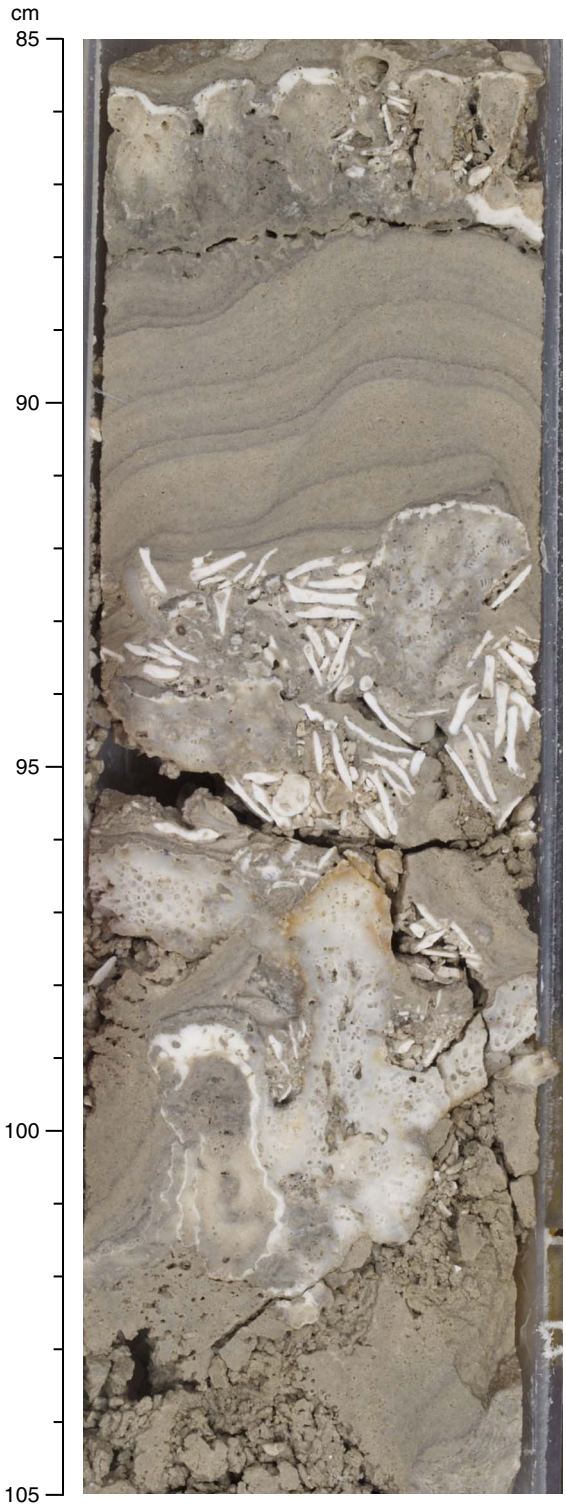

Figure F23. Robust branching *Pocillopora* framework with *Halimeda*-bearing sediment in primary vugs (Subunit 1B; interval 310-M0017A-13R-1, 21–36 cm).

Figure F24. Thick coralline algal crust on tips of tabular *Acropora* branches (Subunit 1B; interval 310-M0017A-13R-1, 3–12 cm).

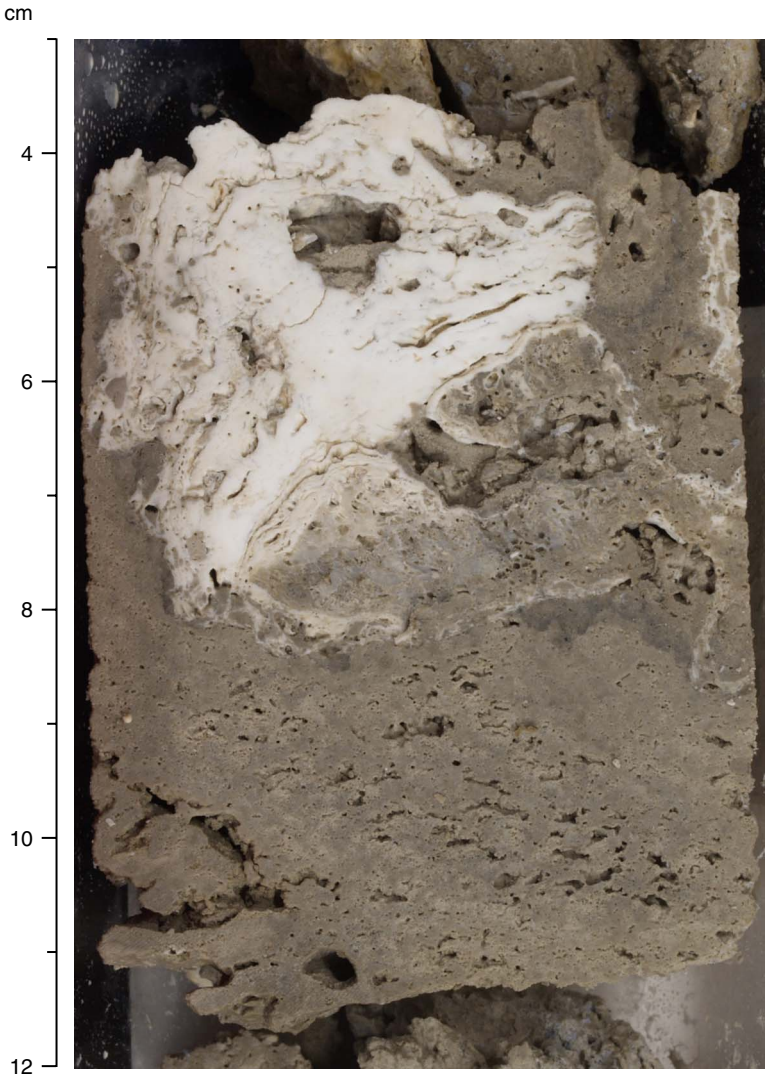

Figure F25. Thick laminated microbialite crusts on top of algal-covered coral (Subunit 1B; interval 310-M0017A-16R-1, 87–98 cm). Note *Halimeda* segments engulfed in the microbialites.

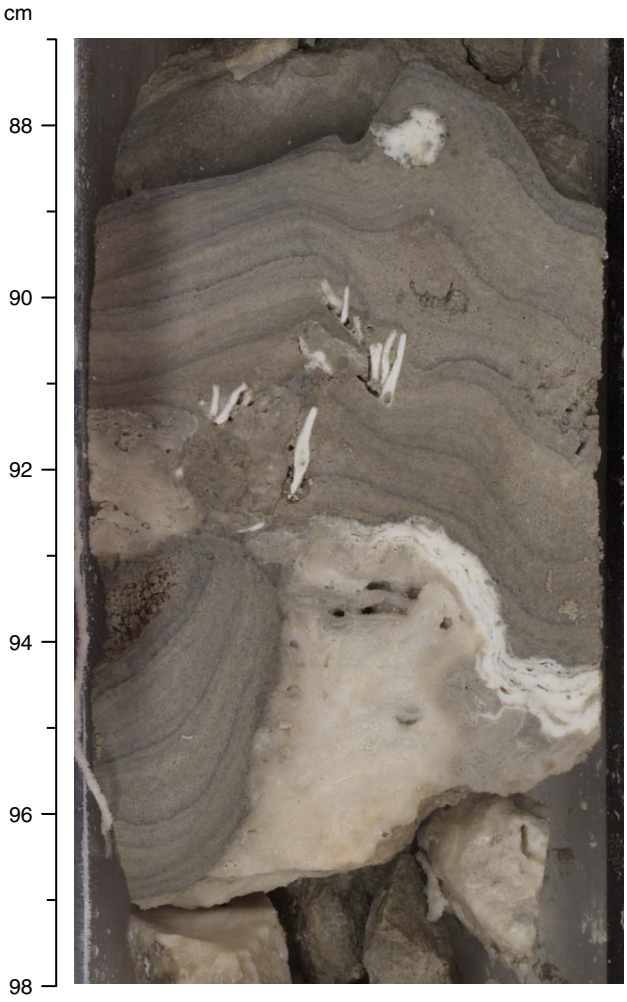

Figure F26. Coral-microbialite framework (Subunit IB; interval 310-M0015B-21R-1, 84–92 cm). Note tabular colonies of *Acropora* in growth position; tips of branches are covered with coralline algal crusts.

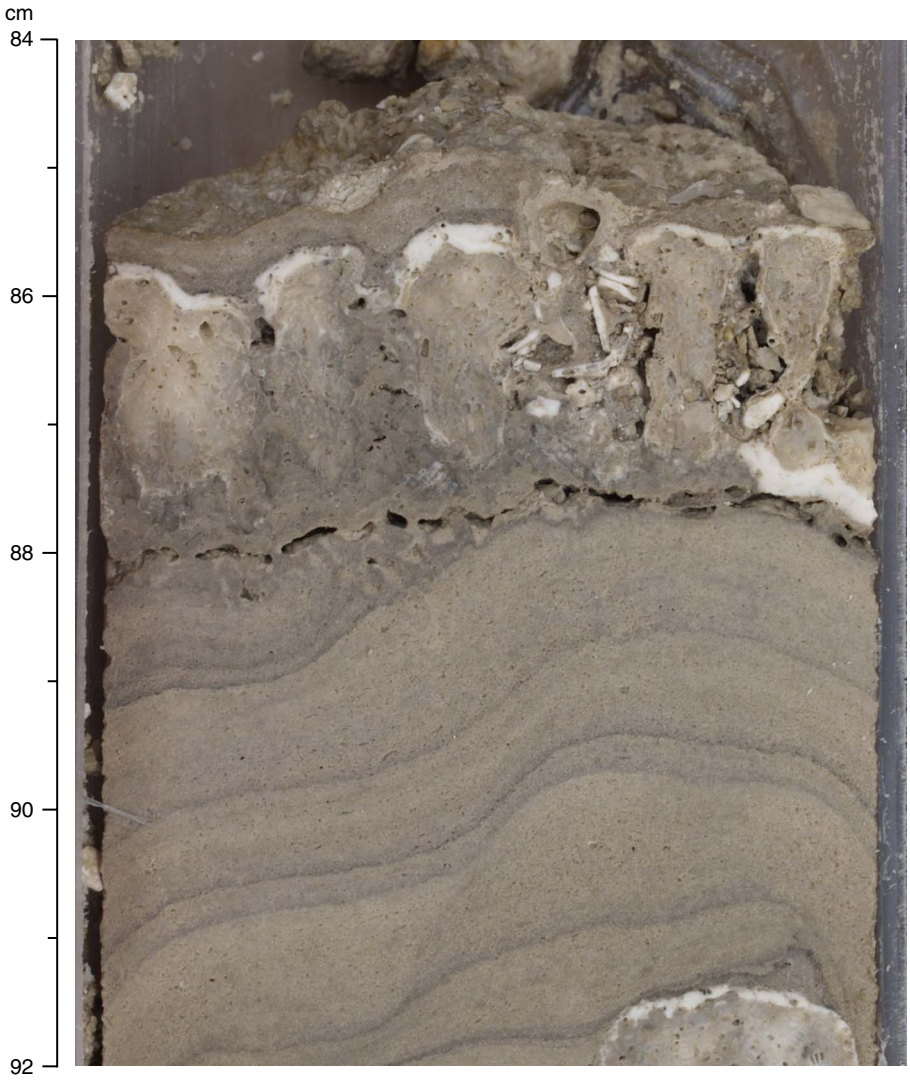

Figure F27. Coral framework of branching *Porites*. Tips of branches are covered with thick coralline algal crusts (Subunit IC; interval 310-M0015A-20R-1, 55–68 cm). Note primary pore space.

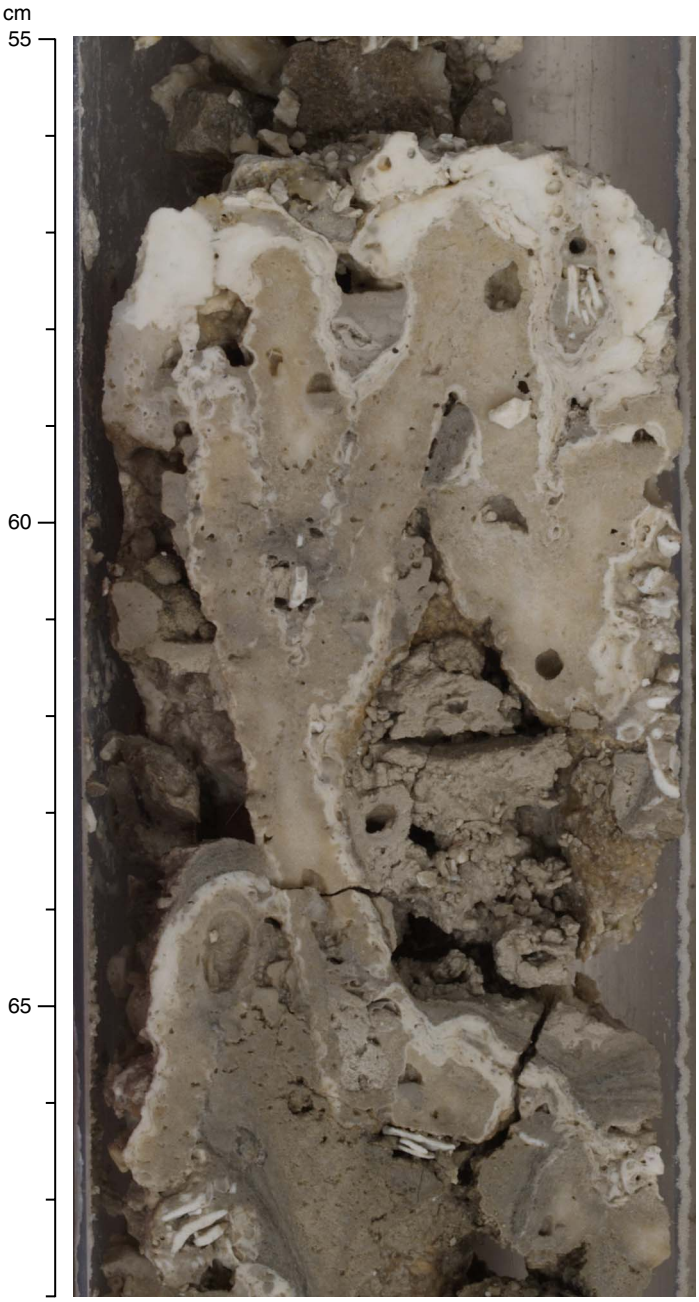

Figure F28. Coralgal-microbialite framework (Subunit IC; interval 310-M0015A-30R-1, 74–89 cm). Note thick coralline algal crusts on tips of branches of *Porites*.

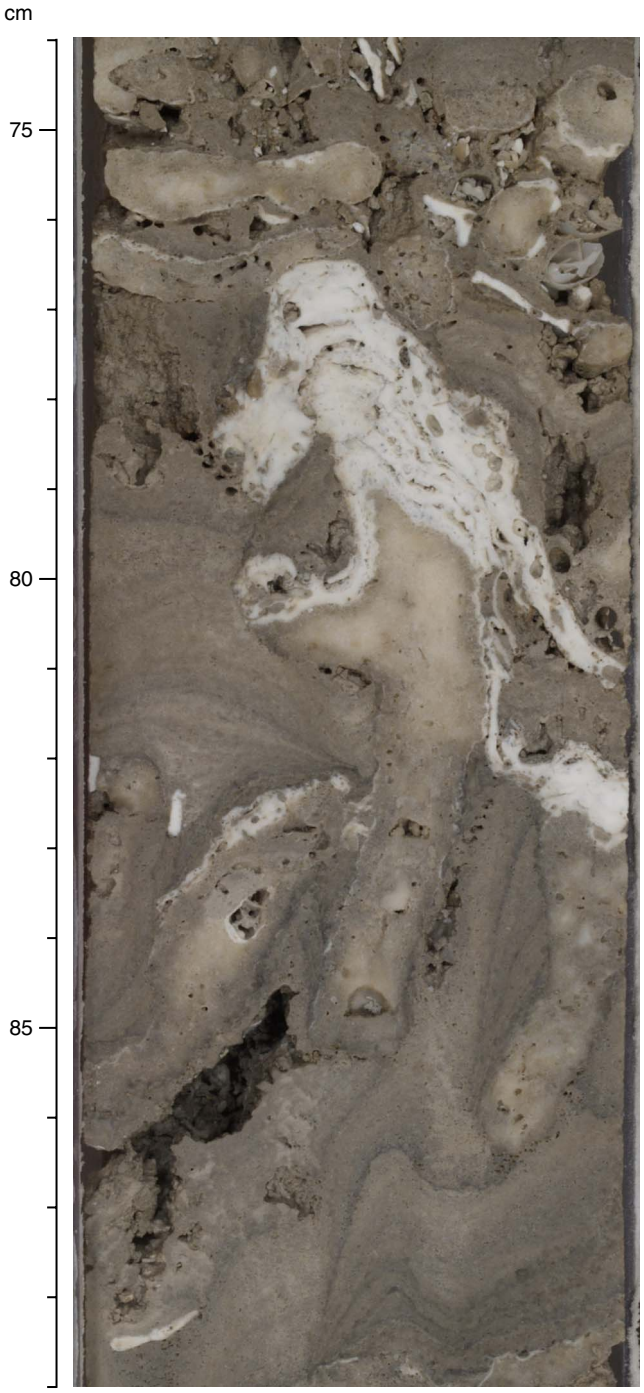

Figure F29. Coralgal framework dominated by branching *Porites* (Subunit IC; interval 310-M0015B-33R-1, 112–139 cm). Sediment in primary vugs contains *Halimeda* segments.

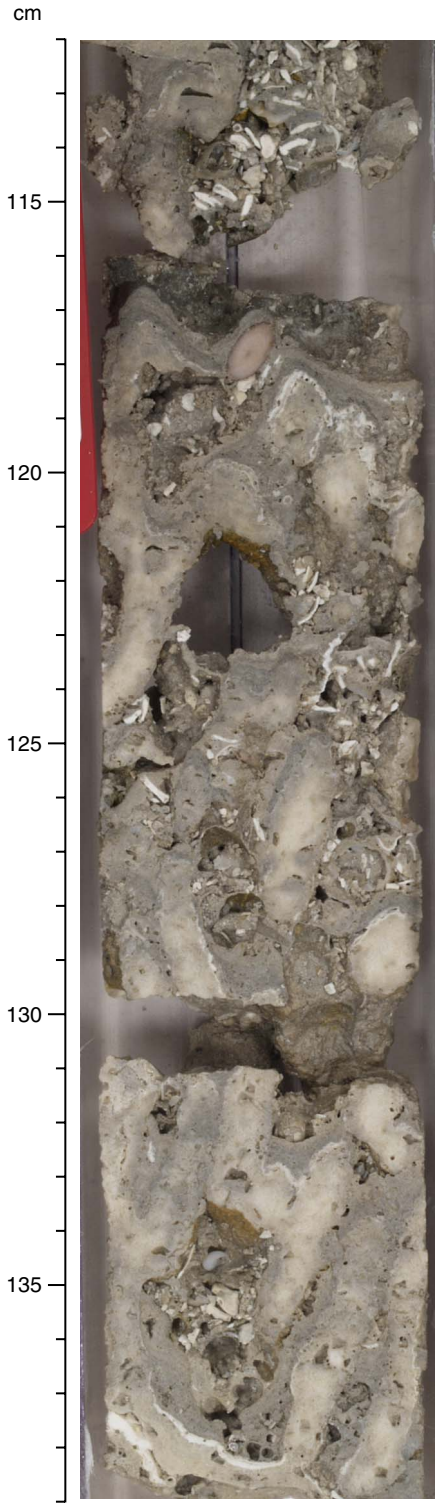

Figure F30. Coral framework composed of branching *Porites* associated with thin encrusting coralline algae and laminated to thrombolitic microbialite crusts (Subunit IC; interval 310-M0015B-34R-1, 13–34 cm).

Figure F31. Coral framework of branching *Porites* encrusted with thin coralline algal crusts and laminated to thrombolitic microbialites (Subunit IC; interval 310-M0016B-11R-1, 20–34 cm). Primary vugs are partly filled with sediment, including *Halimeda* segments.

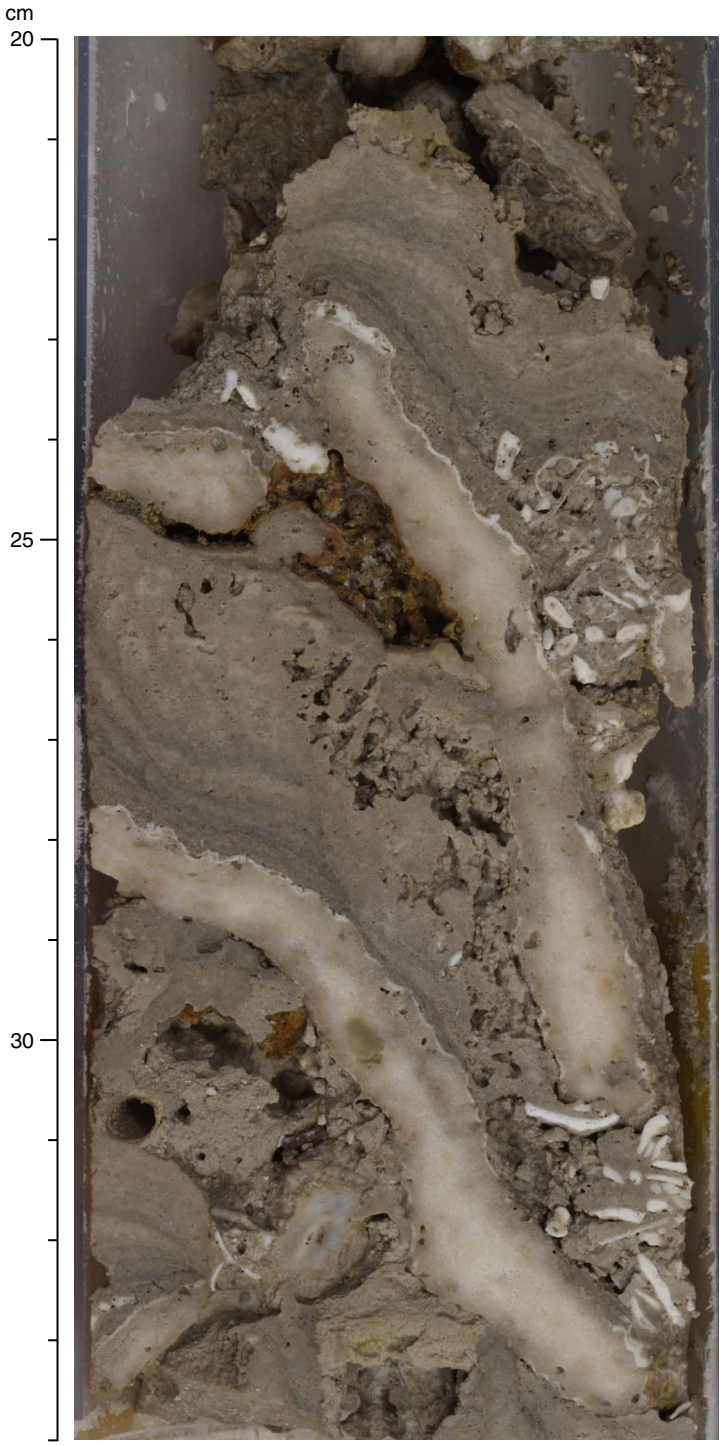

Figure F32. Framework of branching and encrusting *Porites* with thick coralline algal crusts on upper surfaces and subsequent thin microbialite crusts (Subunit 1C; interval 310-M0017A-18R-1, 77–91 cm). Primary vugs are filled with *Halimeda*-bearing sediment.

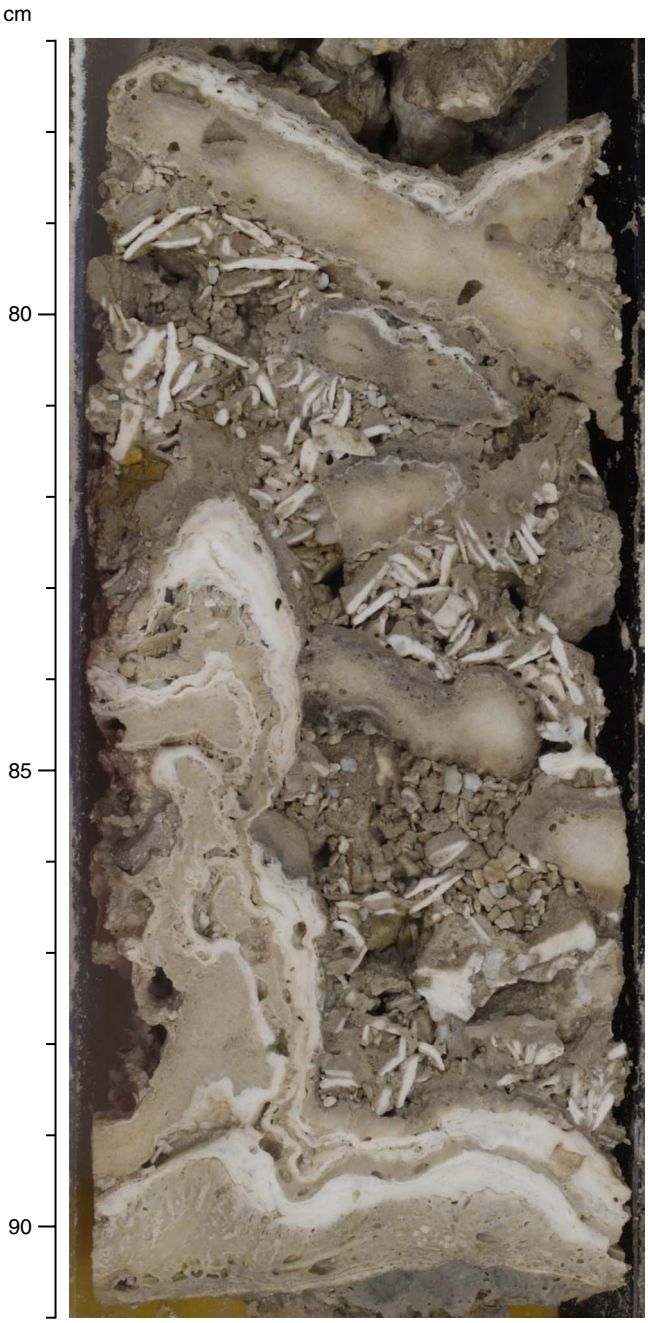

Figure F33. Coralgal framework (Subunit IC; interval 310-M0015A-23R-1, 18–42 cm). Encrusting colonies of *Porites* and *Montipora* are encrusted with coralline algae; last stage of encrustation is microbialite.

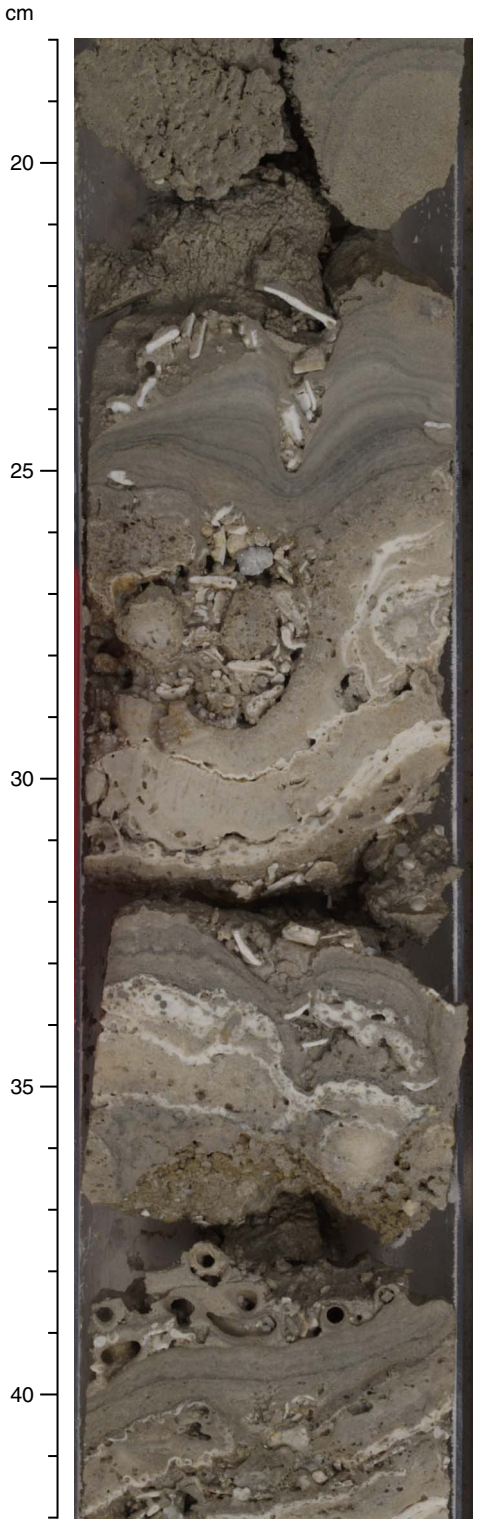

Figure F34. Coralgal framework mainly composed of tabular *Acropora* with thick microbialite crusts (Subunit IC; interval 310-M0015A-26R-1, 8–31 cm).

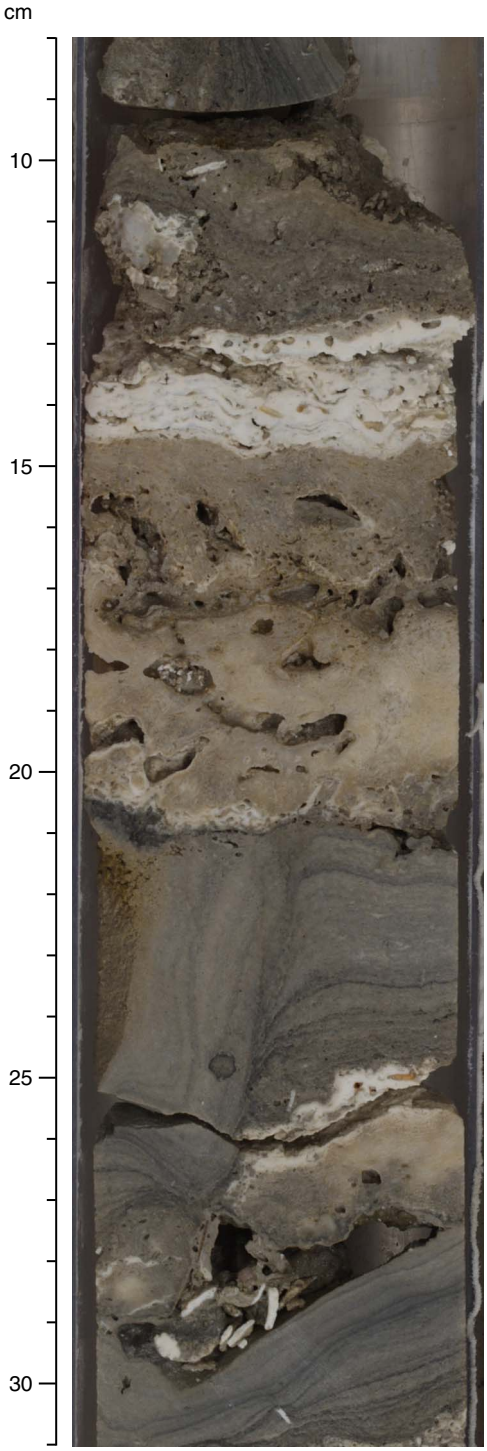

Figure F35. Robust branching *Pocillopora* framework with dominant laminated microbialite crusts (Subunit IC; interval 310-M0015B-25R-1, 40–65 cm).

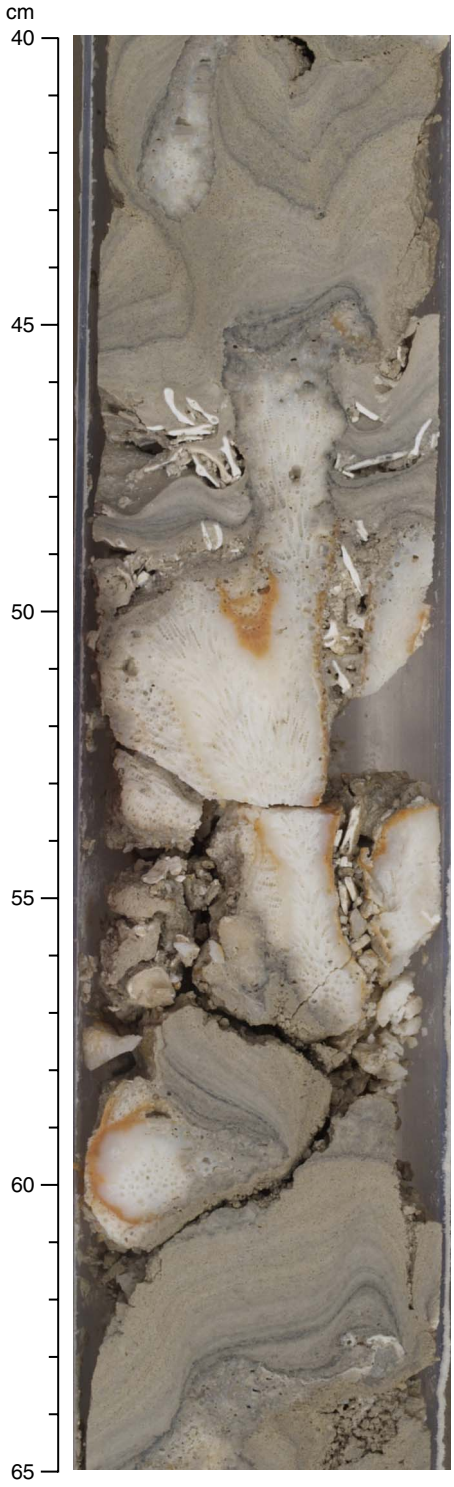

Figure F36. Coral assemblage dominated by encrusting *Leptastrea* with tabular *Acropora* covered with coralline algal crusts and subsequent microbialite crusts (Subunit IA; interval 310-M0016A-22R-1, 13–20 cm).

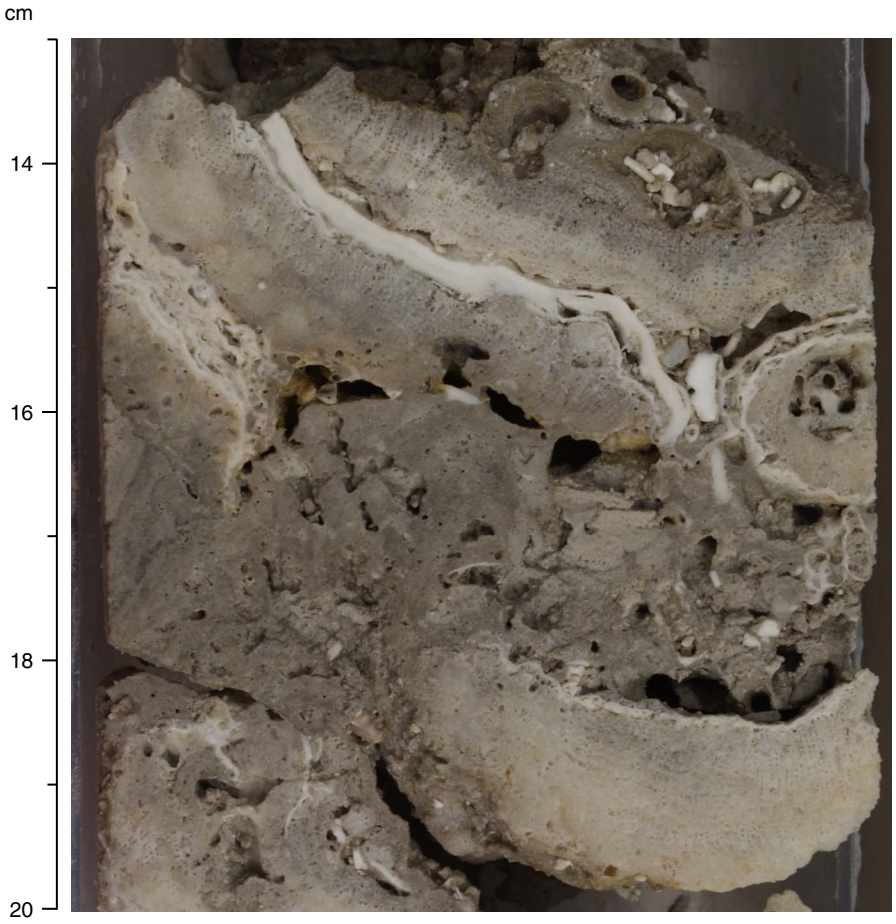

Figure F37. Coral framework composed of encrusting *Montipora* and agariciids with multiple coralline algal encrustations and subsequent microbialite crusts (Subunit IC; interval 310-M0016A-23R-1, 0–16 cm).

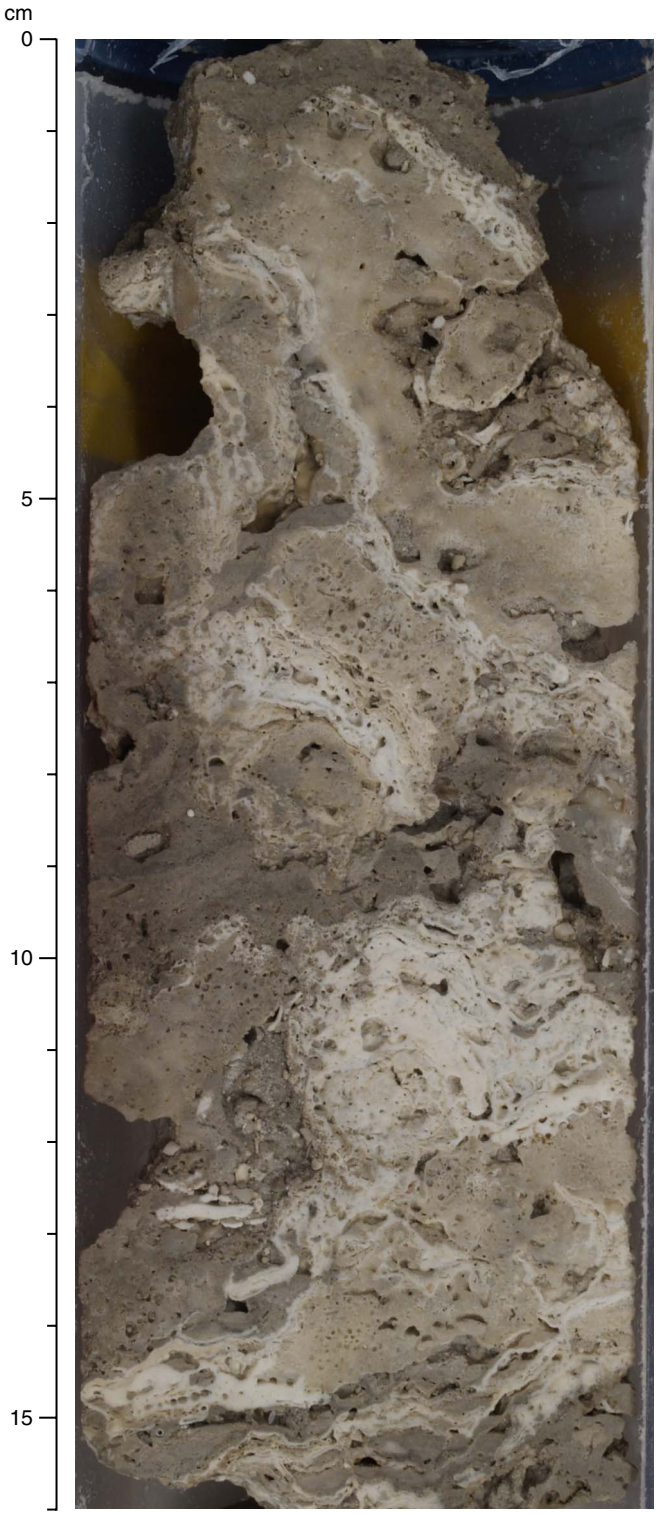

Figure F38. Coral framework of branching *Porites* and encrusting agariciids with coralline algal and thick microbialite encrustations (Subunit IC; interval 310-M0016A-29R-1, 38–60 cm).

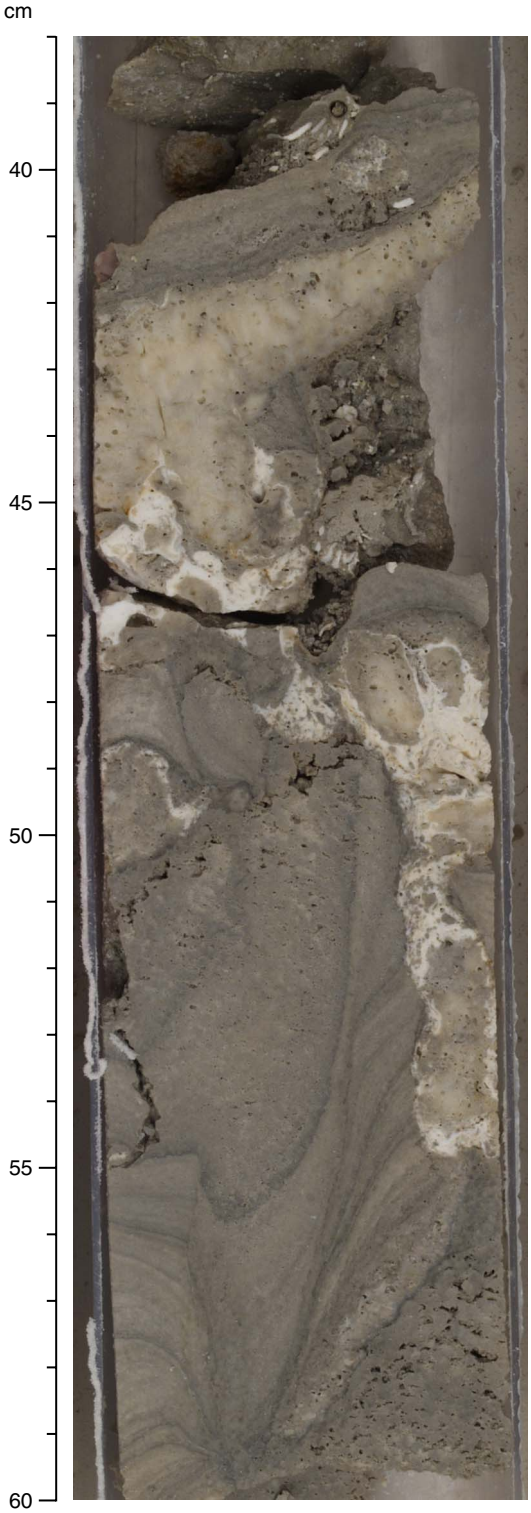

Figure F39. Coralgal bindstone with interlayered encrusting colonies of *Pavona* and coralline algae (Subunit IC; interval 310-M0016A-30R-1, 14–24 cm).

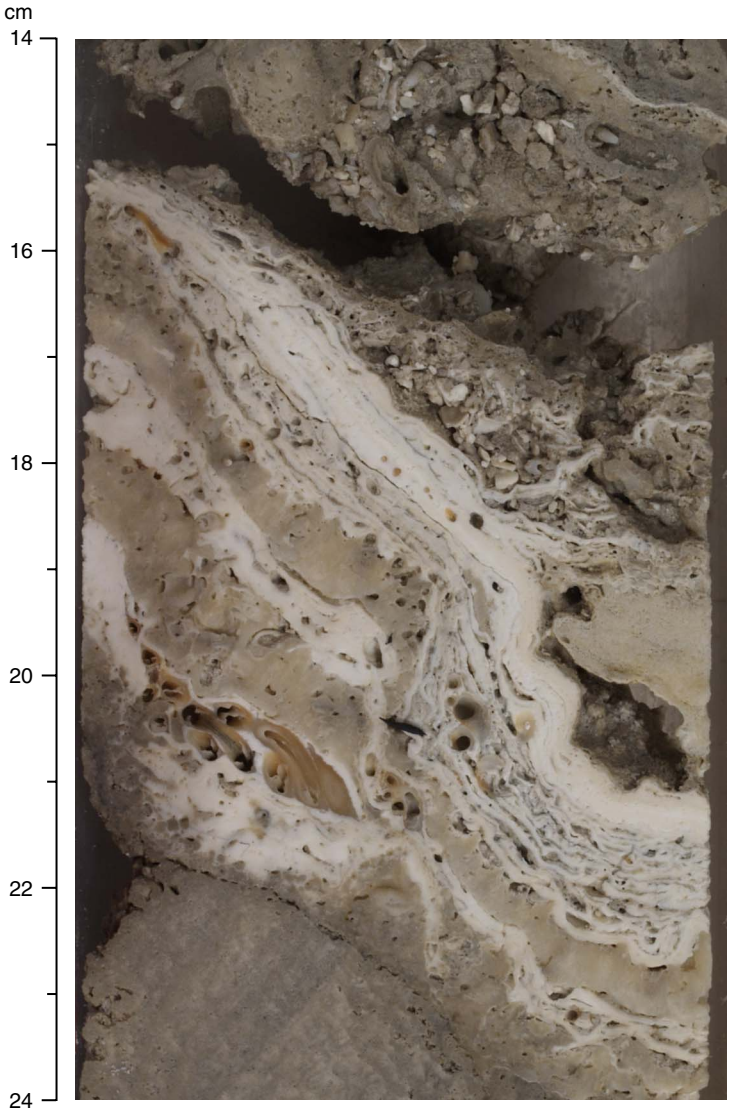

Figure F40. Massive colonies of *Montastrea* encrusted with thick coralline algal crusts (Subunit 1C; interval 310-M0017A-21R-1, 52–66 cm). Note strong bioerosion of coral surfaces.

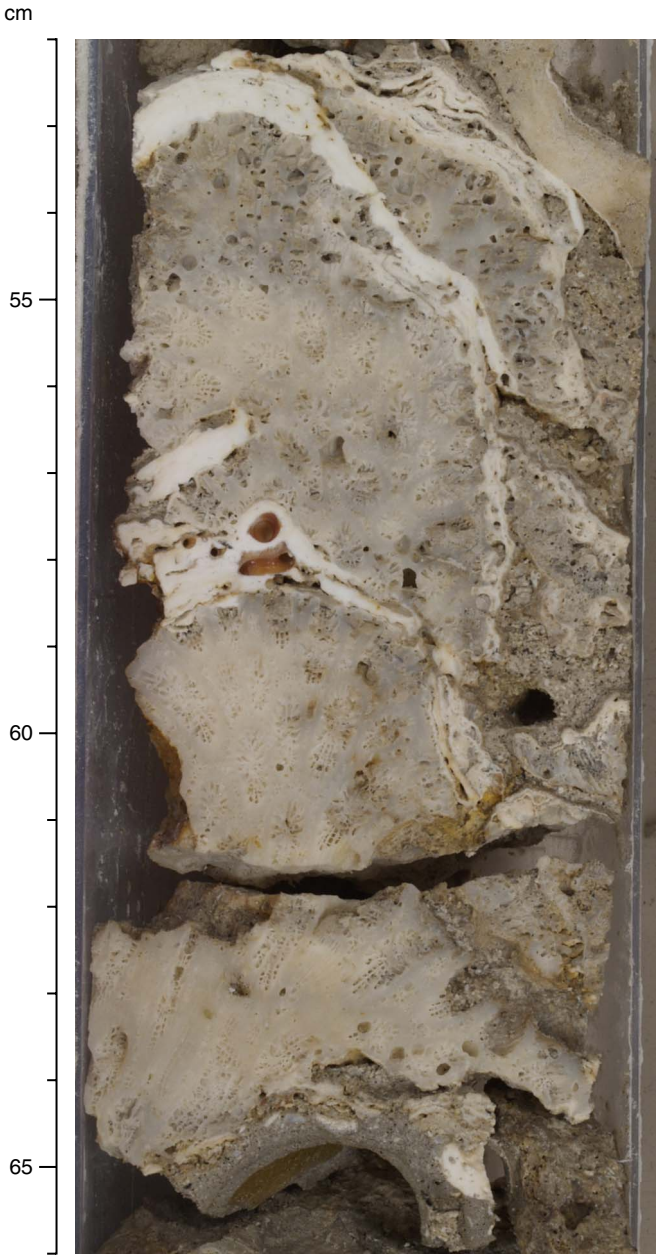

Figure F41. Colonies of encrusting *Leptastrea* and branching *Porites* encrusted with thick coralline algal crusts and microbialites (Subunit IA; interval 310-M0018A-13R-1, 25–35 cm).

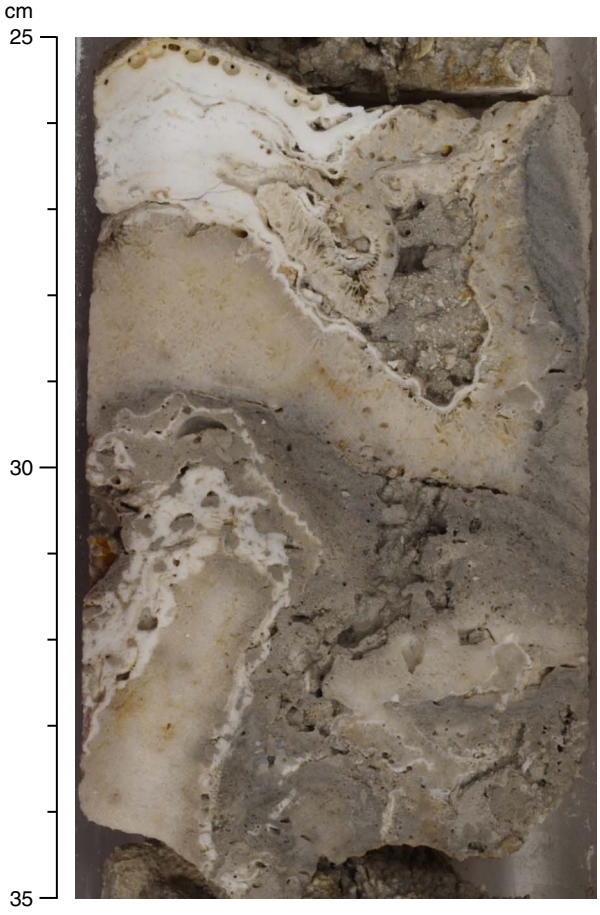

Figure F42. Encrusting and robust branching coral framework locally encrusted with thick coralline algal crusts (Subunit IC; interval 310-M0015A-14R-1, 23–49 cm). Thick laminated microbialite crusts represent last stage of encrustation.

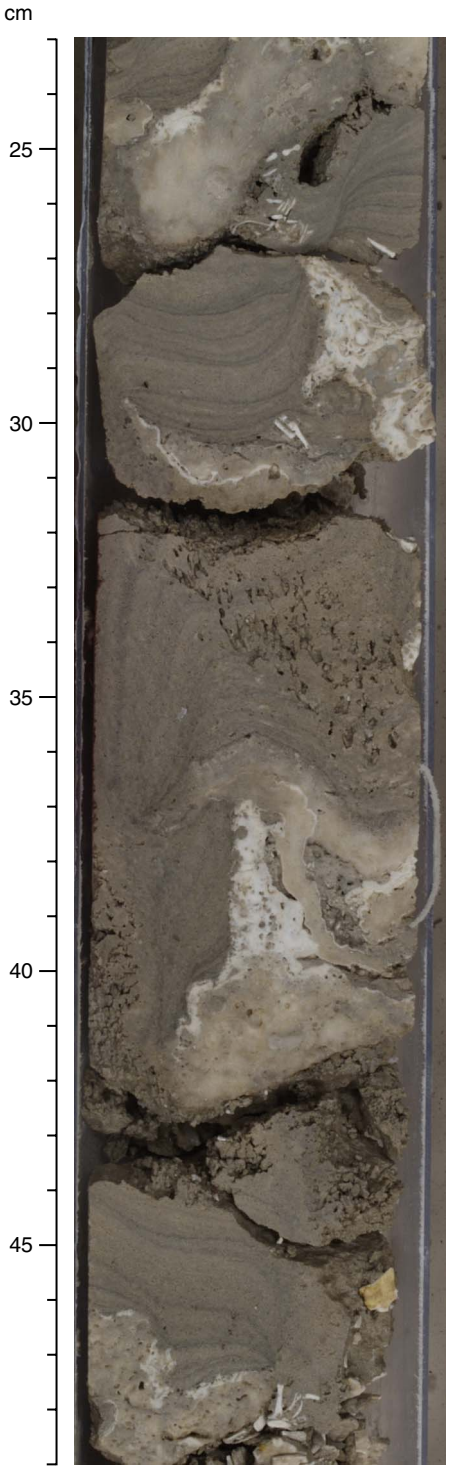

Figure F43. Primary cavity in coralgal-microbialite framework infilled with sediment, including *Halimeda* segments (Subunit IC; interval 310-M0015A-14R-1, 48–60 cm).

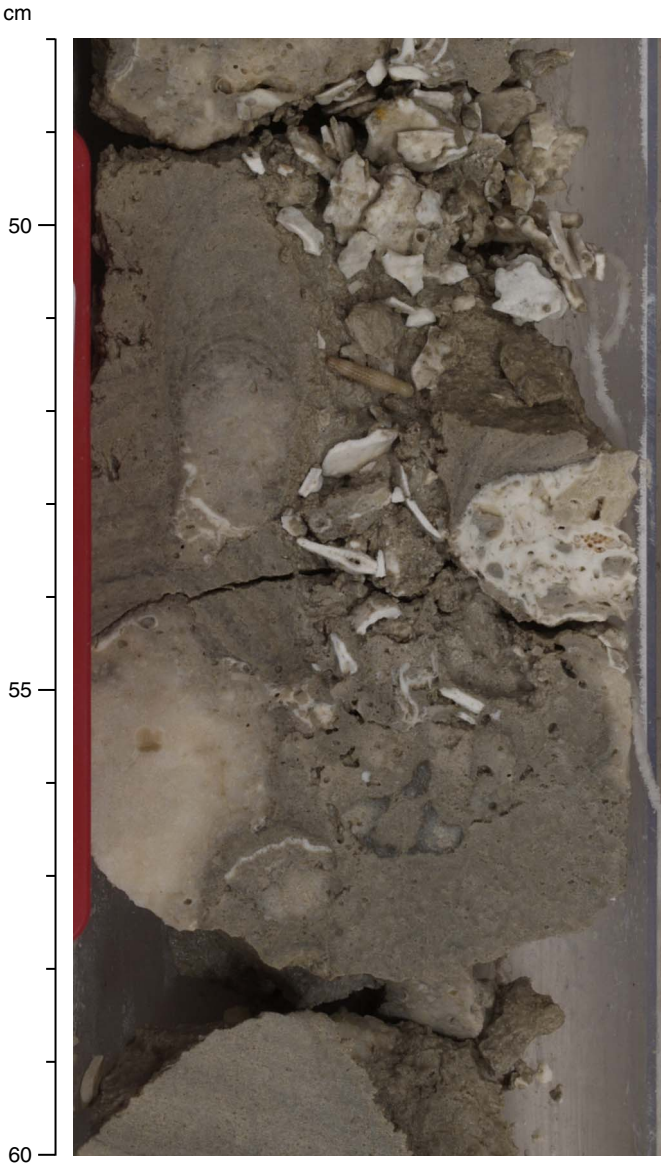

Figure F44. Laminated to thrombolitic microbialite crusts growing on coral framework (Subunit IC; interval 310-M0015A-21R-1, 19–31 cm). Primary vugs are filled with *Halimeda*-rich sediment.

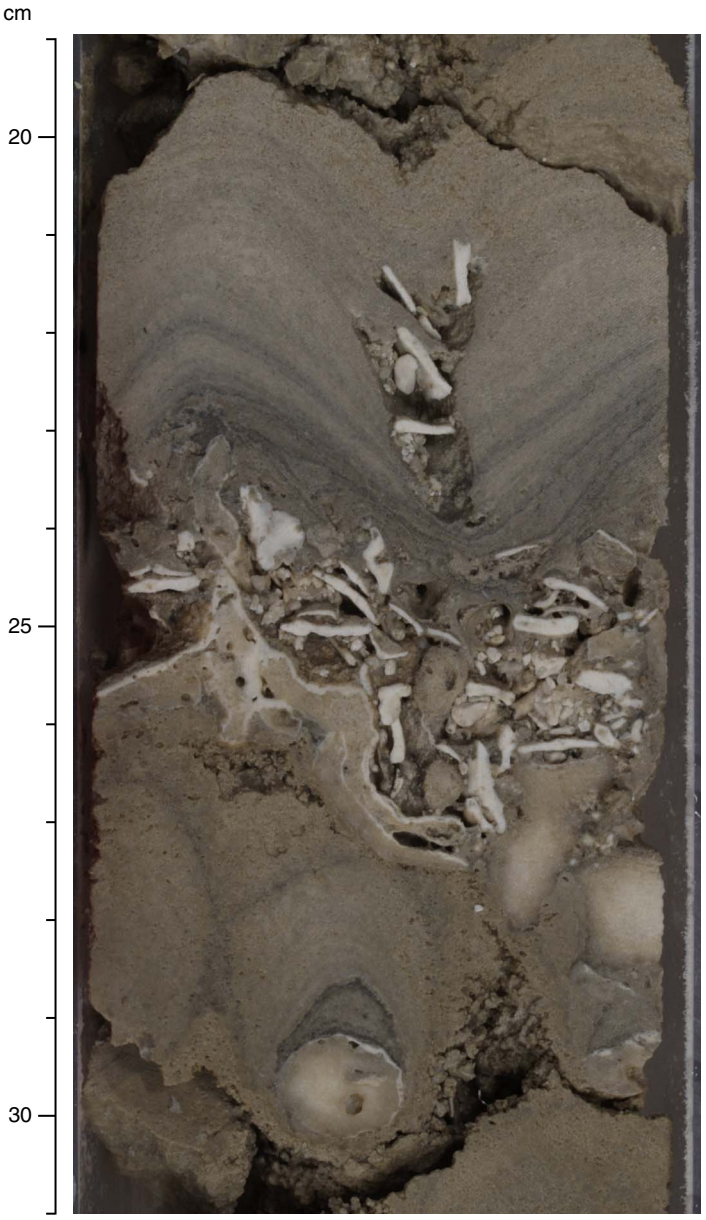

Figure F45. Coralgal-microbialite framework with dominant laminated microbialite (Subunit IC; interval 310-M0015B-26R-1, 50–75 cm). Primary cavities are filled with sediment, including *Halimeda*.

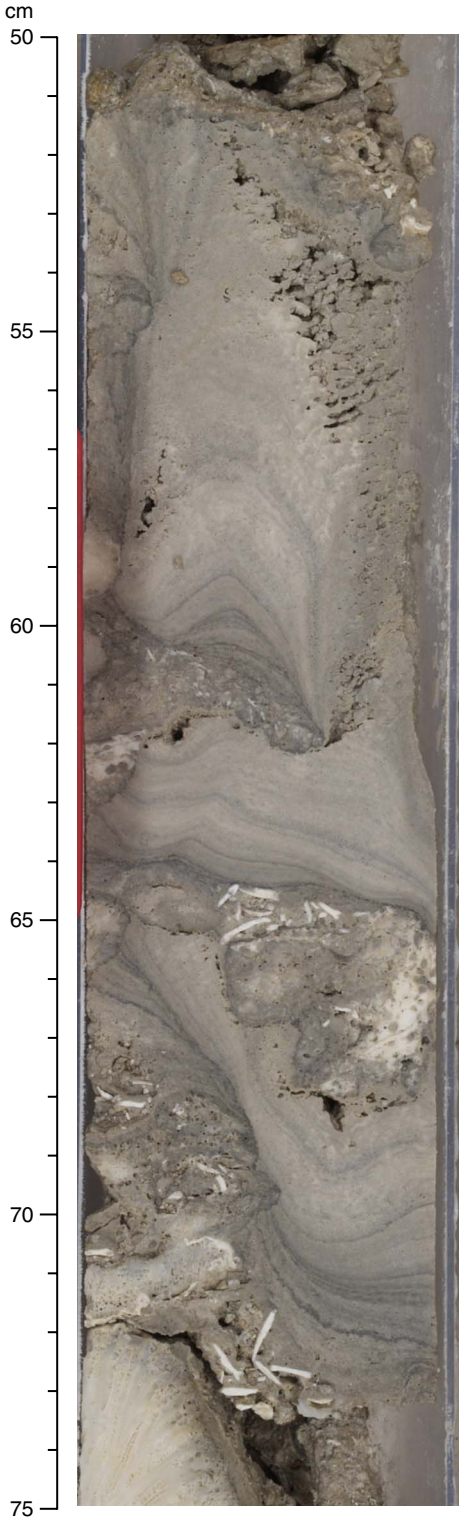

Figure F46. Skeletal rudstone with *Halimeda* segments and fragments of branching corals (Unit II; interval 310-M0015A-40R-1, 10–24 cm). Note solution cavities with dark stained surfaces.

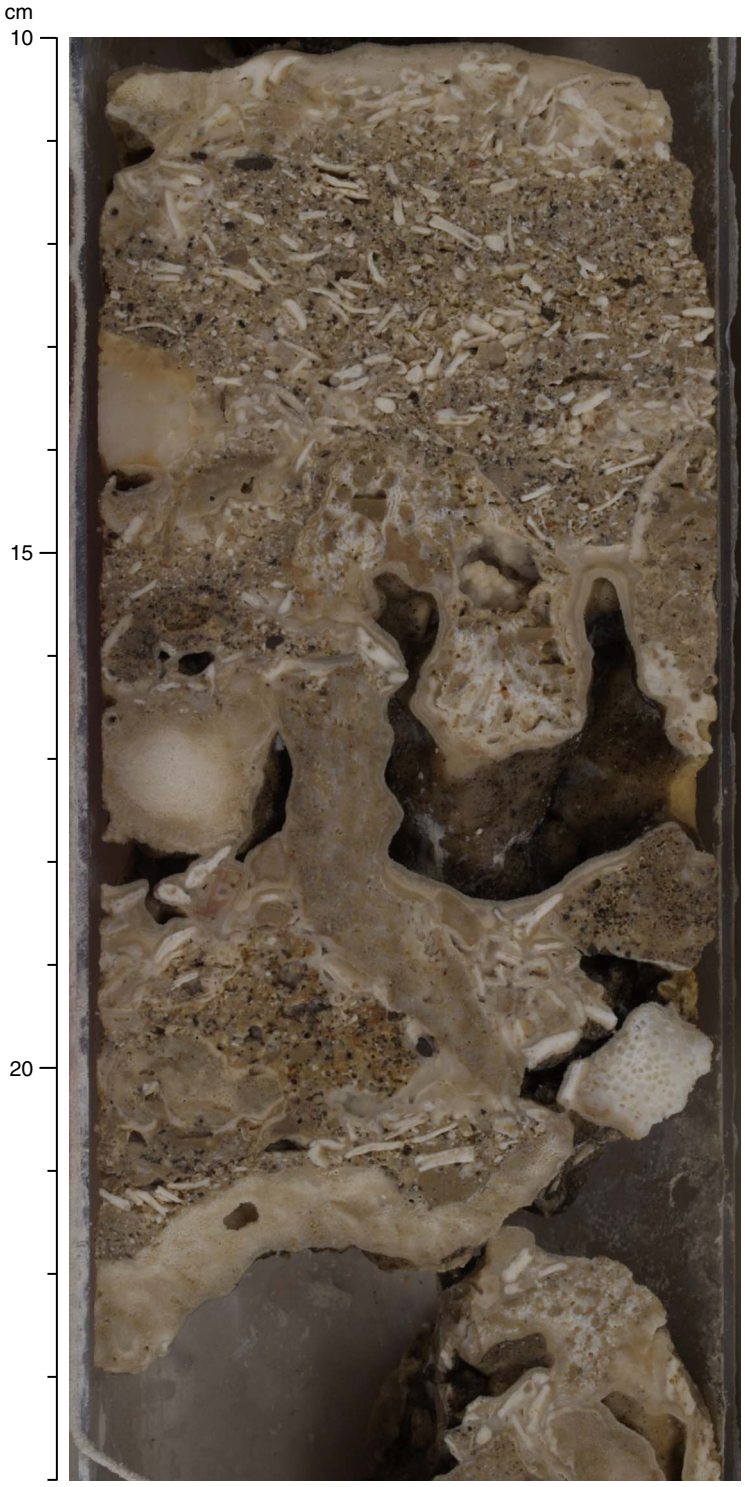

Figure F47. Poorly sorted skeletal rudstone with large cement crystals (botryoidal?) (center of figure) (Unit II; interval 310-M0015A-41R-1, 105–118 cm).

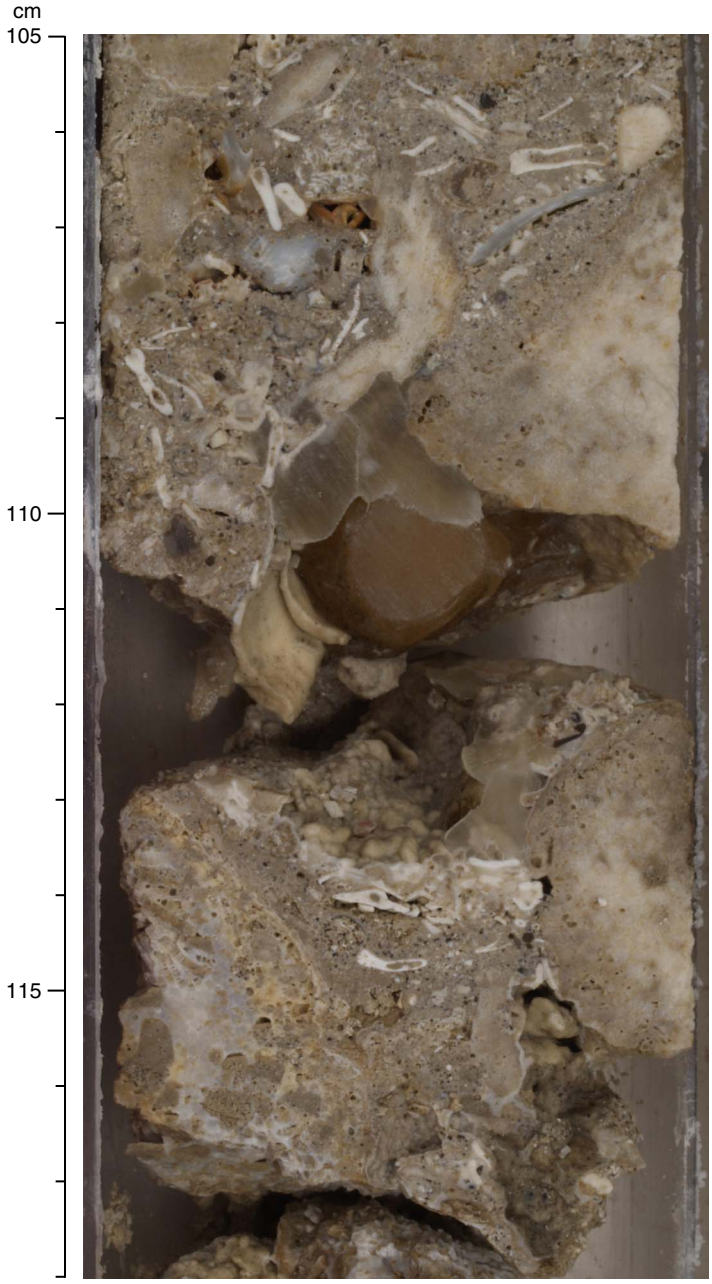

Figure F48. Solution vugs with dark stained walls (Unit II; interval 310-M0015B-38R-3, 92–102 cm).

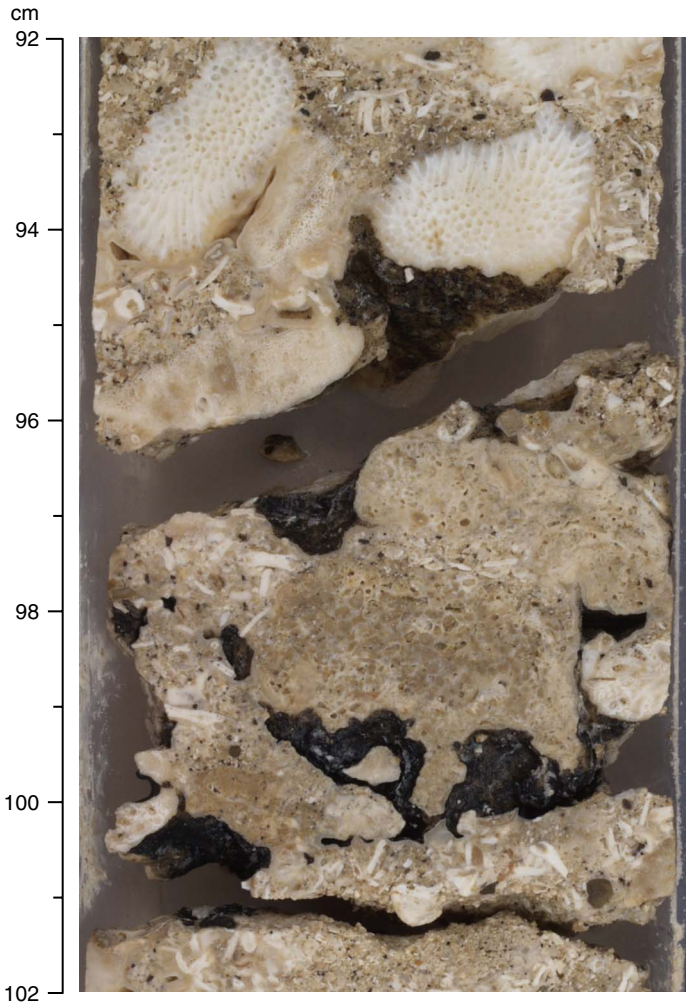

Figure F49. Solution cavities lined with cement (Unit II; interval 310-M0015A-40R-1, 30–38 cm).

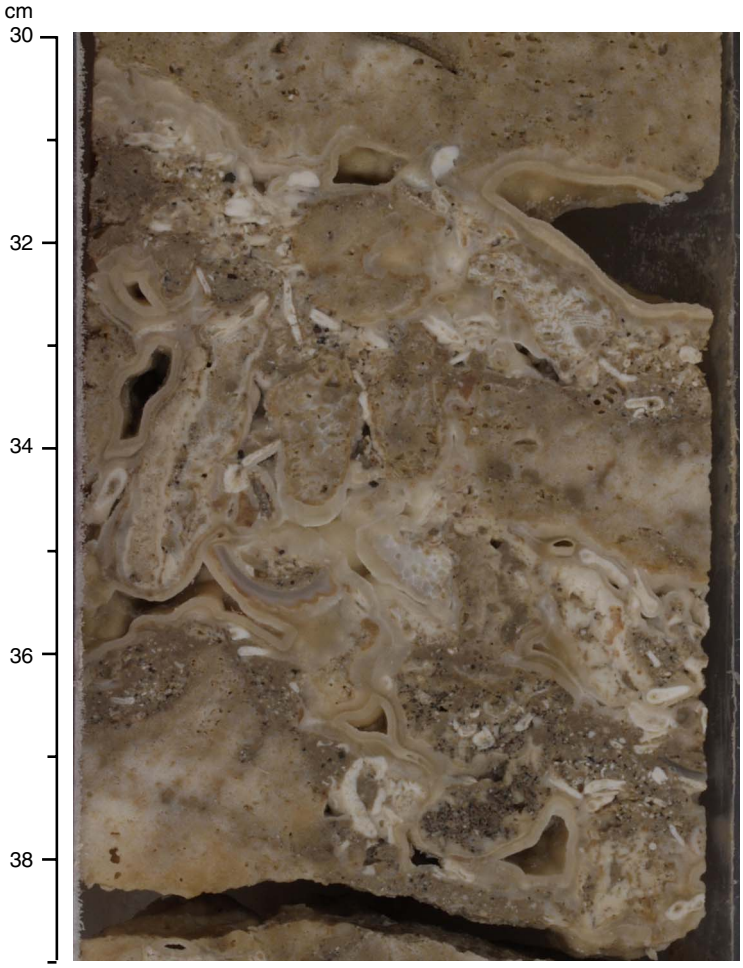

Figure F50. Skeletal floatstone with *Halimeda* segments and coral fragments (Unit II; interval 310-M0015A-37R-1, 40–55 cm).

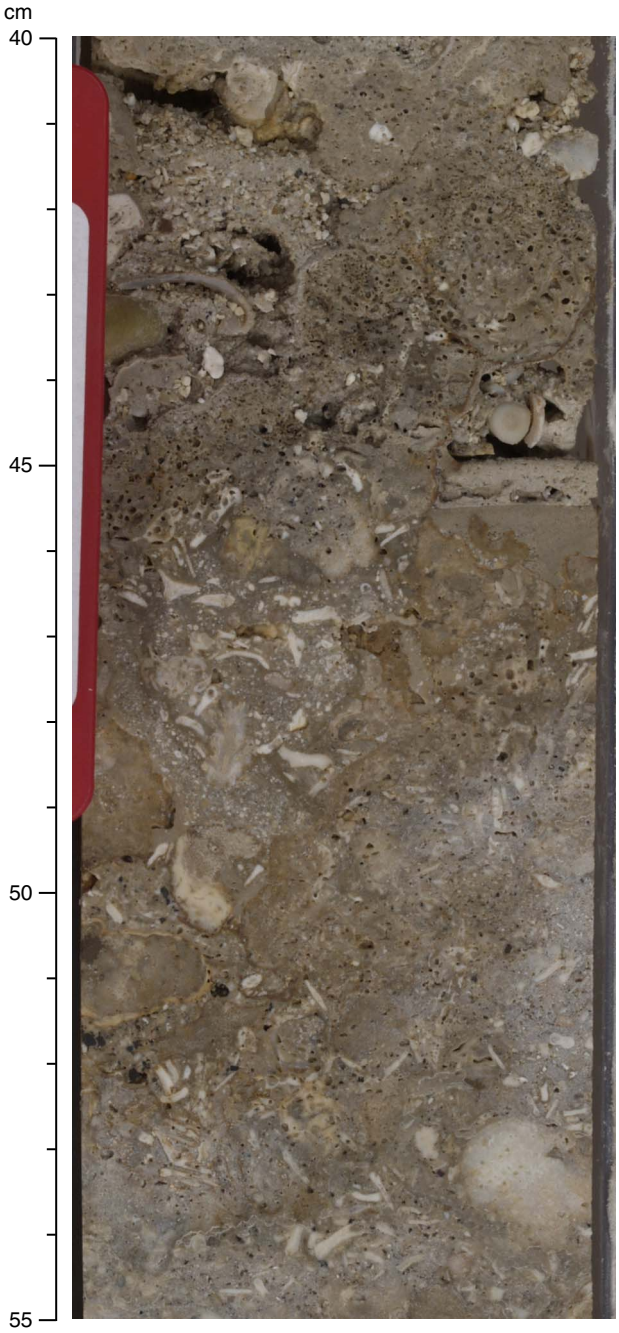

Figure F51. Coral rudstone mainly composed of robust branching *Pocillopora* (Unit II; interval 310-M0015A-39R-1, 63–80 cm).

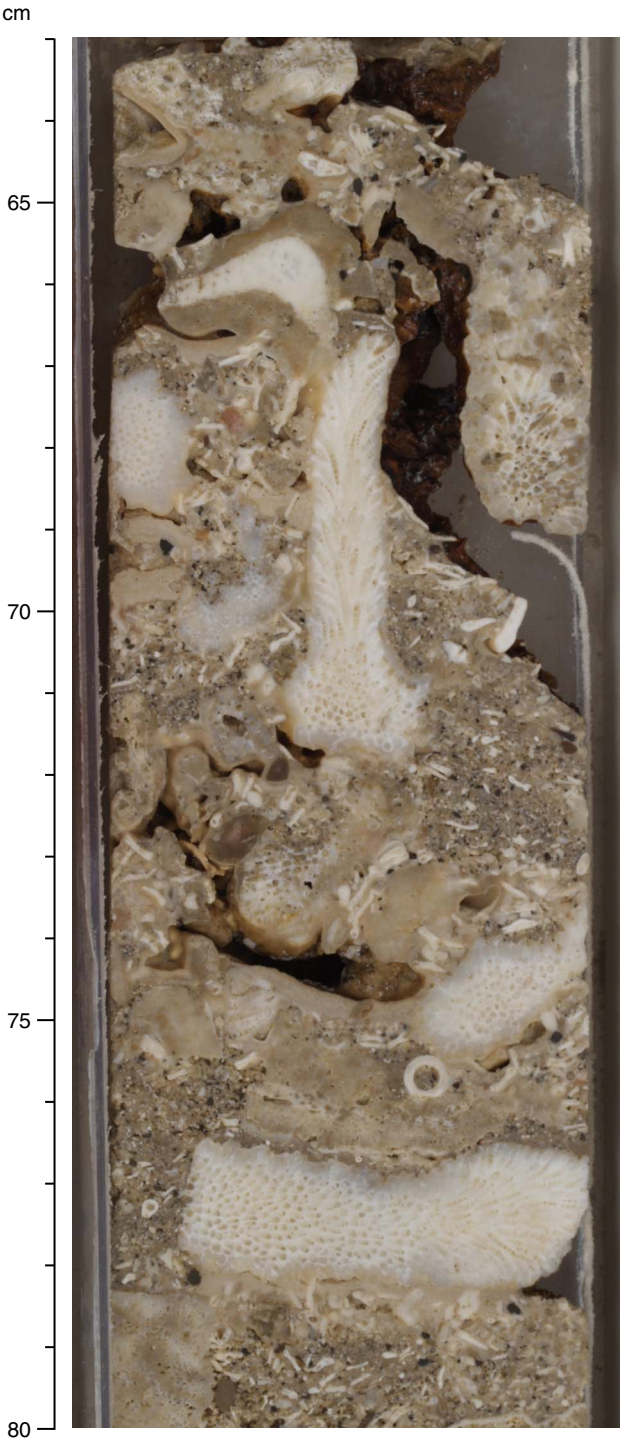

Figure F52. Poorly sorted skeletal floatstone with coral fragments and *Halimeda* segments (Unit II; interval 310-M0015A-39R-1, 115–129 cm). Note stained surfaces in solution cavities.

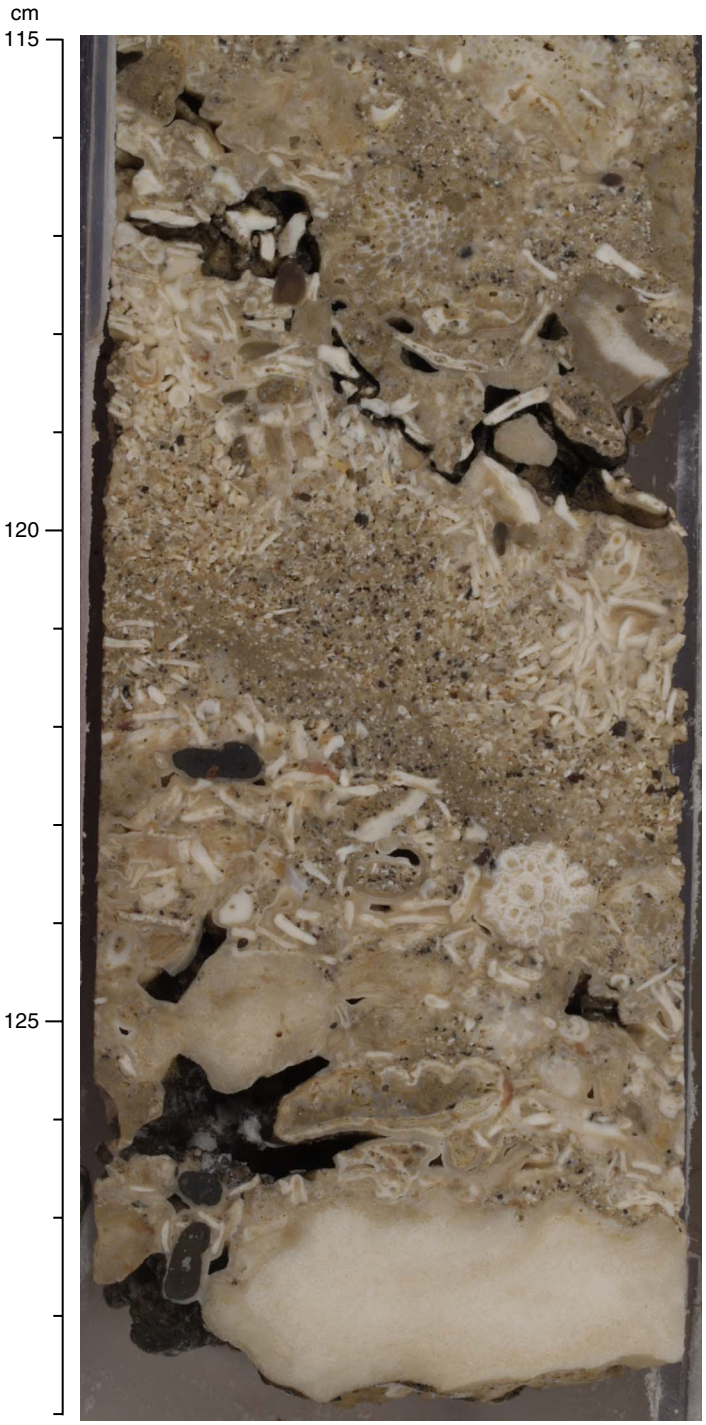

Figure F53. Poorly sorted rudstone with fragments of tabular and branching coral fragments (Unit II; interval 310-M0015A-41R-1, 25–35 cm). Note dark stained surfaces of solution cavities.

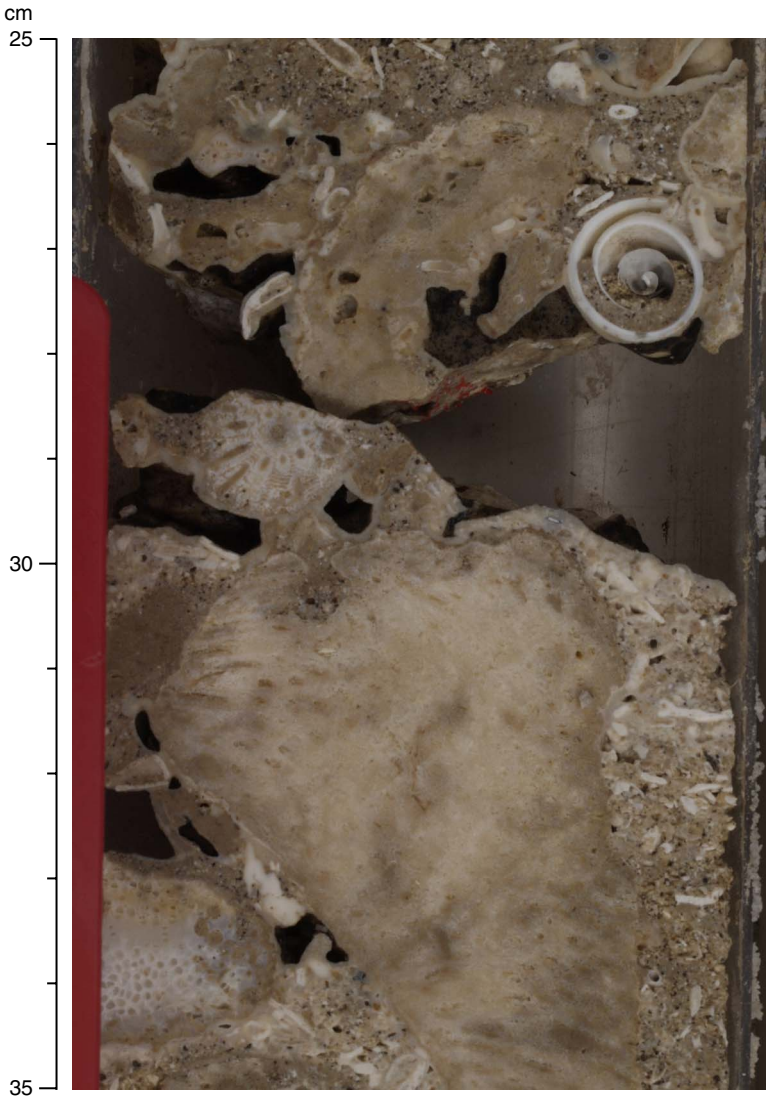

Figure F54. Skeletal rudstone with *Halimeda* segments, coral fragments, and reworked carbonate cobble (Unit II; interval 310-M0015B-38R-3, 40–55 cm).

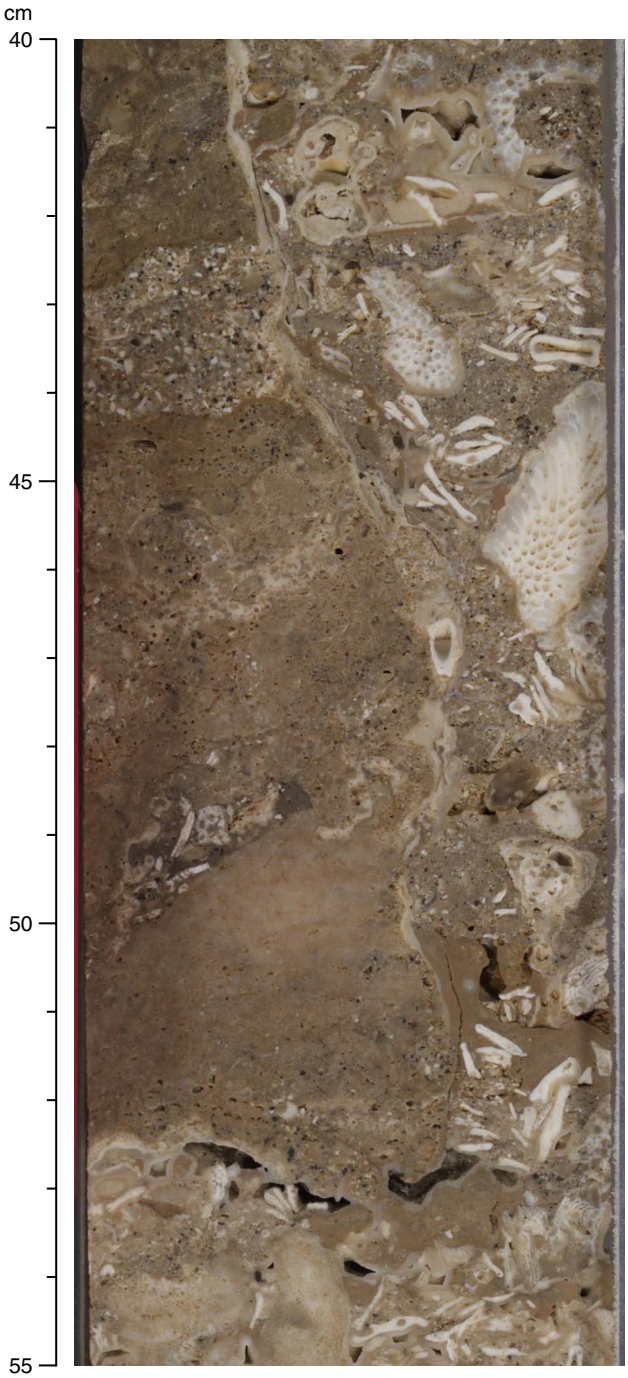

Figure F55. Poorly sorted skeletal rudstone with coral fragments and *Halimeda* segments (Unit II; interval 310-M0016B-22R-CC, 10–24 cm).

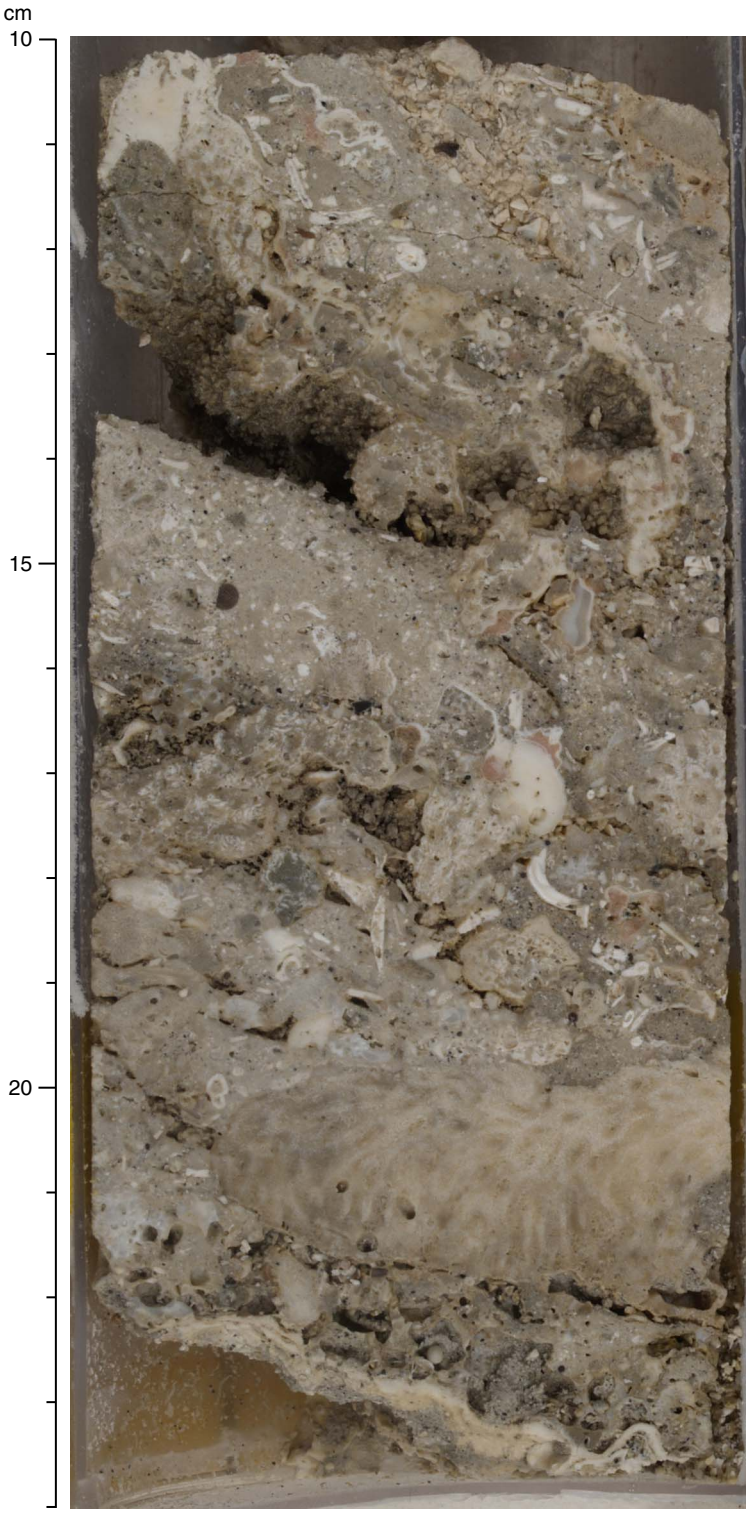

Figure F56. Poorly sorted skeletal rudstone with rhodoliths and *Halimeda* segments (Unit II; interval 310-M0016B-24R-1, 57–70 cm).

Figure F57. Poorly sorted skeletal rudstone with coral fragments and *Halimeda* segments (Unit II; interval 310-M0016B-24R-1, 79–94 cm).

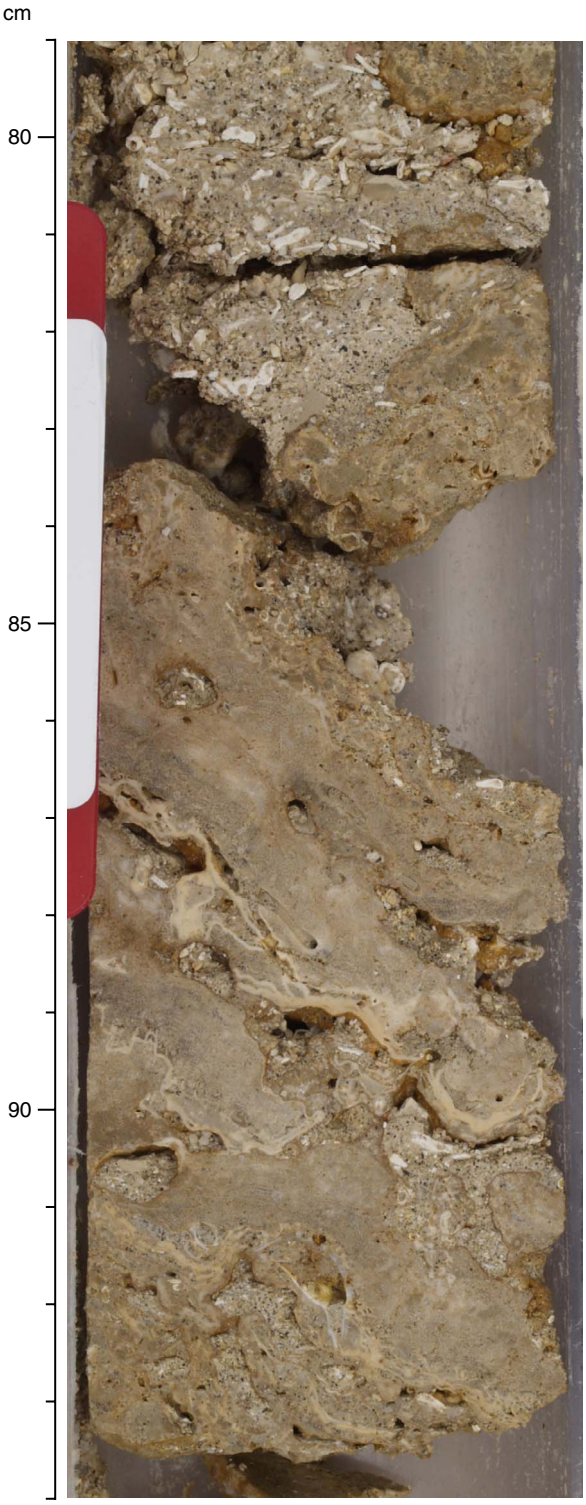

Figure F58. Poorly sorted skeletal rudstone with coral fragments and volcanic grains (Unit II; interval 310-M0017A-21R-3, 92–119 cm).

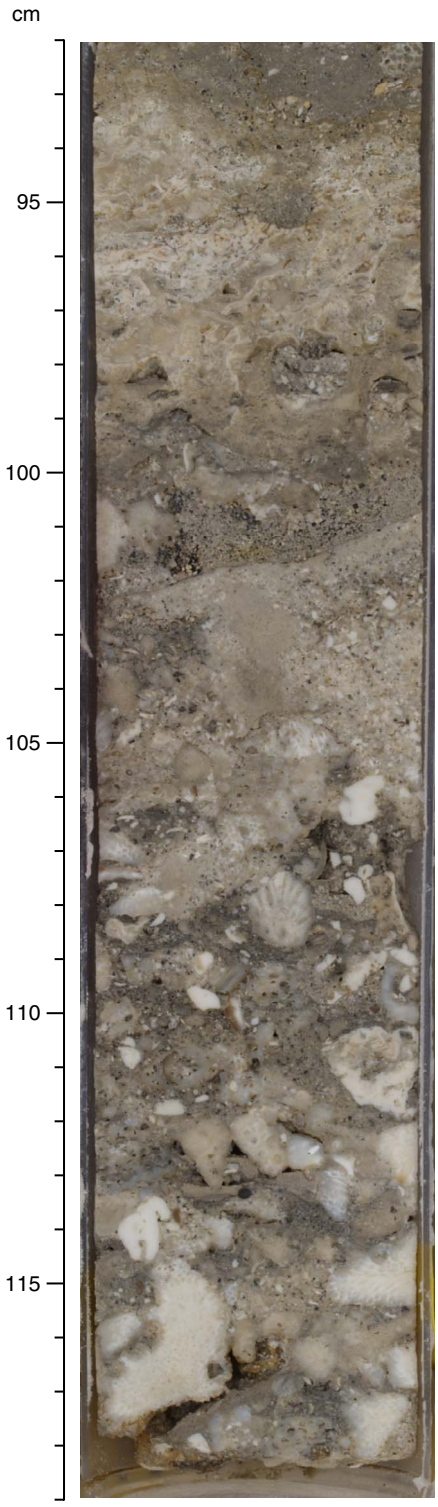

Figure F59. Large fragments of massive and encrusting corals covered with coralline algal crust (Unit II; interval 310-M0015A-38R-1, 63–75 cm).

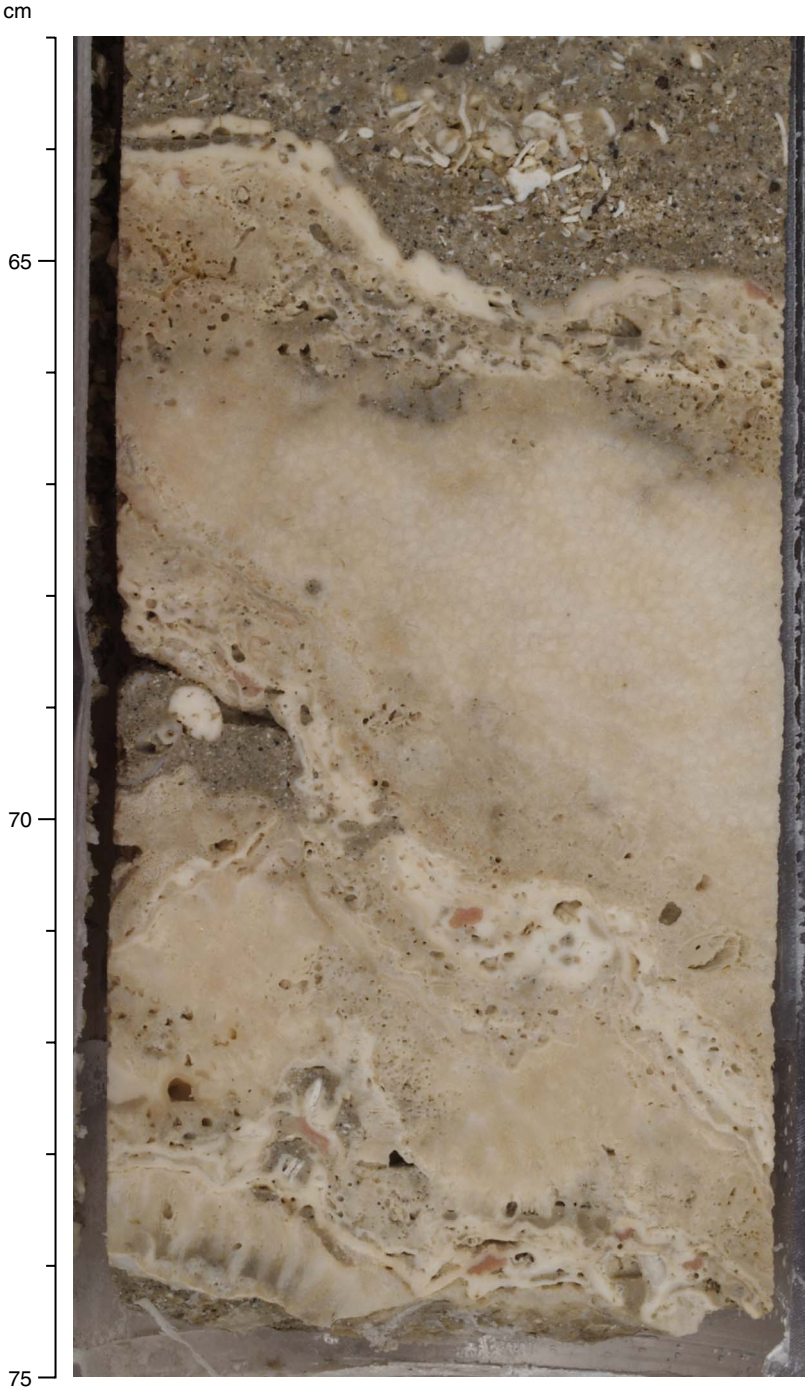

Figure F60. Coralgal framework dominated by encrusting corals with thick coralline algal crusts (Unit II; interval 310-M0017A-21R-1, 98–118 cm). Sedimentary matrix contains large portions of volcanic grains.

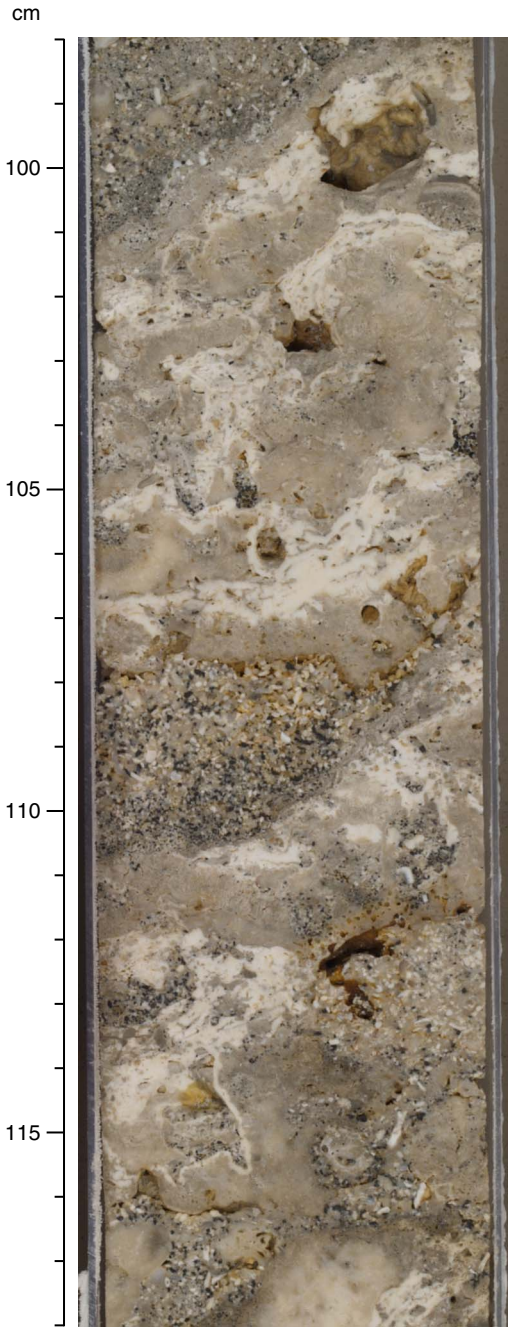

Figure F61. Coralgal framework dominated by encrusting corals with thick coralline algal crusts (Unit II; interval 310-M0017A-21R-2, 32–64 cm). Sedimentary matrix contains large portions of volcanic grains.

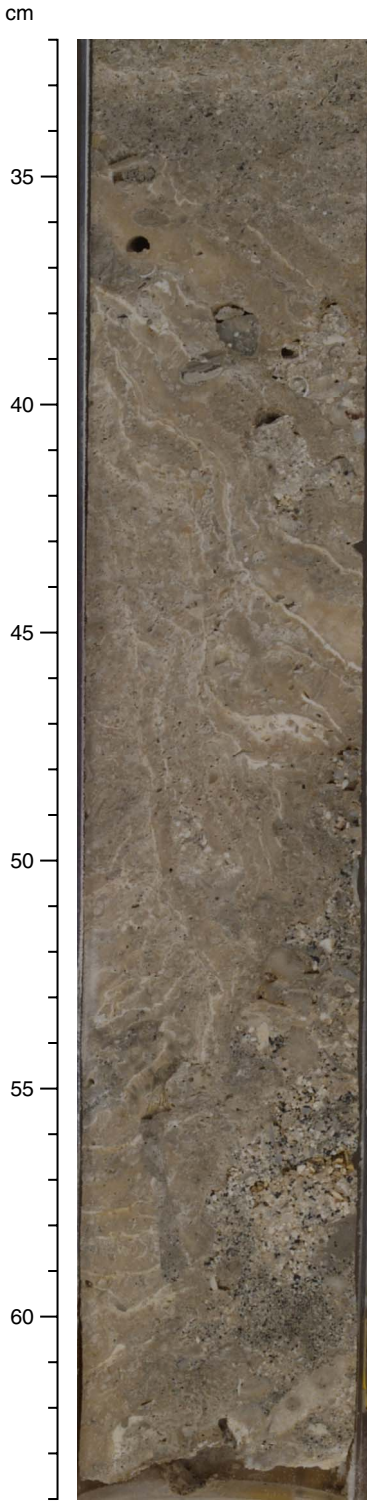

Figure F62. Velocity, bulk density, magnetic susceptibility, and porosity as a function of depth in Hole M0016A. Discrete measurements are superimposed (red circles).

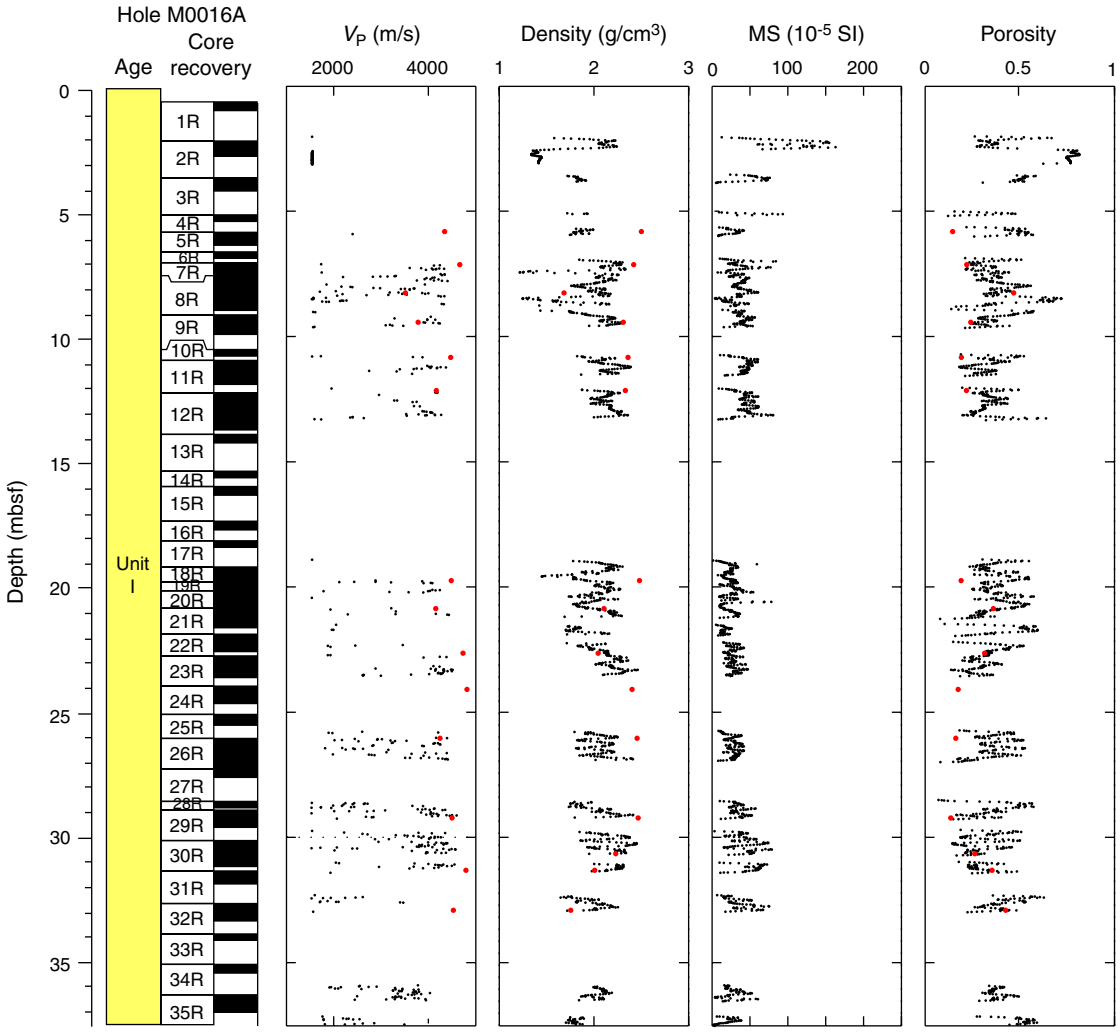

Figure F63. Velocity, bulk density, magnetic susceptibility, and porosity as a function of depth in Hole M0016B. Discrete measurements are superimposed (red circles).

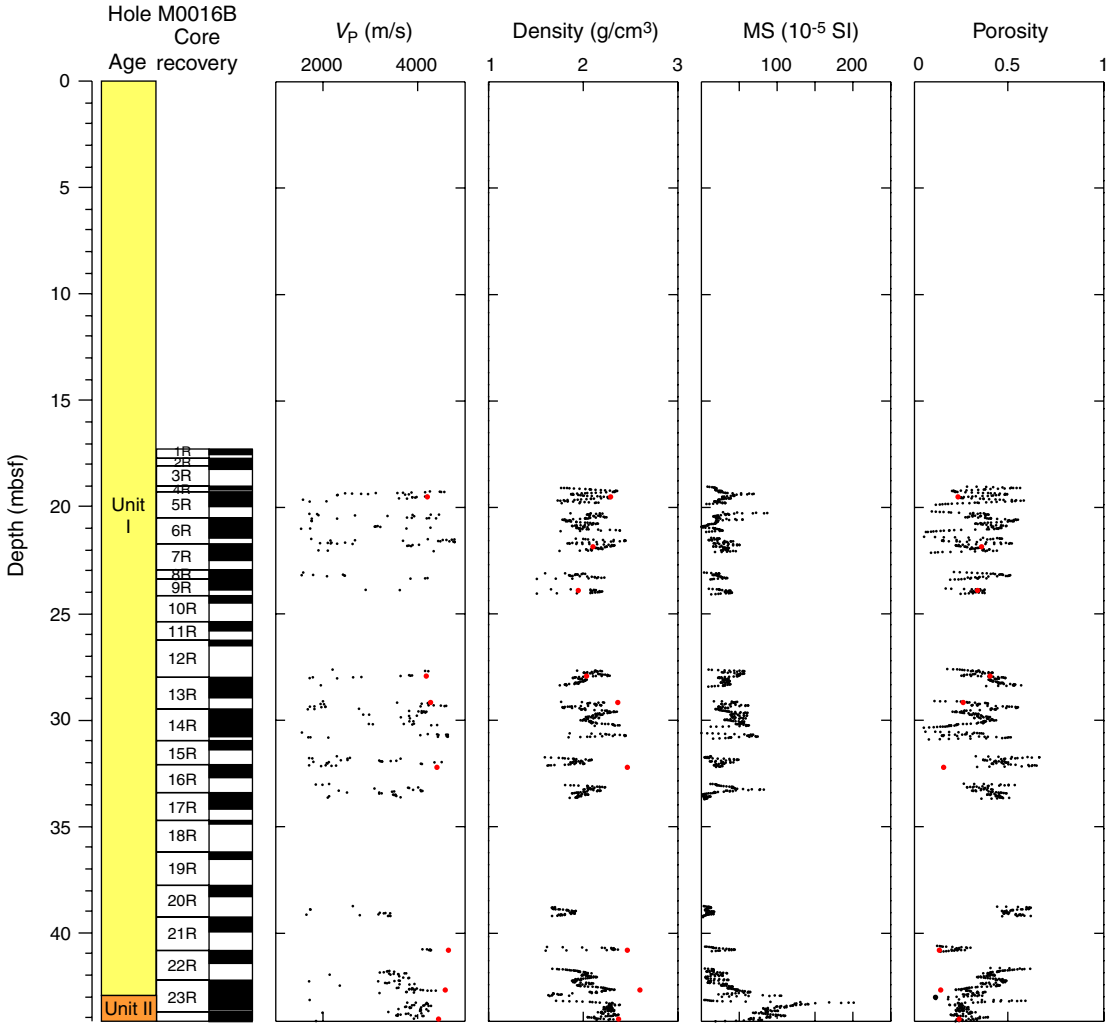

Figure F64. Velocity, bulk density, magnetic susceptibility, and porosity as a function of depth in Hole M0017A. Discrete measurements are superimposed (red circles).

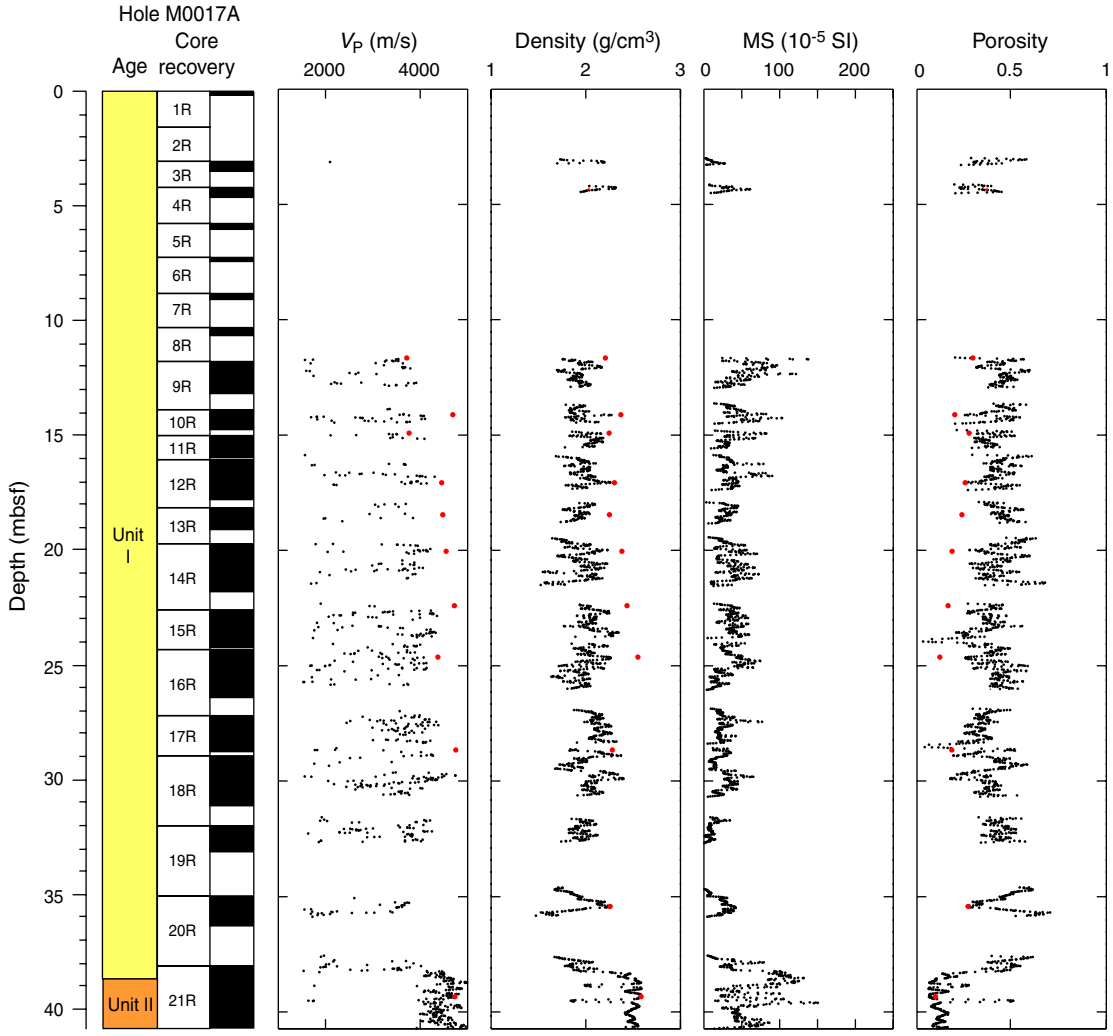

Figure F65. Velocity, bulk density, magnetic susceptibility, and porosity as a function of depth in Hole M0018A. Discrete measurements are superimposed (red circles).

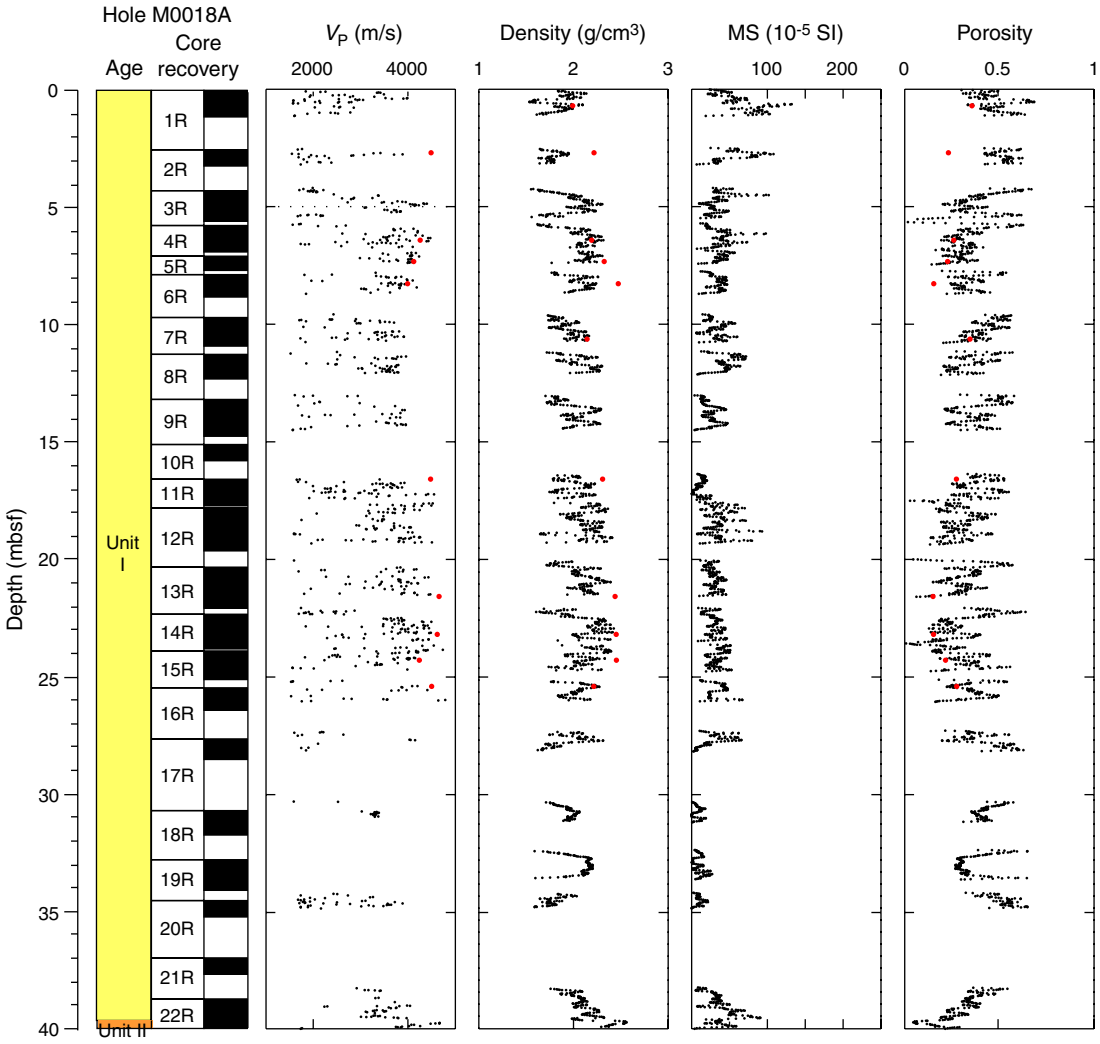

Figure F66. Velocity, bulk density, magnetic susceptibility, and porosity as a function of depth in Hole M0015A. Discrete measurements are superimposed (red circles).

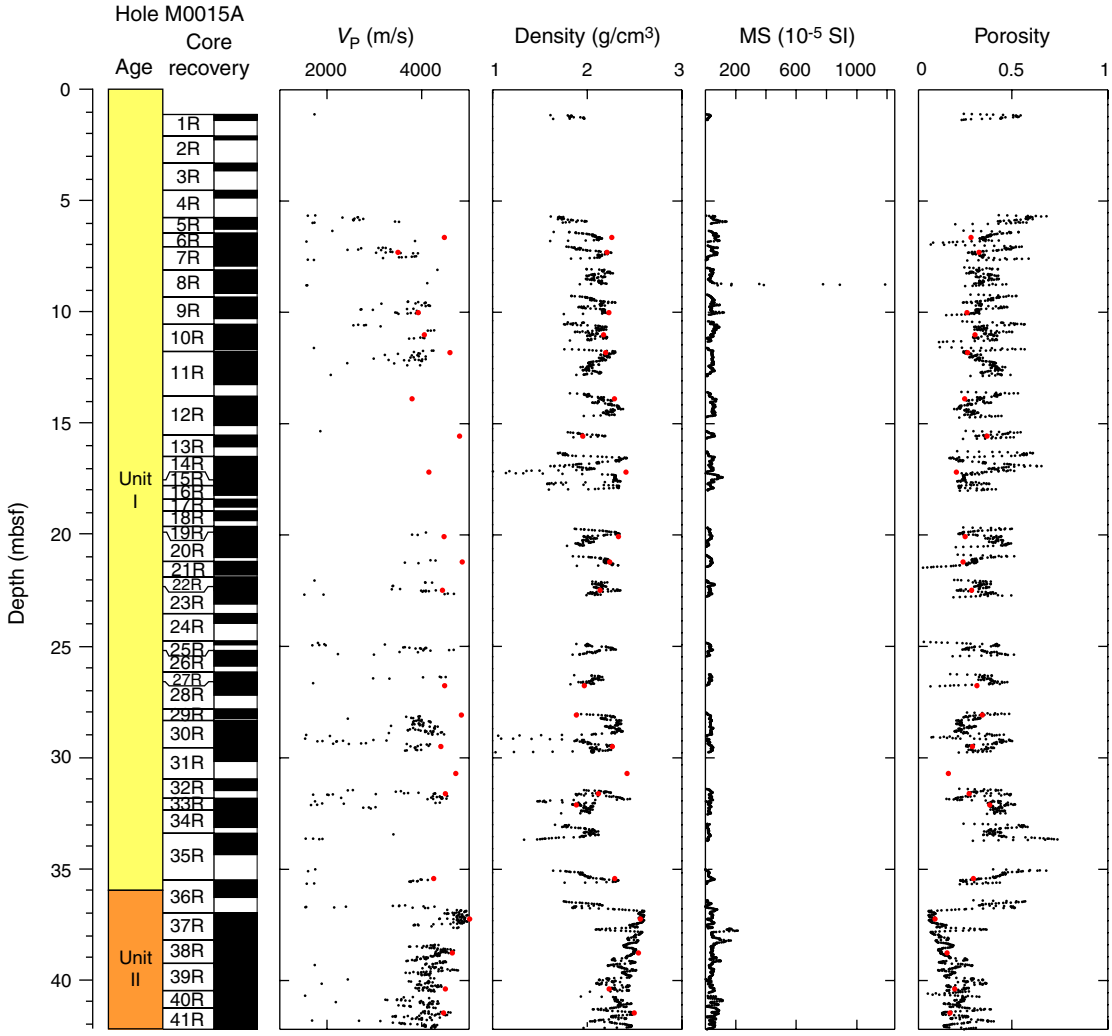

Figure F67. Velocity, bulk density, magnetic susceptibility, and porosity as a function of depth in Hole M0015B. Discrete measurements are superimposed (red circles).

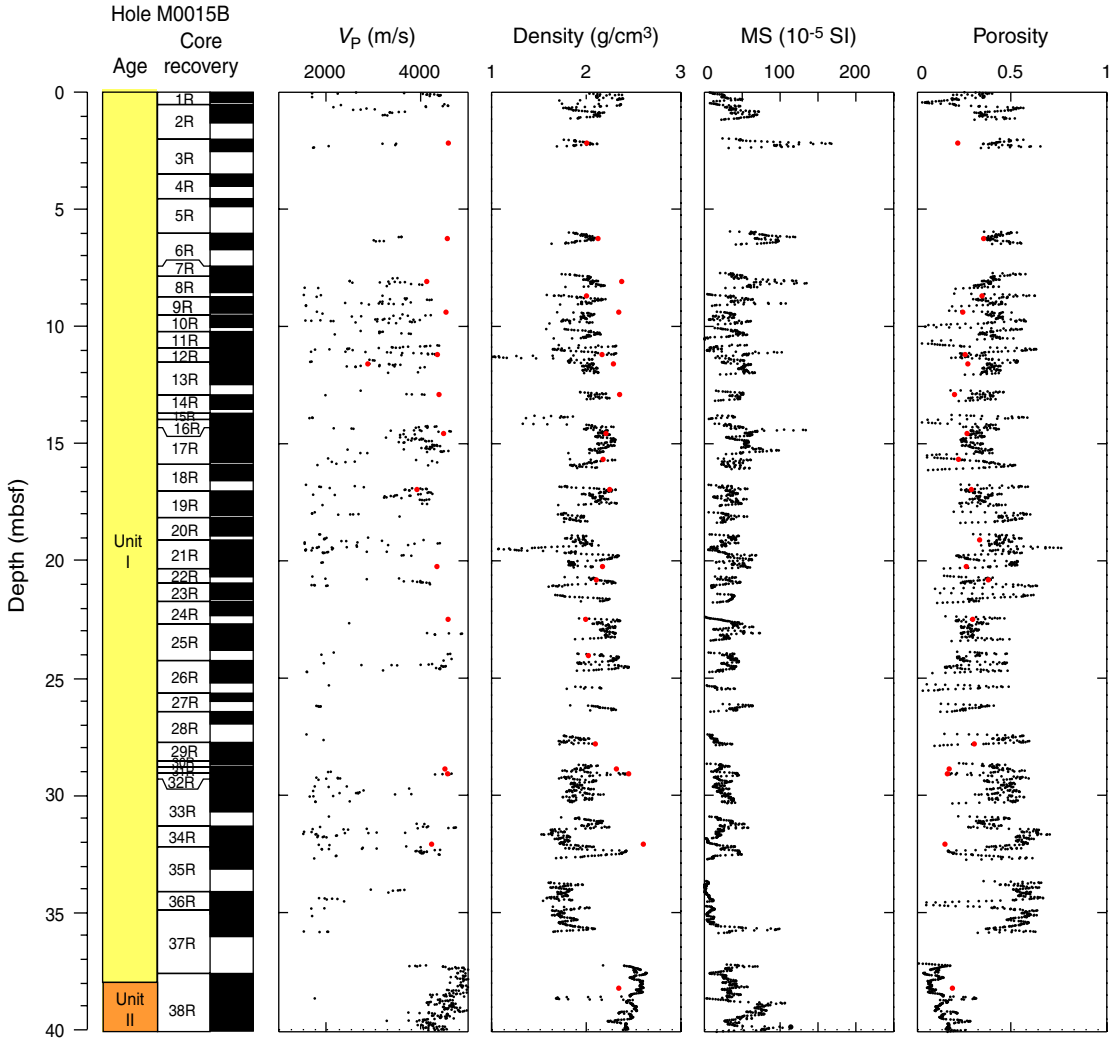

Figure F68. Cross plot of porosity with velocity for Hole M0017A. Solid lines refer to the Wyllie time average equation (red) and Raymer modified time average equation (green) for a matrix velocity of calcite (6530 m/s). Discrete measurements are superimposed (red circles).

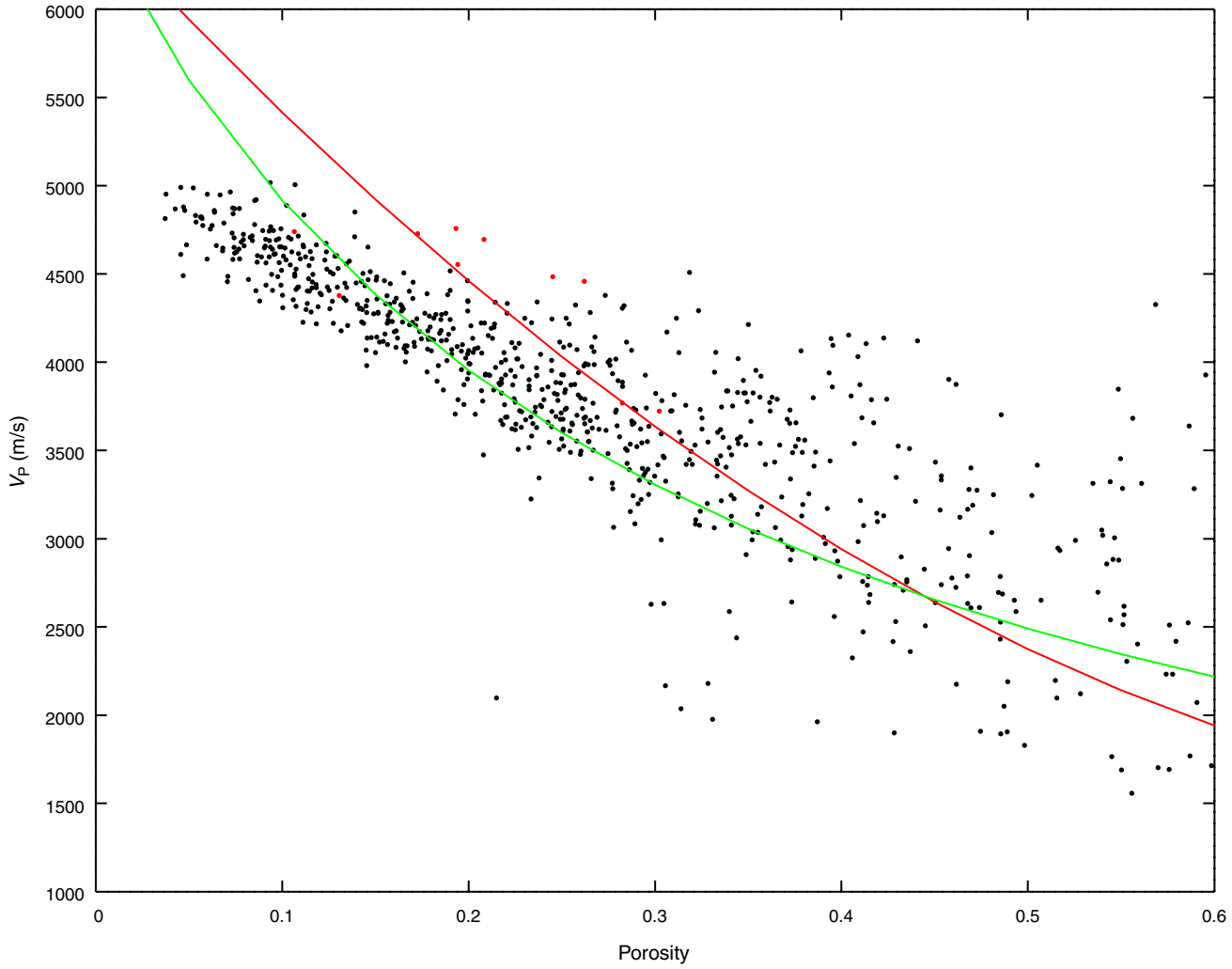

Figure F69. Comparison of MSCL velocity data (solid circles), downhole sonic log data (blue line), and discrete measurements (red circles) as a function of depth for Hole M0017A.

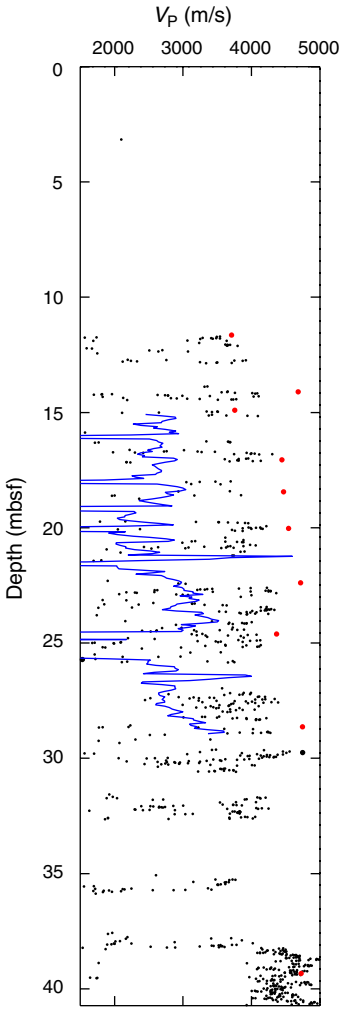

Figure F70. Color reflectance (L*) data from Holes M0015A, M0015B, M0016A, M0016B, M0017A, and M0018A. Holes M0015B, M0016A, M0016B, M0017A, and M0018A are offset from Hole M0015A by 40, 90, 130, 180, and 230 L* units, respectively.

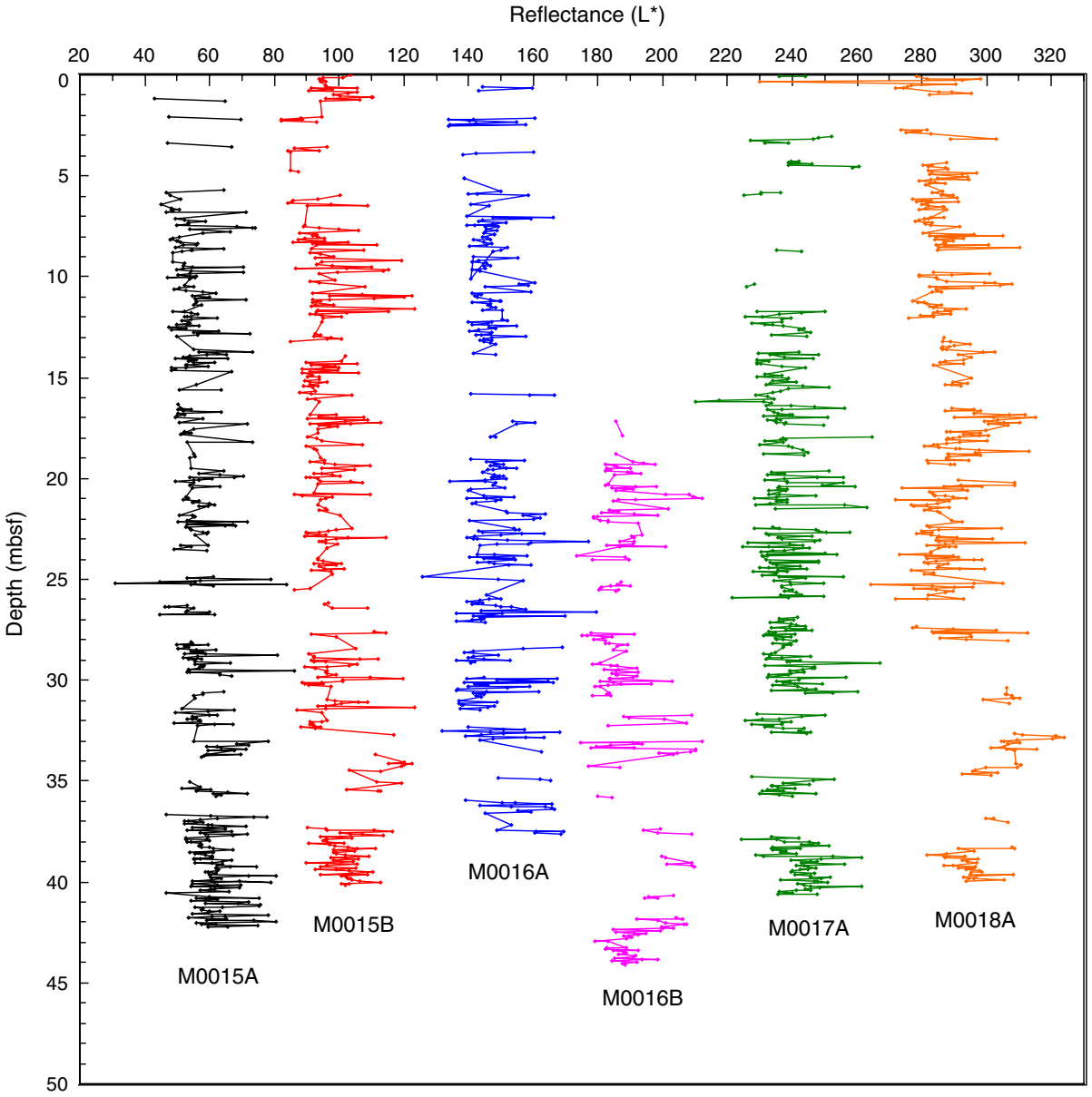

Figure F71. Wireline logging data, Hole M0015A. Mec. cal. = mechanical caliper, Ac. cal. = acoustic caliper extracted from ABI40, res. = resistivity.

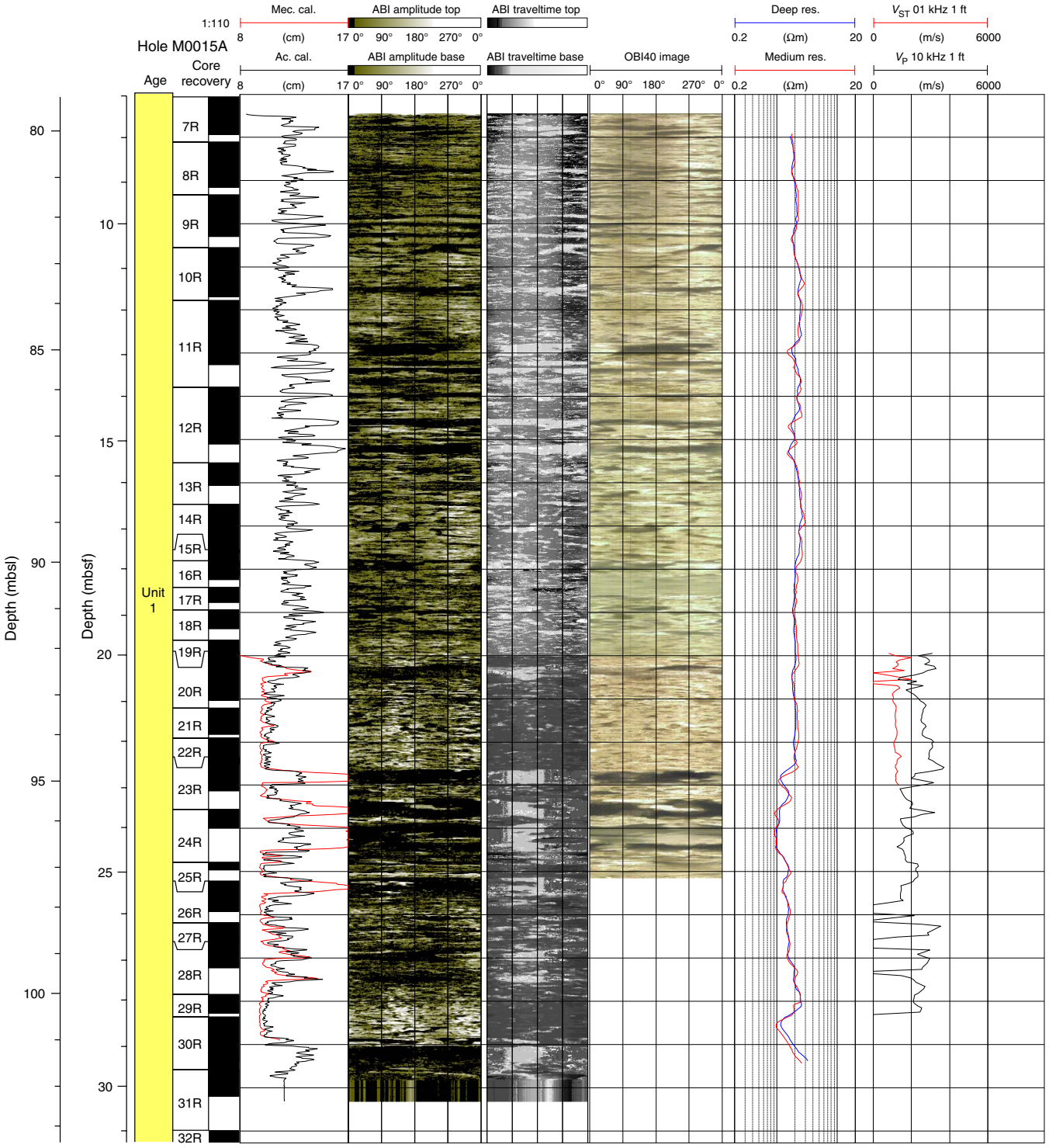

Figure F72. Wireline logging data, Hole M0015A. (See the "DOWNHOLE" folder in **"Supplementary Material"** for the complete multipart figure in PDF format.)

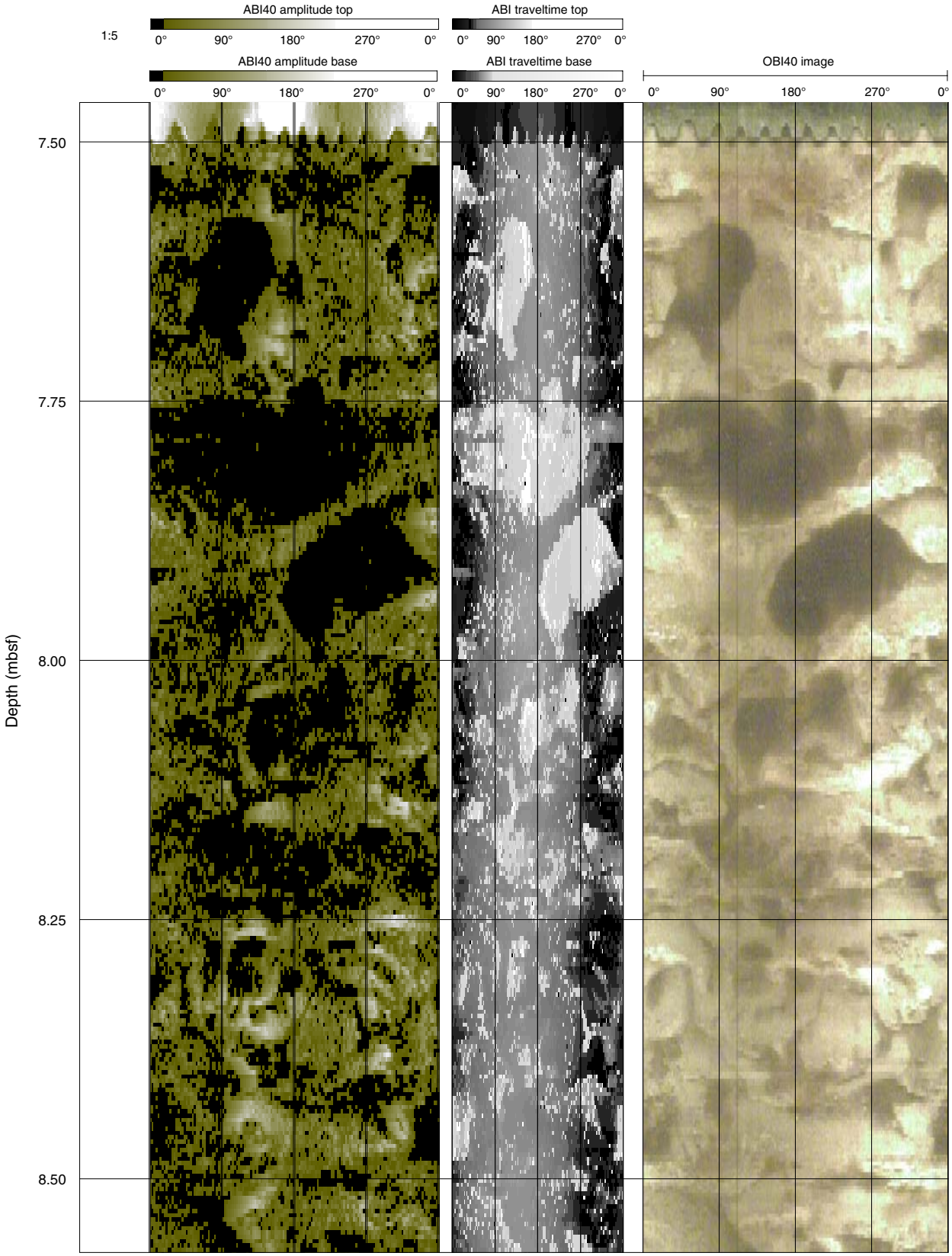

Figure F73. Wireline logging data, Hole M0017A. Ac. cal. = acoustic caliper extracted from ABI40. (See the "DOWNHOLE" folder in **"Supplementary Material"** for the complete multipart figure in PDF format.)

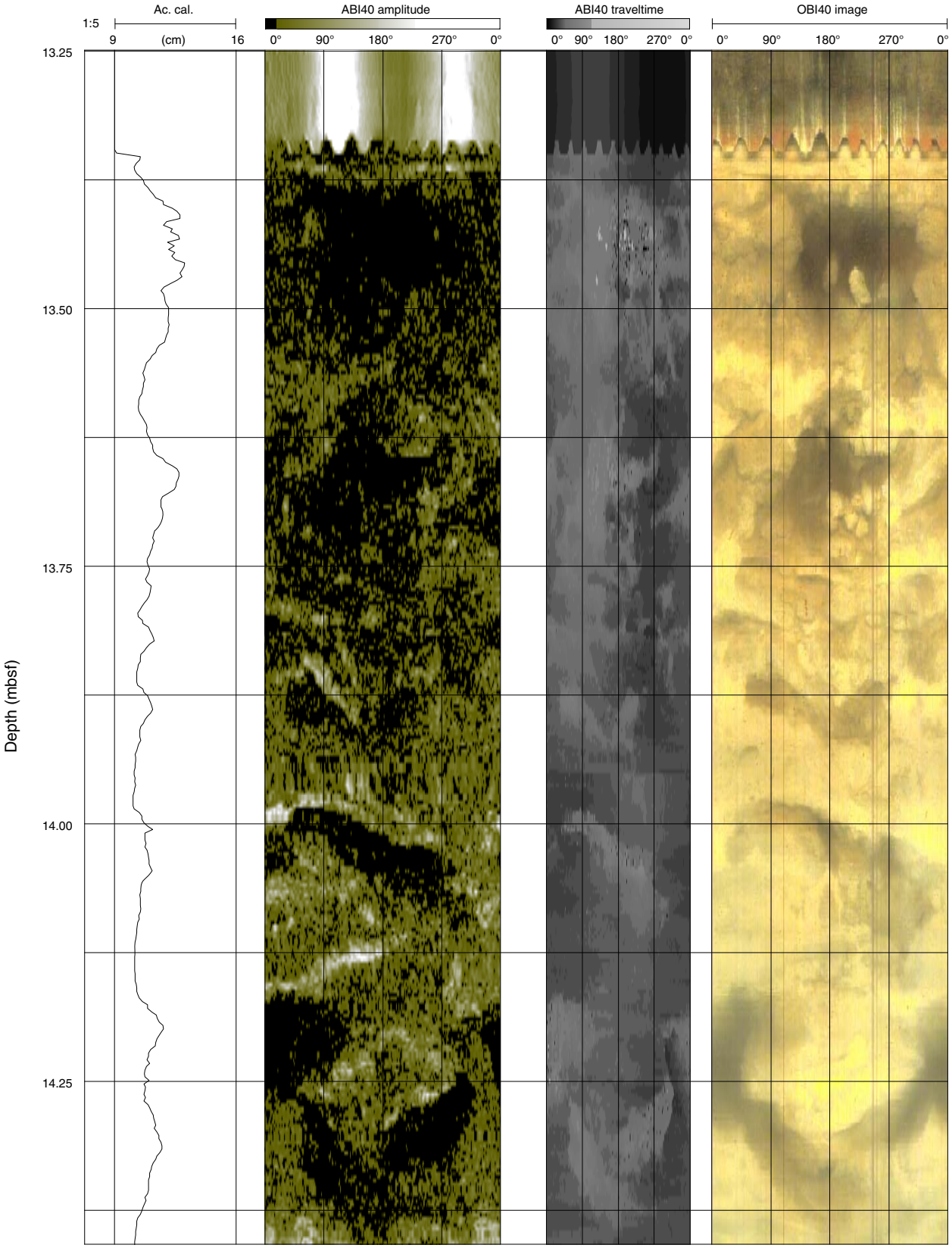

Figure F74. Wireline logging data, Hole M0017A. Ac. cal. = acoustic caliper extracted from ABI40, Mec. cal. = mechanical caliper, res. = resistivity, T = borehole fluid temperature, C = borehole fluid conductivity.

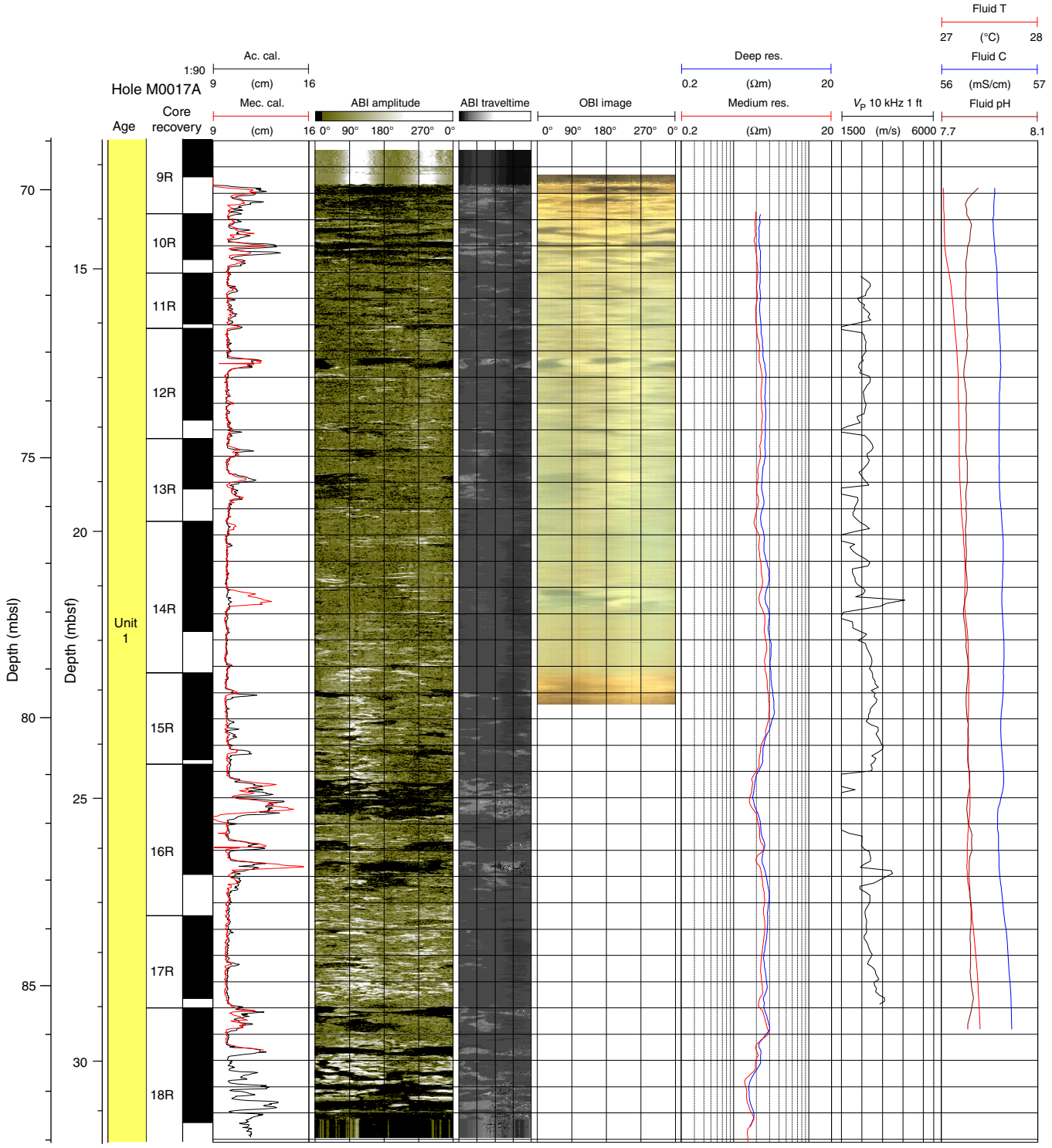

Figure F75. Wireline logging data comparing all Maraa sites. Res. = resistivity, ILD = induction electrical conductivity of greater investigation depth, ILM = induction electrical conductivity of medium investigation depth, TGR = total gamma ray. Unit II boundary in Hole M0015A is at ~108.65 mbsl.